# WAVELET AND MULTIFRACTAL ANALYSIS OF TRANSIENTS IN POWER SYSTEMS

by

LEILA S. SAFAVIAN

A Thesis
Submitted to the Faculty of Graduate Studies
in Partial Fulfillment of the Requirements
for the Degree of

MASTER OF SCIENCE

Department of Electrical and Computer Engineering
University of Manitoba
Winnipeg, Manitoba, Canada

Thesis Advisor: Prof. W. Kinsner, Ph.D., P.Eng.

(xvii + 122 + A-2 + B-28) = 169 pp.

THE UNIVERSITY OF MANITOBA

FACULTY OF GRADUATE STUDIES

*****

COPYRIGHT PERMISSION

Wavelet and Multifractal Analysis of Transients in Power Systems

BY

Leila S. Safavian

A Thesis/Practicum submitted to the Faculty of Graduate Studies of The University of Manitoba in partial fulfillment of the requirement of the degree

Of

Master of Science

*To Shaahin*

# ABSTRACT

This thesis is an investigation into the characterization and classification of power system transients, using advanced signal processing and pattern classification techniques. In the system developed in this thesis, which is intended to act as an artificial consultant to power systems operators, wavelet and multifractal analyses have been used to characterize transients in power systems and to extract features from them. The Daubechies wavelet family used in this thesis decomposes the signal into details and approximations, which contain the high and low frequency content of the signal, respectively. The variance fractal dimension trajectory method characterizes the complexity of the signal using a sequence of fractal dimensions. The thesis considers the usefulness of each of these methods in characterizing the transients as well as their combination. Various classification methods, namely the Bayes rule (based on the method of maximum likelihood, ML), the nearest neighbor (*k*-NN), and the probabilistic neural networks (PNN) have been used to identify the corresponding class of a transient.

The performance of the system is evaluated both on simulated transients and recorded data obtained from Manitoba Hydro. For the simulated data, the ML-based Bayes rule produced an average accuracy of 82.92% with the VFDT-based features, an average accuracy of 96.25% with the wavelet features and 100% with the combined features. The PNN yielded an average accuracy of 95% with the training set and 88.75% with the testing set of data. Classification of the recorded data produced an average of 82% using the *k*-NN classifier. The results show superior performance to previous work, both in the accuracy of the classification and significant reduction of the number of features used.

# ACKNOWLEDGEMENT

I would like to express my most sincere thanks to my thesis advisor, Prof. Witold Kinser, for his guidance, encouragement and support throughout this project. Completion of this thesis could not be reached without useful discussions with him that produced much insight into this work.

I would also like thank Manitoba Hydro for their financial support; special thanks go to Dr. Hilmi Turanli and Mr. Ray Armstrong from Manitoba Hydro for their assistance and making recorded data available to this research project.

I also acknowledge the members of the Delta research group, both past and present, including Robert Barry, Dr. Hakim El-Boustani, Stephen Dueck, Aram Faghfouri, Neil Gadhok, Dr. Bin Huang, Michael Potter, Sharjeel Seddiqui, and Lily Woo, for their support and useful discussions throughout this work.

I would also like to thank my parents for their belief in me through all the stages of my life, and for encouraging me endlessly to learn more.

Last but not least, I would like to thank my beloved husband, Shaahin, for his help and encouragement, and for staying beside me in the most difficult times. Without his unwavering support, the completion of this work was impossible.

# TABLE OF CONTENTS

# LIST OF FIGURES

# LIST OF TABLES

# LIST OF ABBREVIATIONS

| | |
|---|---|
| PSCAD® | **P**ower **S**ystem **C**omputer-**A**ided **D**esign |
| EMTDC® | **E**lectro**m**agnetic **T**ransients including **DC** |
| VFD | **V**ariance **F**ractal **D**imension |
| VFDT | **V**ariance **F**ractal **D**imension **T**rajectory |
| ML | **M**aximum **L**ikelihood |
| CWT | **C**ontinuous **W**avelet **T**ransform |
| DWT | **D**iscrete **W**avelet **T**ransform |
| FIR | **F**inite **I**mpulse **R**esponse |
| DB | **D**au**b**echies wavelet family |
| Var | **Var**iance operator |
| *k*-NN | *k*-**N**earest **N**eighbor |
| PNN | **P**robabilistic **N**eural **N**etwork |
| HVDC | **H**igh **V**oltage **D**irect **C**urrent |
| FORTRAN | **For**mula **Tran**slation (computer programming language) |
| PLL | **P**hase-**L**ocked **L**oop |
| SNR | **S**ignal to **N**oise **R**atio |

NOTE

The spelling used in this thesis follows the Canadian spelling, and not the American or British.

# LIST OF SYMBOLS

| | |
|---|---|
| $W(a,b)$ | Wavelet transform for scale $a$ and shift $b$ |
| $t$ | Time |
| $\psi(t)$ | Wavelet function |
| $h(n)$ | Wavelet decomposition low-pass filter |
| $g(n)$ | Wavelet decomposition high-pass filter |
| $U_d(z)$ | Down-sampled approximation signal |
| $V_d(z)$ | Down-sampled detail signal |
| $U_u(z)$ | Up-sampled approximation signal |
| $V_u(z)$ | Up-sampled detail signal |
| $\phi(t)$ | Scaling function |
| $\Re^n$ | $n$-dimensional real space |
| $\Delta t$ | Time incerement |
| $\sigma^2$ | Variance |
| $H$ | Hurst exponent |
| $E$ | Euclidian dimension |
| $D_\sigma$ | Variance fractal dimension |
| $g(x)$ | Probability density function of the random variable $x$ |
| $P(\omega_i \mid \mathbf{x})$ | Probability of class $\omega_i$ given the pattern $\mathbf{x}$ |
| $g(\mathbf{x}\|\omega_i)$ | Class-conditional pdf |
| $P(\omega_i)$ | Prior probability of class $\omega_i$ |
| $C$ | Number of classes |
| $\boldsymbol{\theta}$ | Parameter set for a pdf |

| | |
|---|---|
| $L(\boldsymbol{\theta})$ | Optimization objective function for the maximum likelihood method |
| $G(\mathbf{x})$ | A mixture model pdf |
| $M$ | The number of constituent models in a mixture model |
| $\pi_i$ | Mixing proportions for mixture models |
| $W(x)$ | Window function (in Parzen pdf estimation) |
| $N_t$ | Total number of training samples |
| $y_i$ | The $i$th output of a PNN |
| $q_i$ | Normalized share of the $i$th PNN output |
| $e(\mathbf{x}_i)$ | Partial objective function for the input $\mathbf{x}_i$ |
| $OF$ | The overall objective function of a PNN |
| $\omega_0$ | Angular frequency of the power system (=367.99 rad/sec in North America) |
| $v_1$ | The estimated magnitude in a PLL |
| $\phi_1$ | The estimated phase angle in a PLL |
| $K$ | Number of wavelet vanishing moments |
| $v_d(n)$ | Detail waveform (in wavelet analysis) |
| $v_{rms^2}$ | The squared RMS of the wavelet detail waveform |
| $N_{ww}$ | The window width parameter in the VFDT analysis |
| $N_{ws}$ | The window shift parameter in the VFDT analysis |
| $f_d$ | Trajectory of the variance fractal dimensions |
| $N_d$ | Total number of fractal dimensions in a trajectory |
| $m_1$ | First moment of a VFDT |
| $m_2$ | Second moment of a VFDT |

# CHAPTER I

# INTRODUCTION

## 1.1 Problem Definition and Motivation

Electric energy systems are the backbones of modern industrial societies. Their purpose is to meet the demand of energy in a safe, secure and reliable manner with the highest quality. Energy transmission and distribution systems are constantly subjected to disturbances that inevitably occur due to planned operations, as well as unforeseen events such as faults and lightning strikes. Such disturbances, which commonly are referred to as electromagnetic transients, affect adversely the quality of electric power delivery and hence are considered as unfavorable events. Consumers of the electric power as well as the equipment used in power systems are affected by the occurrence of transients. The impact of transients can vary from hardly-noticeable flicker of incandescent lamps to massive service interruptions and blackouts affecting millions of consumers.

The recent awareness of the power quality concepts has driven the power systems industry to devize intelligent methods for the operation of the existing and design of emerging infrastructure so that the adverse impact of transients is minimized.

Signal processing techniques can be used to assist effectively power system operators in making appropriate decisions when transients do occur. Such techniques can be used to detect, characterize and classify transients accurately and in the shortest time possible, so that the system operators or other components of the protection system can initiate the appropriate corrective measures. The ultimate goal of the research activities in this field

is to devize an artificial-intelligence agent that gives instant, accurate consultation to the power system operators. A critical task in developing such a system is to use suitable signal analysis techniques to extract and examine the underlying features of transients, and then to carry out identification and classification.

The major steps that need to be taken in order to develop such a system are

(i) to obtain an abundant, rich collection of various waveforms of transients in power systems either through simulation or by using recorded data;

(ii) to develop robust, accurate methods for the extraction of a suitable number of features that precisely describe the underlying transient phenomena; and

(iii) to develop methods for rapid classification of the transients to provide the power systems operator with a reliable means of identifying as to what has initiated such a transient.

Although some details about each of these essential tasks are provided next, comprehensive treatment of the subjects is presented in the subsequent chapters of the thesis.

## 1.2 Power System Transients

In order to develop the classification algorithms, several instances of transients in power systems are required. In this research, two sets of such waveforms have been used, namely simulated transients and real, recorded transients. The simulated waveforms, which are obtained using the PSCAD/EMTDC electromagnetic transient simulation

program, include transients caused by three-phase faults, capacitor switchings and breaker operations.

The recorded data that has been used for the final testing of the overall system contains several instances of such transients as those caused by (i) lighting, (ii) switching, (iii) birds, (iv) storm, and (v) mis-operation, such as transients caused by operator's error.

Use of recorded transients for the verification of the usefulness of the proposed methods is a salient feature of this research that gives further credibility to its results.

## 1.3 Feature Extraction Algorithms

Features are underlying properties of signals that can be used to distinguish them from one another. It is desirable to have as small number of features as possible, while being able to uniquely identify signals using their features. Feature extraction involves use of methods that condense a given signal into a number of features while preserving its fundamental properties. The choice of the feature extraction algorithm depends largely on the nature of the signals to be analyzed.

Transients in power systems are short-term, non-stationary, and normally non-periodic waveforms. While conventional signal analysis methods, such as the Fourier transform, find numerous applications in the analysis of various signals, their capabilities fall too short when applied to transient waveforms. This is mainly because transients are non-periodic, whereas Fourier methods are based essentially on periodic waveforms. Moreover, the analysis of power system transients usually involves the study of both time

and frequency content of a signal and as such more advanced signal processing techniques are to be employed.

In this research two signal analysis methods, namely the wavelet analysis and multi-fractal analysis have been used. Both methods provide useful means for the investigation of the non-stationary signals and preserve both time and frequency/dimension information. They are also efficient in compressing the signals and thus can provide condensed, yet very rich sets of features. The features obtained from either of these two methods are assessed individually and then are combined and used as the input to the classifier.

## 1.4 Classification Unit

Classification refers to the task of assigning appropriate labels (classes) to the transient waveforms based on their features. There are several options as to what classification algorithm should be used. In the majority of the research activities conducted in this area, artificial neural networks have been used. While neural networks do demonstrate acceptable performance in the classification of transients in power systems, there are other options, such as Bayes rule (with estimated probability density functions) and the nearest neighbor classifier, which can be of comparable performance. The study carried out in this research has incorporated two important tasks. Firstly, unlike the majority of the previous studies, the classification has been made with the aim of identifying what event has caused the transient, rather than identifying the type of the transient. This provides an insight to the actual cause of the event and provides the operator or the protection system with invaluable information as to what needs to be done

in reaction to the observed transient. Secondly, the study has considered other classifiers in conjunction with the neural networks and has performed critical assessment of their suitability for the classification of transients in power systems.

It is important to note that the existence of elements such as transformers with nonlinear cores (due to saturation, hysterises and many interacting subsystems) makes power systems nonlinear. Nonlinear systems give rise to the question about uniqueness of solutions. The system studied in this thesis is stable and our solutions have shown convergence; therefore, eliminating the concern over non-uniqueness of the solution.

## 1.5 Statement of Objectives of the Thesis

The main goal of this thesis is to establish a firm groundwork for the development of an artificial intelligence consultant to assist the power system operator with a powerful, reliable means for the detection, analysis and classification of the transients and to provide them with appropriate input to enable them to decide what type of corrective measure needs to be taken in response to the identified event.

In order to achieve this goal, it is necessary to develop:

1. Suitable methods for the extraction of a minimal number of features that can describe accurately the nature of the transients, and

2. Classification methods that are rapidly adaptable and produce accurate results.

As a major outcome of thesis, care has been devoted to the study of a fairly wide range of possible options and to assess the suitability of various options in a critical manner.

Unlike prior works in this area, e.g., [KiAg00], [LiMo99], and [Yous03], which either focused on extraction of features or development of classifiers, this work has a comprehensive approach to the problem and places equal emphasis on both feature extraction and classification. Reduction of the number of features without sacrificing the accuracy of the classifier has been another major focus of this thesis.

## 1.6 Organization of the Thesis

Following the introduction presented in this chapter, the remaining chapters are organized to present a logical transition from technical and mathematical background to the system design and finally to the experiments carried out.

Chapter 2 presents a qualitative overview of the transient phenomena in power systems, and the protection schemes deployed to react to such transients. It also discusses the need for an intelligent transient processing and classification from the viewpoint of power systems operation.

Chapter 3 is devoted to the theory of wavelet analysis. In particular, the chapter discusses the suitability of the method for the analysis of transient signals. Implementation of the method using filter banks is also presented.

Chapter 4 presents the essentials of the fractal analysis, including fractals and fractal dimensions, and their suitability for characterization of transients in power systems. Particularly, the variance fractal dimension trajectory (VFDT) method is described and its benefits for the intended application in this thesis are highlighted.

Chapter 5 is dedicated to the theory and mathematical essentials of pattern classifications. The chapter begins with an overview of the statistical foundations of classification and the Bayes rule. The implications of practical limitations (such as lack of probability density functions) on the Bayes rule are then discussed, which lays the foundation for other classification methods discussed, including the Bayes rule using maximum likelihood (ML), the nearest neighbor (NN) and the probabilistic neural network (PNN). The treatment presented in Ch. 5 is organized so that the underlying common foundations of the classification methods discussed are revealed.

The material presented in Chs. 3 to 5 form the mathematical basis of the thesis, followed by a description of the system design in Ch. 6, which provides details on the design and implementation of various components.

In Ch. 7, the experimental results obtained using the simulated transients as well as recorded data obtained from Manitoba Hydro are presented. In particular, the performance of individual feature extraction methods and their combination is presented.

Chapter 8 provides a summary of conclusions and specifies the contributions made through this research. Recommendations for further research in the area conclude this chapter.

# CHAPTER II

# POWER SYSTEM TRANSIENTS

## 2.1 Electric Power Systems – An Overview

Electric power systems are known to be the largest dynamical systems created by man. They are used for the generation, transmission and distribution of electric energy. Normally, generation of power is done in remote locations and then the energy is transmitted to load centers, e.g. metropolitan areas, through high voltage, long transmission lines. Distribution systems are often located within or very close to densely populated areas, and are used primarily for stepping down the voltage to the levels used by the consumers [GlSa87].

Power systems are often interconnected with each other resulting in even larger systems. This is to increase the reliability and stability of power delivery. Such interconnected power systems usually span vast geographical areas; they may include several power generation plants producing power from different sources (such as hydro-electric, thermal or nuclear plants), a large number of transmission lines of various lengths, and thousands of transformers, and they can provide power to millions of energy consumers. Figure 2.1 shows a schematic diagram of a typical power system. In an actual power system the loads are complex combinations of thousands of consumer apparatus; such complex combinations as well as the dynamic behaviour of other system components make the operation and control of a power system a task that requires advanced control and protection schemes.

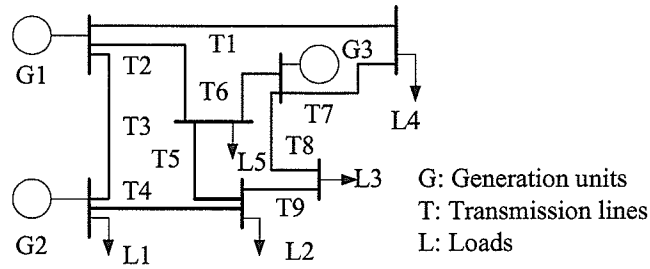


**Fig. 2.1** Schematic diagram of a power system.

In order to ensure safe and reliable delivery of electric energy, several layers of control and protection are used to ensure proper operation of the network as well as sufficient protection for the network equipment and energy consumers [Kund95]. The role of interconnected power systems is to provide the users with a reliable, secure, and clean source of energy.

## 2.2 Transient Phenomena in Power Systems

Under ideal circumstances, ac power systems should operate at the specified frequency, e.g. 60 Hz in North America, with all the voltages and currents being within their safe operating ranges. However, this is hardly the case, as there are a large number of events that can cause deviations in the frequency as well as voltage and current waveforms from their specified values. Some of these changes are so small that can be tolerated without causing any significant impact of the quality of electric power delivery. For example, switching on a mid-size electric motor in a factory in the suburbs of a city will result in a momentary voltage drop; however, this voltage drop can be noticed hardly by energy consumers inside the city, although these electric power systems are interconnected. However, in many cases, the deviations are more significant so that they impact the performance of the systems and deteriorate its performance below acceptable

limits. A well-known example of these minor, yet irritating, transients is the voltage flicker that is caused by loads such as arc furnaces and causes fluctuations in the brightness of incandescent lamps. In severe cases, such unfavorable events can lead to line outages, instability of the network and massive blackouts, which affect vast areas and a large number of consumers and cause significant economical losses.

In many cases, these deviations are short-term and impact the system in a relatively short period of time, and hence are referred to rightfully as transients. Transients can be initiated by an abundance of causes, including natural, unplanned events such as lighting strikes, storms, birds, and a wide variety of faults, as well as planned operations such as switching of large capacitor banks, opening and closing of transmission lines and changes in the settings of power system controls.

Two examples of actual power system transients are shown in Fig. 2.2. These recorded waveforms show how the pre-transient sine waves are disturbed by the presence of transients. In Fig. 2.2 (a), the impact of the transient on the voltage waveform persists for a relatively large number of cycles and finally causes interruption in the voltage waveform. The other waveform shows significant distortion of the waveform during the transient followed by restoration of the voltage waveform caused by the removal of the cause of the event.

Taking into account that power systems physically span large areas, it is easy to imagine that transients, at least the ones initiated by natural causes, are quite likely to occur. For example, even the most well-designed transmission systems will be still prone to lightning strikes. Although it is possible to reduce the unfavorable impact of transients,

it is impractical to design systems with no risk of transients. Presence of transients deteriorates the quality of electric power delivery by disturbing the frequency of operation and also the voltages and currents supplied to the consumers. The undesirable impact of transients tends to become even further pronounced as the number of sensitive loads, such as computers and other digital devices, increases.

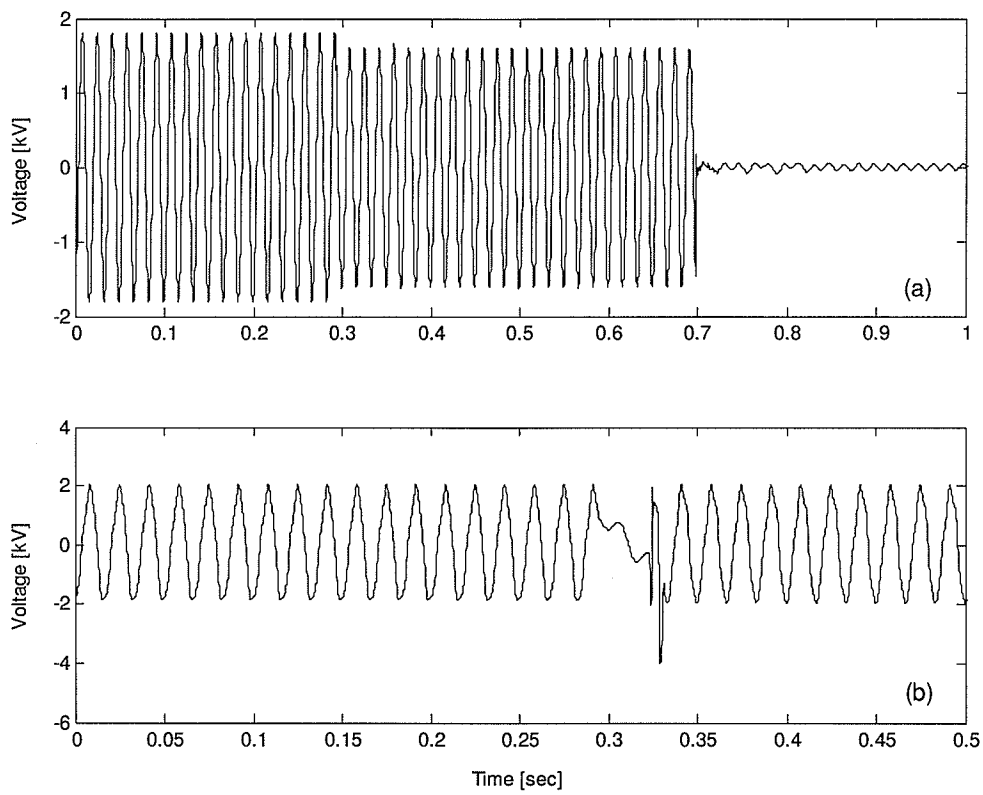


**Fig. 2.2** Examples of transients in power systems.
(a) Transient caused by a bird; (b) Transient caused by lightning.

It is possible to simulate transient waveforms of a power system using a computer program. Electromagnetic transient simulation programs do exactly this. It is a very safe approach to studying transient phenomena in a power system without disturbing the actual power system, which can be expensive, unsafe and hazardous. Simulated transients have been extensively used in this thesis for feature extraction and classification. Figure

2.3 shows two samples of simulated transients cause by three-phase faults (Fig. 2.3 (a)) and capacitor switching (Fig. 2.3 (b)).

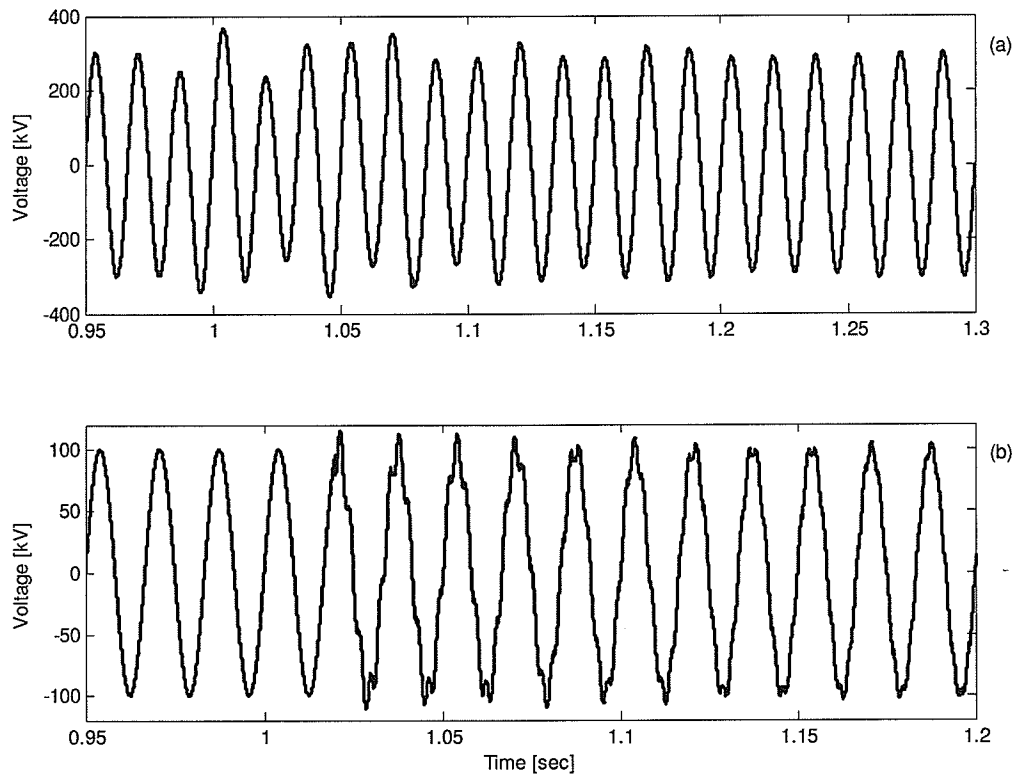


**Fig. 2.3** Samples of simulated transients.
(a) Three-phase fault; (b) Capacitor switching.

## 2.3 Signal Processing for Power System Protection

Power systems protection systems are designed to react to the cause of transients by temporary or permanent removal of the faulted section of the network. In general, a number of relays are installed in appropriate locations in a power system and they constantly monitor various quantities, such as voltage, current, impedance, phase angle, rotor angle, real and reactive power, in their respective protection zone. As soon as a transient causes the measured quantities to fall outside their specified safe limits, the

relays generate command signals to switches that would react by switching out the faulted section. An essential task is to identify correctly the true cause of a transient, so that appropriate corrective measure can be taken. For example, a protection system may tolerate the presence of a capacitor switching transient but its reaction to a line stricken by lighting will be to disconnect it until it is repaired. Misjudgment about the true nature of a transient will result in an incorrect protective reaction that can cause actually further damage, e.g., by interrupting service to critical loads.

Older generations of protective relays used electromechanical systems to detect the occurrence of transients. Later generations have incorporated successfully digital systems in the relays, thus improving the longevity of relays as well as their accuracy. Although digital relays have shown superior performance over their electromechanical predecessors, they still mainly rely on conventional methods for detection of transients. It is evident that an intelligent signal processing unit that constantly monitors the voltage and/or current waveforms, detects correctly the occurrence of transients, analyzes the waveforms and identifies the cause of transients can be an invaluable asset to the power system operators and an integral part of a comprehensive power system protection scheme. The output of such a system will assist greatly the protection system or the operator to initiate correctly the necessary remedial action with minimal risk of further deteriorating the operation of the system by making incorrect decisions.

High performance fault recorders are becoming essential components of modern power systems, where high quality power delivery is a prime concern. An artificial intelligence consultant, as described above, in conjunction with modern transient recorders and advanced protection algorithms can enhance significantly the reliability of

power systems and contribute greatly to its quality. Development of such a system is the subject of the following chapters.

## 2.4 Chapter Summary

This chapter presented a brief overview of some essential concepts related to power systems operations and protection. It was mentioned that occurrence of transients, even in the most well-designed systems, is inevitable due to the vast geographical span of power systems that exposes them to a wide range of natural events such as lightning strikes, birds, falling tree branches. Other planned operations such as line or capacitor switching also cause transients.

Proper operation of a power system requires high quality, disturbance-free delivery of power to consumers. Signal processing techniques can be used effectively to improve the performance of protection system by enabling them to detect and identify transients and by enabling them to respond to such events appropriately. Such tools and techniques are discussed in detail in the upcoming chapters.

# CHAPTER III

# WAVELET ANALYSIS

## 3.1 Introduction

Characterization of the transients and extraction of their features is an important task in the identification and classification of power system transients. Several techniques for the analysis of signals exist, including Fourier transform, windowed Fourier transforms, and wavelets. These techniques are based on characterizing signals using known waveforms with either infinite or finite support. Other techniques such as the multi-fractal analysis also exist; however, their consideration is postponed to the next chapter.

Fourier transform techniques are based on characterizing a given signal using sine waves with different frequencies, phase shifts and amplitudes. In other words, a given waveform is represented as a combination of various sine waves. This combination may contain only a limited number of terms or on the other hand may require an infinite number of sinusoidal components to represent the original waveform accurately. This technique is best suited for the analysis of periodic waveforms, which repeatedly represent the same pattern. The reason is that sine waves are not limited to a bounded interval (in time) and extend over the entire time axis. Figure 3.1 shows the reconstruction of a periodic square-wave signal using its Fourier components. It is worth examining this figure as it reveals some of the important properties of the Fourier transform. As shown the original waveform has sharp edges resulting from instantaneous jumps between +1 and -1. These sharp edges translate in terms of high frequency components in the Fourier domain. Incorporating more frequency components (with

increasing frequencies) results in a more accurate estimation of the original waveforms, especially better approximation of the sharp edges. An infinite number of components are required to obtain accurately the original waveform. Since such an approach is not feasible, in practice the number of components used for reconstruction (approximation) is limited, and therefore an approximation error will be associated with process.

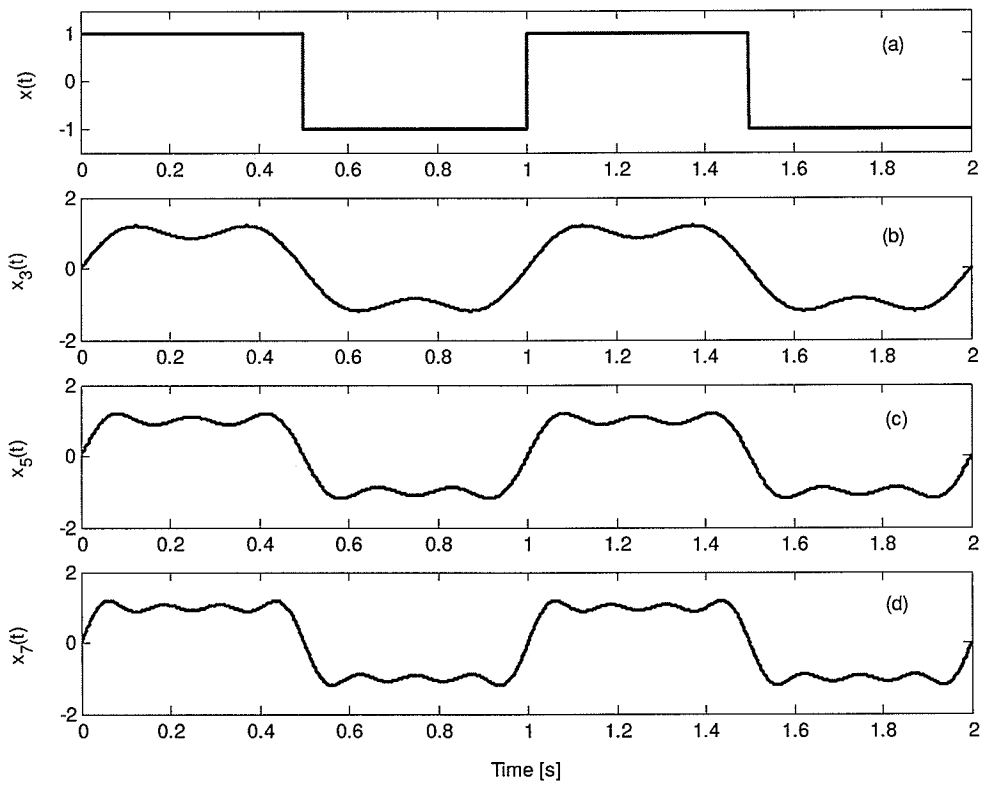


**Fig. 3.1** Reconstruction of a square-wave signal using its Fourier components. (a) Original square wave; (b) Signal reconstruction using first two components; (c) Signal reconstruction using first three components; (d) Signal reconstruction using first four components.

Transients in power systems, however, are not periodic waveforms. They are usually short-term, abrupt changes that last for a short while. Originally the characterization of transients was attempted also using conventional signal analysis tools, e.g. Fourier

transform and windowed Fourier transform; however, soon it was realized that enhanced methods are required to best describe such short-term phenomena.

One of the techniques that have found numerous applications in the analysis of short-term, non-stationary phenomena is the wavelet transform [KiAg00], [KiAg01], [PaSa98], [Yous03], [SPGH96], [SaPG97]. Unlike the Fourier analysis, which transforms totally a signal from time domain to frequency domain, the wavelet analysis extracts the frequency contents of the signal while preserving its time-domain properties [Mall99]. In other words, the wavelet analysis is a time-frequency transformation. The analysis of transients in power systems often requires both time and frequency contents of the signal to be characterized and as such the wavelet analysis is suited completely for studying them.

## 3.2 Wavelet Analysis: Essentials

The underlying idea in the wavelet analysis is to decompose the original waveform into the shifted and scaled versions of a short-term waveform called a wavelet. Since the original wavelet is a short-term waveform, it provides a localized representation of the signal. Depending on the local complexity of the original signal, this representation can contain low or high frequency components. This variability is the reason why it is also called the multi-resolution analysis.

Mathematically, the continuous wavelet transform $W(a,b)$ of the signal $x(t)$ can be represented using the following formula

$$W(a,b) = \frac{1}{\sqrt{a}} \int_{-\infty}^{\infty} x(t)\psi(\frac{t-b}{a})dt \tag{3.1}$$

where, $\psi(t)$ is the mother wavelet function and $a$ and $b$ are the scaling and shifting parameters, respectively [SSAS98], [SaSu98]. Parameter $a$ determines how much the original wavelet function $\psi(t)$ is contracted (for $a < 1$) or stretched (for $a > 1$). Parameter $b$ determines how much the original wavelet function is shifted to the right (for $b > 0$) or to the left (for $b < 0$). Altogether, various combinations of these two parameters correspond to the shifted and scaled versions of the wavelet function. For every such combination, Eq. (3.1) is a measure of the closeness (or correlation) of the waveform $x(t)$ with $\psi(\frac{t-b}{a})$. Apparently, a closely similar $x(t)$ with a given $\psi(\frac{t-b}{a})$ results in a corresponding $W(a,b)$ of a large value. In other words, Eq. (3.1) yields a localized measure of the correlation between the two waveforms.

Unlike Fourier analysis, where infinite-duration, periodic sine waves are used, wavelet analysis uses short-term wave(lets) as the analyzing function. A wavelet function is a short-term, oscillatory function with an average equal to zero and with both ends vanishing to zero. Such a choice of the analyzing function makes wavelet transform an ideal choice for the analysis of signals with transients in them, e.g. power system transients.

It was mentioned that the parameters $a$ and $b$ in (3.1) represent the scaling and shifting of the original wavelet. In continuous wavelet transform (CWT), these two parameters can assume any value on a continuous basis. Such an approach results in a tremendous amount of information, which will be very inconvenient for further processing. To facilitate convenient and accurate analysis, $a$ and $b$ are selected to be powers of 2, the so-called dyadic or discrete wavelet transform (DWT) [SSAS98].

Both versions of the wavelet analysis are based on determining the closeness (correlation) of the original signal with shifted and scaled versions of the wavelet function. In other words, the wavelet coefficients obtained by finding the closeness between the two waveforms will attain larger magnitudes, as the two waveforms become more similar.

## 3.3 Discrete Wavelet Analysis: Implementation and the Filter Bank Theory

Close examination of the properties of the wavelet transform reveals that the analysis can be thought of as filtering the original using a carefully selected set of filters. The rationale behind this is that the scaled versions of the mother wavelet are in fact similar to filters (in frequency domain) that select sub-bands of the original signal. A large value of $a$ corresponds to an expanded wavelet, which has smoother changes and so extracts low frequency content of the waveform, while lowering $a$ results in a compressed wavelet, which has more abrupt changes and hence is suitable for extracting high frequency contents.

Figure 3.2 shows the filter bank implementation of the discrete wavelet transform (DWT). Before proceeding any further into the details, it should be noted that the filter bank implementation is demonstrated in such a way to establish the underlying ideas of wavelet decomposition and reconstruction. In other words, the input signal $\dot{x}(n)$ is decomposed (for example at the sending end) and reconstructed (at the receiving end) using filters that implement the wavelet transform. The idea is to design filters such that the input signal could be retrieved at the receiving end without any artifacts.

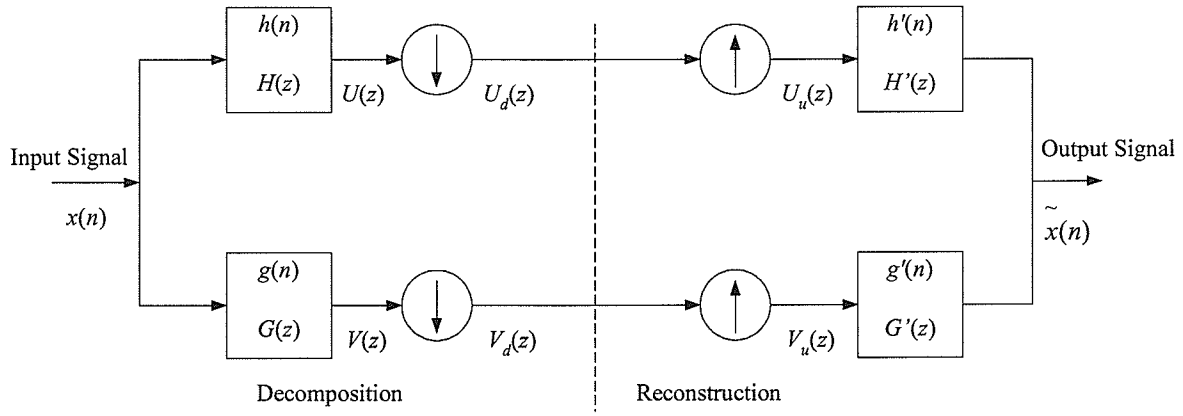


**Fig. 3.2** Filter bank implementation of the wavelet transform.

The low-pass and high-pass filters $h(n)$ and $g(n)$ generate approximation and detail waveforms, respectively. The approximation and detail waveforms are so named because they contain low-frequency and high-frequency contents of the original signal, respectively. Note that filtering of a signal with a given number of samples generates a signal with the same number of samples; therefore, one can expect that after performing the low-pass and high-pass filtering, the total number of samples to be doubled (note that the number of input and output samples in a filter are the same; therefore the total number of samples at the output of two filters will be twice as large as the number of samples of the original signal). The doubling of the number of samples following each stage of filtering is undesirable as it complicates the processing of samples. In order to address this, each filtering stage is followed by down-sampling operation (denoted by the down arrow), which eliminates samples alternatively. Figure 3.3 shows the process of down-sampling on a given signal. Such sequence of operations is known as the decomposition part of the wavelet transform, and can be repeated in several stages resulting in multiple approximations and details.

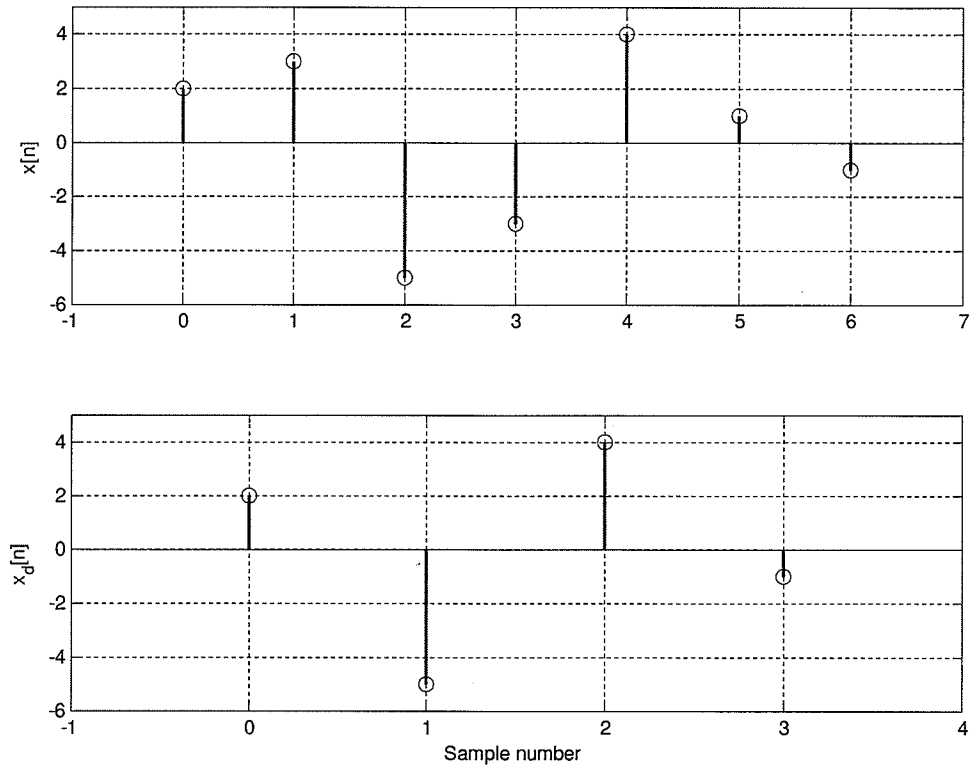


**Fig. 3.3** Down-sampling of a discrete signal.

The reconstruction part of the transform consists of up-sampling operations (the up arrow), followed by filtering of the approximation and detail waveforms. The up-sampling is done by inserting zeros alternatively between the sample numbers.

In order for the process to be useful, it should be possible to recover the original signal $X(z)$ ($X(z)$ is the $z$-transform of $x(n)$) at the output. Let us investigate how the original signal $X(z)$ is related to the output $\tilde{X}(z)$ [SSAS98]. It is observed that

$$U(z) = H(z)X(z) \tag{3.2}$$

$$V(z) = G(z)X(z) \tag{3.3}$$

The down-sampled signals can be obtained using the following formulae

$$U_d(z) = \frac{1}{2}(U(\sqrt{z}) + U(-\sqrt{z})) \tag{3.4}$$

$$V_d(z) = \frac{1}{2}(V(\sqrt{z}) + V(-\sqrt{z})) \tag{3.5}$$

Appendix A contains a proof of the above formulae. For the reconstruction part, the decimated signals $U_d(z)$ and $V_d(z)$ are up-sampled, resulting in $U_u(z)$ and $V_u(z)$, which are expressed as follows (see Appendix A for proof)

$$U_u(z) = U_d(z^2) = \frac{1}{2}(U(z) + U(-z)) \tag{3.6}$$

$$V_u(z) = V_d(z^2) = \frac{1}{2}(V(z) + V(-z)) \tag{3.7}$$

Thus, the output signal can be expressed as follows

$$\tilde{X}(z) = \frac{1}{2}\{G(z)G'(z) + H(z)H'(z)\}X(z) + \frac{1}{2}\{G(-z)G'(z) + H(-z)H'(z)\}X(-z) \tag{3.8}$$

The output signal is therefore a combination of the original signal $X(z)$ and an aliased part $X(-z)$. Suitable choice of the filter coefficients can eliminate the aliased component by setting its coefficient equal to zero. Usually FIR filters are used in the filter bank implementation of the DWT. It can be shown that with a low-pass filter $H(z)$ of the form

$$H(z) = h(0) + h(1)z^{-1} + \cdots + h(N)z^{-N} \tag{3.9}$$

and with the three remaining filters described as

$$H'(z) = z^{-N}H(z^{-1}) \quad \text{i.e.,}\ h'(n) = h(N-n) \tag{3.10}$$

$$G'(z) = z^{-N}H(-z^{-1}) \quad \text{i.e.,}\ g'(n) = -(-1)^n h(n) \tag{3.11}$$

$$G(z) = -z^{-N}H(-z^{-1}) \quad \text{i.e.,}\ g(n) = (-1)^n h'(n) \tag{3.12}$$

the aliased component in the output signal vanishes. By substituting the above four equations into (3.8) it can be shown that if the filter coefficients for $h(n)$ (and hence for the rest of the filters) are chosen, through a simultaneous system of equations, in a way so that

$$H(-z)H(-z^{-1}) + H(z)H(z^{-1}) = 2 \tag{3.13}$$

then the reconstructed signal will be as follows

$$\tilde{X}(z) = z^{-N}X(z) \quad \text{i.e.,}\ \tilde{x}(n) = x(n-N) \tag{3.14}$$

In other words, the output signal will be a delayed version of the input signal, and has no other artifacts. Note that the delay is determined by the order of the filters used. Equation (3.13) usually yields a system of simultaneous equations (in terms of the filter coefficients) with more unknowns than the equations. Other conditions, such as the smoothness of the filters, are usually imposed on the filters to produce an adequate number of equations.

The filter bank implementation is linked to the original waveform representation of the wavelets through a recursive equation, which yields the following scaling and wavelet functions, respectively. These equations are given as follows

$$\phi(t) = \sqrt{2}\sum_{m=0}^{N} h(N-m)\phi(2t-m) \tag{3.15}$$

$$\psi(t) = \sqrt{2}\sum_{m=0}^{N} -(-1)^N h'(N-m)\phi(2t-m) \tag{3.16}$$

To solve for the scaling function in Eq. (3.15) one needs to start with an initial guess and recursively substitute it until the difference between the two successive iterations becomes negligibly small. For a third-order filter ($N$ = 3), four parameters need to be determined. The system of equations obtained using (3.13), yields 2 simultaneous equations, and therefore 2 extra equations need to be established. One equation is obtained by observing that for a high-pass filter $G(z)$, one can impose $G(0) = 0$; the fourth equation can be obtained by imposing smoothness on the low pass filter $H(z)$; i.e., zero slope at $\omega = 0$. Solution of the systems of simultaneous equations so obtained yields the four coefficients as follows

$$h(0) = \frac{1-\sqrt{3}}{4\sqrt{2}}, h(1) = \frac{3-\sqrt{3}}{4\sqrt{2}}, h(2) = \frac{3+\sqrt{3}}{4\sqrt{2}}, h(3) = \frac{1+\sqrt{3}}{4\sqrt{2}} \tag{3.17}$$

The wavelet corresponding to the four-coefficients found above is called the Daubechies 4 (DB4) wavelet after Ingrid Daubechies [Daub92], who proposed the method of smoothness for creation of the extra equations. In case more than one equation is required to complete the system of equations, higher order derivatives also can be set to zero [SSAS98].

Figure 3.4 (a) and (b) show the scaling and the wavelet functions for the Daubechies 4 family, respectively. The scaling and wavelet functions for another wavelet family

(biorthogonal 2.2) are also shown in Fig. 3.4 (c) and (d), respectively. As shown the wavelet functions in both cases have many singular points, where derivatives are not defined; such details make wavelets suitable for the analysis of signals such as transients, which contain singular points.

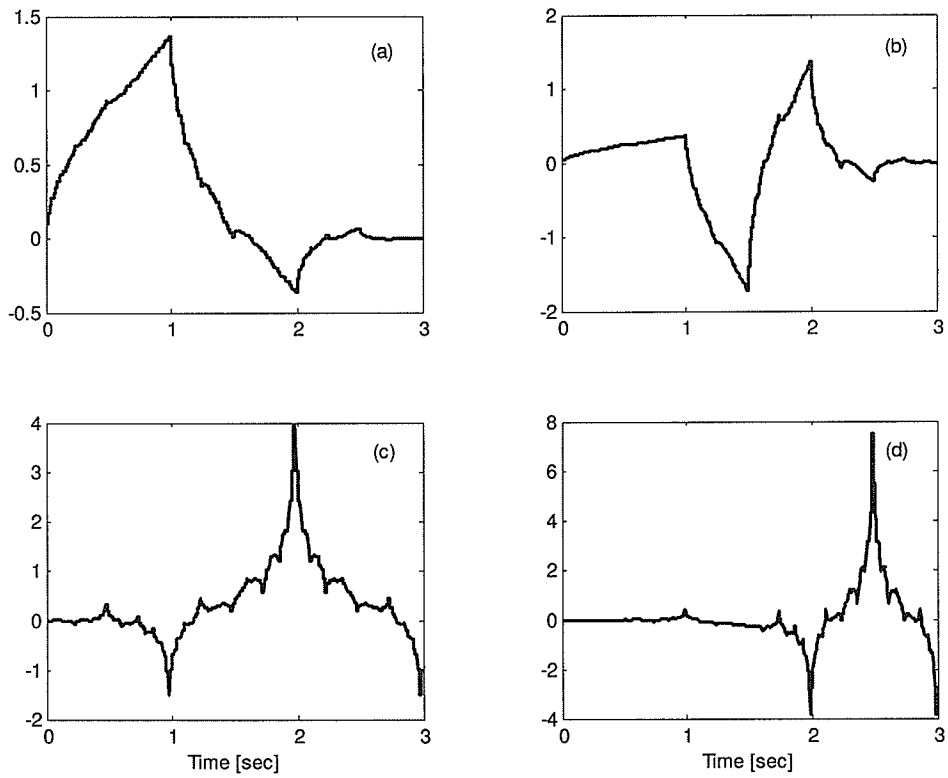


**Fig. 3.4** Scaling and wavelet function waveforms.
(a) Scaling function; and (b) Wavelet function for the DB4;
(c) Scaling function; and (d) Wavelet function for biorthogonal 2.2.

Figure 3.5 shows an example of a transient waveform that has been analyzed using the DB4 wavelet. Two levels of detail and approximation waveforms have been shown, which clearly show how the low- and high-frequency components of the original signal have been decomposed into the approximation and detail waveforms, respectively. In the first stage of filtering the original waveform is decomposed into a detail and an

approximation waveform. The approximation waveform becomes smoother than the original signal as some of the high frequency components will be contained in the detail waveform. Second stage filtering is done on the approximation waveform, which results in an even smoother approximation waveform and a second detail that contain some high frequency components.

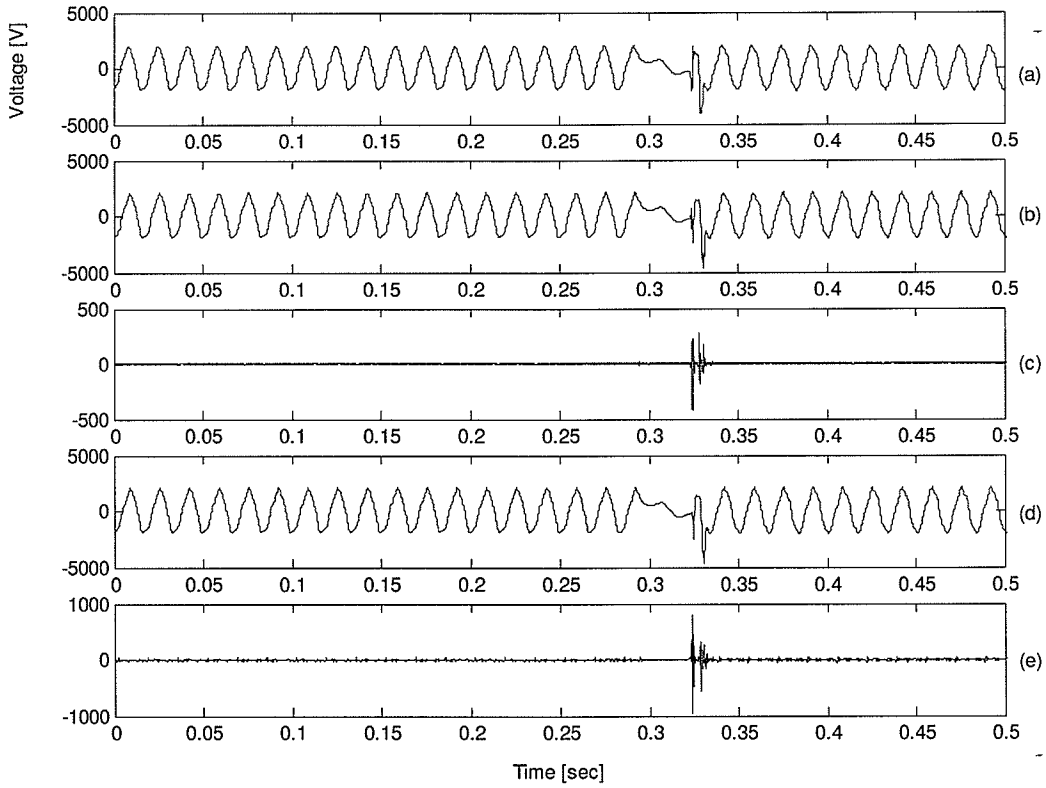


**Fig. 3.5** Wavelet analysis of a signal with a transient.
(a) The original signal; (b) First level of approximation; (c) First level of detail; (d) Second level of approximation; (e) Second level of detail.

Since the resolution of the analysis can vary along the signal, the wavelet transform can act as a suitable tool for the analysis of signals with varying complexity, such as the ones with transients.

Choice of a particular mother wavelet for a given application is an important task that needs careful examination of the signals to be analyzed as well as awareness of the properties of the wavelet family [SaKT05]. Study of transients in power systems is no exception in this regard and this issue is dealt with in Ch. 6, where the design of the overall system is discussed.

## 3.4 Chapter Summary

This chapter presented a short mathematical background on the wavelet analysis of signals containing transients. Implementation of the wavelet transform using an equivalent filter bank was demonstrated. As an example, development of a wavelet family, namely the Daubechies 4, was shown. The process, in general, usually starts with the design of appropriate filters that have a number of specified properties, and then the filter is translated into the corresponding scaling and wavelet functions.

The wavelets have several advantages over conventional signal analysis tools (such as the Fourier-based methods), including multi-resolution representation of signals with varying local complexity, and preservation of time and frequency content of the signal. These two important features prove to be very essential in the analysis of transients in power systems and will be further discussed in later chapters.

# CHAPTER IV

# MULTIFRACTAL ANALYSIS

## 4.1 Introduction

As mentioned in previous chapters, transients in power systems are short-term phenomena that occur due to various events and disturb the original waveforms of voltage and current in the network.

Characterization of transients could be tackled using various methods, including wavelet analysis presented in the previous chapter. Another method, called the multifractal analysis, could also be employed [Chen01], [Shaw97]. Multifractal analysis is based on characterizing the signal using the notion of complexity. In particular, the variance fractal dimension trajectory (VFDT) will be addressed. This method has several favorable features, such as capability for real-time implementation, which make it very suitable for real-time characterization of transients in power systems.

## 4.2 Fractals – An Overview

The term fractals and fractal analysis deal with the study of objects that demonstrate immense complexity. As one may expect from the words, this study involves objects, e.g. images, which look rough and contain intricate complexity. The word "fractal" was first introduced by Mandelbrot and it originates from the Latin adjective fractus, which means broken [Mand82].

In order to provide a better understanding of the concept, two well-known fractals, the Koch curve (Fig. 4.1) and Sierpinski carpet (Fig. 4.2) are shown below. For each of

these two objects, the first few steps taken to generate the final object are also shown. It is interesting to see that each of these fractals are generated by repeating a simple procedure on an initially plain object (a line segment for the Koch curve and a square for the Sierpinski carpet); however, the resulting image that starts to appear after a few iterations demonstrates significant complexity as well as visual appeal. It is also very important to see that the images all share similar components that can be observed at various scales.

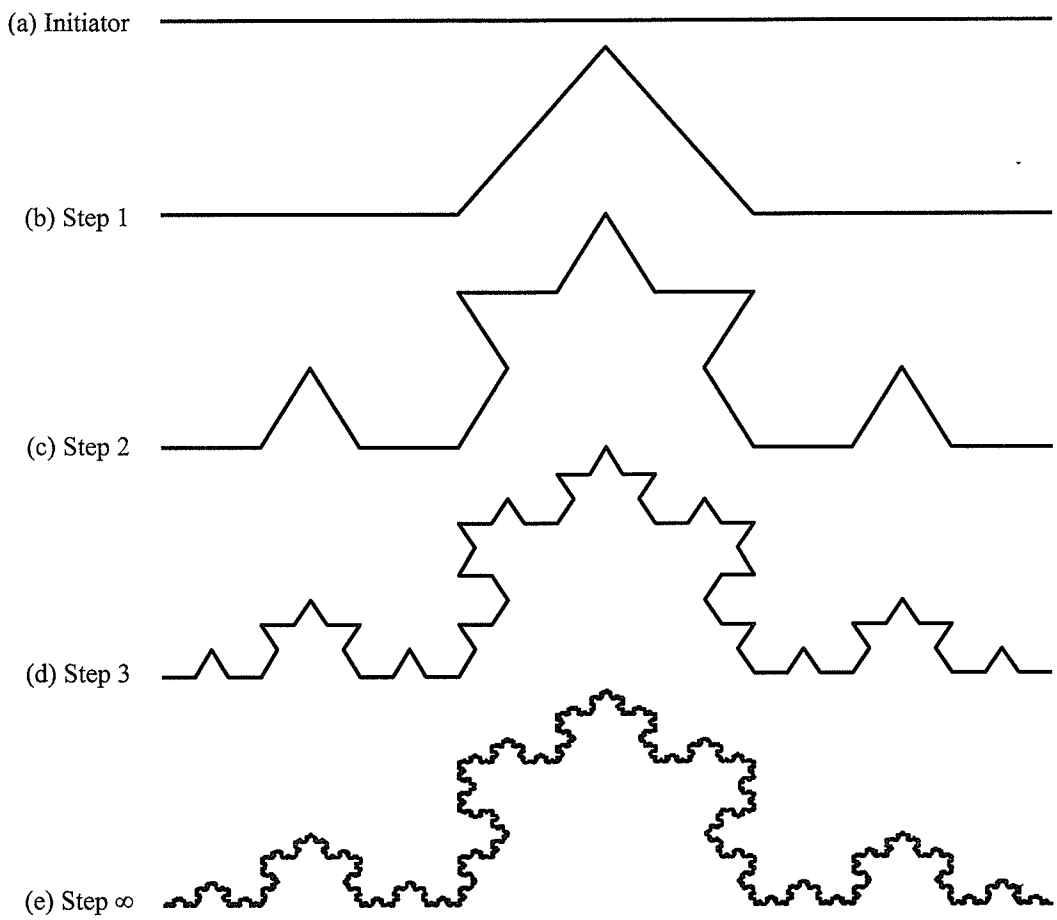


**Fig. 4.1** Koch curve fractal. (After [PeJS92])

Visual inspection of these two objects reveals that the fractals are self affine; i.e., part of the object is related to the whole through the property of scaling; this is fundamental to the understanding of the fractals.

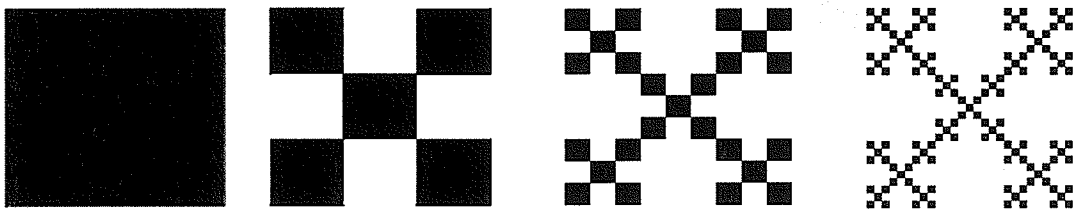

(a) Initiator (b) Step 1 (c) Step 2 (d) Step 3

**Fig. 4.2** Sierpinski carpet fractal. (After [Kins95])

It is noted that the final objects has details (singularity and transition) and as such the Euclidian, Riemannian, and Lobachevskiy geometries fail to describe the objects properly. One can define a fractal as a subset in $\Re^n$, which is self-similar and whose fractal dimension exceeds its topological dimension [Kins95].

Further analysis of fractals leads to the notion of fractal dimensions, which are non-integer values (contrary to the common Euclidian dimensions). In broad terms, a fractal dimension is a measure of roughness or irregularity of the object. Intuitively, the concept of fractal dimension is derived from the self-similarity property (power law) [Kins94a].

It is interesting to note that fractals have a profound existence in the nature and are not limited only to mathematical ones, such as the two examples given above. Mathematical fractals usually can be generated using relatively simple mathematical procedures. The overall procedure has two components, namely the initiator and the generator. In case of the Koch curve, the initiator is the straight line segment shown in

Fig. 4.1(a). To move on to the next stage, the line segment is divided into three equal line segments and the middle one is replaced with two line segments of equal length (and equal to the length of the removed segment) that meet at a 60° angle. Note that each of the line segments in the object in stage 2 has the same length (1/3 of the length of the original line). The objects in the following stages are obtained by performing the same procedure on each of the line segments. The resulting objects can become increasingly complicated, but careful analysis reveals profound similarity, simplicity and beauty within the object.

Another example of a mathematically generated fractal, the 2-dimensional (2D) Mandelbrot set, is shown in Fig. 4.3. The object has intricate details, but it could be generated using a simple mathematical procedure.

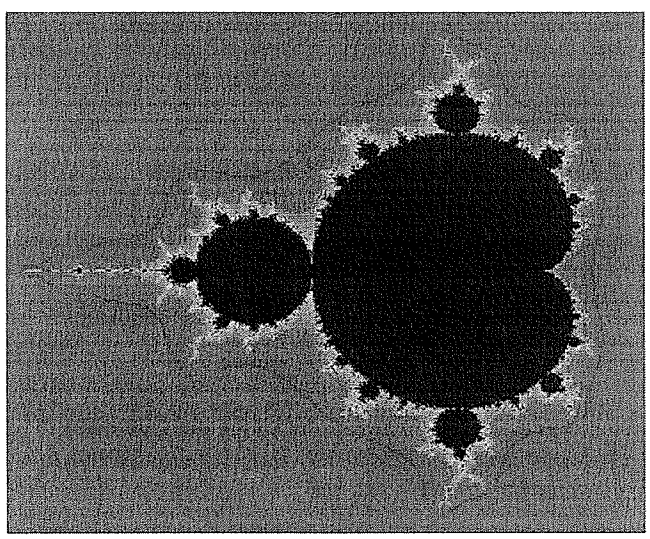

**Fig. 4.3** Mandelbrot set. (From Technical University of Athens)

Fractals also exist in nature, but are much more complicated in their design and description. In other words, while mathematical fractals, such as the Mandelbrot set, can be generated using an initiator and an iterative process, natural fractals are far more

complex and can be described hardly using such mathematics. As an example of a natural fractal, Fig. 4.4 shows a picture of an electric discharge in a lightning. As shown, the object has a very complex form that possesses the fundamental properties observed in mathematical fractal; i.e., parts of the object show similar pattern to those observed in whole. For example, the tiny portions that branch out form the main branches, still show similar patterns to those of the larger ones. Naturally, it is expected that the Euclidian geometry should fail to provide an accurate description of such an object.

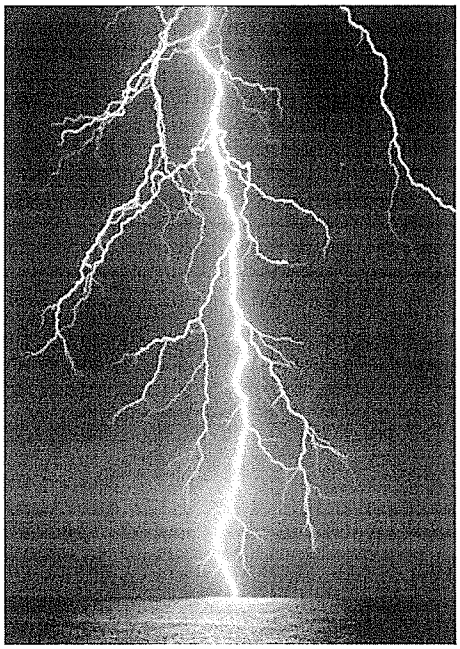

**Fig. 4.4** Electric discharge in a lightning. (From www.flatrock.org.nz)

## 4.3 Fractal Dimensions

Fractals have a ubiquitous presence and as such it is important to be able to study them quantitatively, so that their description and comparison becomes possible. As stated before, fractal dimension is an approach for measuring the roughness or irregularity of such objects. The fractal dimension has its roots in the similarity that exists in a fractal at

different scales, and hence has strong connections with the power law relationship. For some fractals, a single fractal dimension is adequate to describe them, while more complex objects may require more than one fractal dimension.

Generally, fractal dimensions may be classified into the following four categories [Kins94a]:

- Morphological-based dimensions, which are based on geometrical properties of the object under consideration and are used if the distribution of a measure (such as probability) is uniform or the information about the distribution is not available [Kins94a];

- Entropy-based dimensions, which take into account a measure of a fractal and therefore deal with inhomogeneous fractals;

- Spectrum-based dimensions, which are based on the fact that the power spectrum or power spectrum density of a signal reveals a power-law relation with frequency, in which the exponent characterizes the persistence or antipersistence of the corresponding fractal object; and

- Variance-based dimensions, (see below for details).

Our focus throughout the rest of this chapter will be on a particular variance-based dimension, namely the variance fractal dimension, which will be shown to be an efficient method for characterizing waveforms with transients such as power system transients.

## 4.4 Variance Fractal Dimension

Analysis of a time series is possible directly in real time by analyzing the spread of the increments in the signal amplitude (variance, $\sigma^2$) [Kins94b]. This approach has its roots in the work done by Mandelbrot and Van Ness [MaVa68]; however, the approach presented in this thesis is based on the work developed by Kinsner [Kins94a].

Let us assume that the signal $x(t)$ is either continuous or discrete in time $t$. The variance $\sigma^2$ of its amplitude increments over a small time increment is related to the time increment according to the following power law

$$\mathrm{Var}[x(t_2) - x(t_1)] \sim |t_2 - t_1|^{2H} \tag{4.1}$$

where Var is the variance operator, and $H$ is the Hurst exponent. By setting $\Delta t = |t_2 - t_1|$, and $(\Delta x)_{\Delta t} = x(t_2) - x(t_1)$, the exponent $H$ can be calculated from

$$2H \log(\Delta t) \sim \log[\mathrm{Var}(\Delta x)_{\Delta t}] \tag{4.2}$$

which $H$ is ½ times the slope of the best fitted line that passes through the points $\log[\mathrm{Var}(\Delta x)_{\Delta t}]$ versus $\log(\Delta t)$, for small values of $\Delta t$. Finally, for embedding Euclidean dimension $E$, the variance dimension can be computed from

$$D_\sigma = E + 1 - H \tag{4.3}$$

In practice, the limit of Eq. 4.2 shown above translates into the slope of a log-log plot with a finite number of time increments. The sequence is usually chosen to be b-adic. For this case, the following formula will hold

$$X_k = \log_b(\Delta t_k)$$
$$Y_k = \log_b(\mathrm{Var}(\Delta x_k)) \tag{4.4}$$

where $k$ is in the range $[k_1,k_2]$. Within the range where power-law relation holds, the slope of the line polynomial whose curve passes through these points is given by

$$s = \frac{(k_2 - k_1)\sum_{i=k_1}^{k_2} X_i Y_i - \sum_{i=k_1}^{k_2} X_i \sum_{i=k_1}^{k_2} Y_i}{(k_2 - k_1)\sum_{i=k_1}^{k_2} X_i^2 - (\sum_{i=k_1}^{k_2} X_i)^2} \tag{4.5}$$

The Hurst exponent $H$ is obtained by

$$H = s/2 \tag{4.6}$$

A useful property of the variance fractal dimension approach is that the result is bounded automatically between 1 (dimension of a straight line) and 2 (dimension of white noise). This is a very appealing feature that can be of importance when such results are used for the purpose of classification as it often requires input data to belong to bounded intervals.

## 4.5 Variance Fractal Dimension Trajectory

Often times there are objects that contain more than a single fractal and are characterized by having a spatial or temporal combination of a number of fractals. Such objects are called multifractals. An extension of the previously discussed variance fractal dimension is used for the characterization of signals with multifractality.

In this method, a window over which the fractal dimension is calculated is shifted along the signals [Kins94b]. Usually the windows are selected to have some overlap. By

calculating the fractal dimension of the portion of the signal within a window, the resulting *variance fractal dimension trajectory* (VFDT) will have smaller samples points, resulting in a significant reduction in the number of characterizing features [Kins94b]. Decision on the width of the sliding window and the overlap between successive windows is very important and will be discussed in detail in Ch. 6, where the system design is presented.

For signals with a single fractal nature, the VFDT approach results in a single value for all the windows; however, for signals with transients, such as the ones considered in this thesis, the variance fractal dimension approach will result in a sequence of dimensions that assumes different values, thus providing an indication of the onset and type of the transient. This is because the presence of transients, which are mostly much more complicated than the signal itself, introduces short-term changes in the complexity of the signal and as such the variance fractal dimension attains a different value during the transient portion. Such sequence is rightfully called the variance fractal dimension trajectory or VFDT.

As an example of how the VFDT actually characterizes a signal, Fig. 4.5 shows a waveform with a transient along with its VFDT. The original sine wave is disturbed by the presence of a short-term transient occurred between [0.29,0.33] sec (approximately). The variance fractal dimension trajectory of the signal shows a relatively constant value before and after the transient period, which corresponds to the fractal dimension of the original undisturbed waveform. During the transient period however, the fractal dimension calculated changes significantly, which is an indication of subtle variation in

the complexity of the signal. The resulting VFDT is automatically scaled between 1 and 2 and has by far less samples than the original waveform.

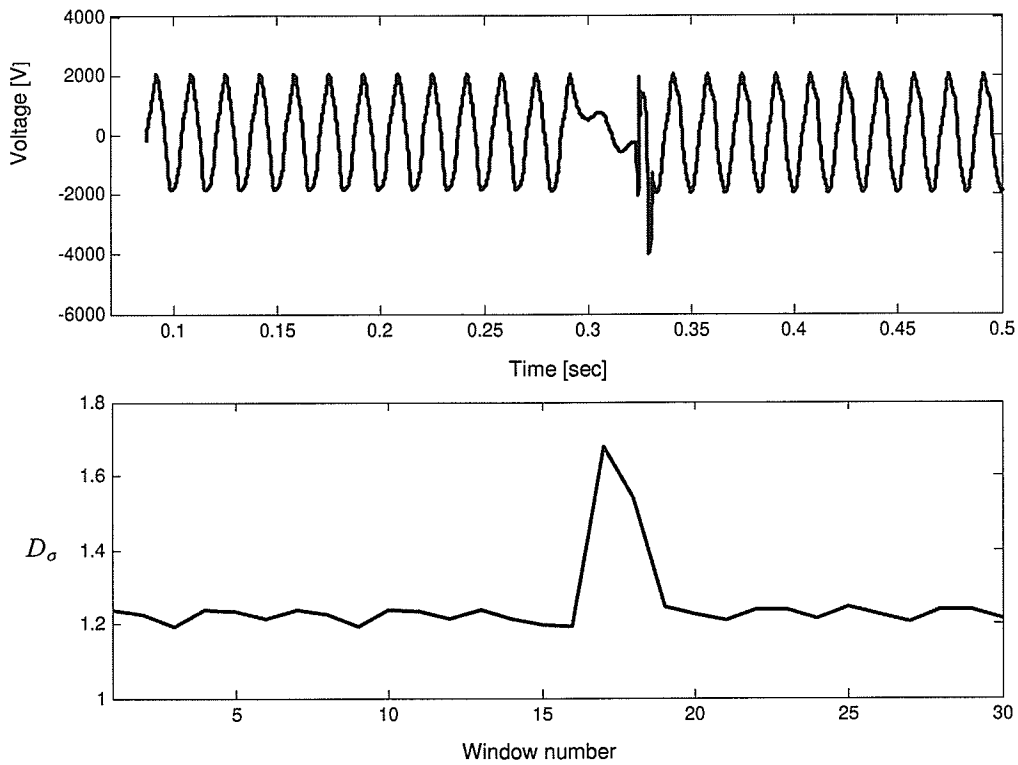


**Fig. 4.5** VFDT analysis of a transient.
(a) Original waveform; (b) VFDT.

## 4.6 Chapter Summary

An efficient approach for the analysis and characterization of complex signals, e.g. signals with non-stationarities, is based on using the notion of fractals and fractal dimensions. It was shown that variance fractal dimensions are suitable measures for describing signals with transients and they reveal important underlying properties of the signals.

In particular, the VFDT approach was described and it was shown that the method lends itself to a fairly straight forward implementation that proves to be useful for real-time applications. The VFDT approach involves calculating the variance-based fractal dimension of the signal in a number of overlapping windows along the signal and results in a trajectory of fractal dimensions that track the changes that occur in the signal as the time progresses. A trajectory so obtained (i) has significantly less number of samples (high compression ratio) and (ii) contains important properties of the original signal that can be used efficiently in a well-designed classifier.

Classification of transients becomes possible once their features are extracted using the method presented in this and the previous chapter. In the next chapter, essentials of the pattern classification are presented.

# CHAPTER V

# PATTERN RECOGNITION AND CLASSIFICATION OF TRANSIENTS

## 5.1 Introduction

Analysis of transients using the techniques mentioned in the previous chapters provides means for characterizing them using a number of properties, also commonly referred to as features, which could be used to distinguish between various transients.

The task of determining the class of an object based on its features is called classification and the procedures that perform such tasks are called classifiers [DuHS01]. Depending on the objectives of the study, the 'class' of an object is defined. For example, in classifying transients in power systems, the classes may be labeled as 'faults', 'breaking operation, 'capacitor switching', and so on. Classification of transients involves their analysis, extraction of features and determination of their true cause (whether they have been caused by faults, breakers operations, capacitor switchings, etc.).

Consider a classification problem with $C$ classes. An input sample, whose class is to be determined, is characterized by $n$ number of features. Each feature can be considered to represent part of the characteristics of an object; for example the length, color, or weight can be the features used to describe a given object. In the study of transients in power systems, features can be extracted from signals using the results of wavelets and multifractal analyses. The task of the classifier is to assign the input sample, using its $n$ features, to one of the $C$ existing classes. Therefore, the classifier is a system with $n$

inputs and $C$ outputs, which uses the statistical properties of the input samples to assign them to one of the classes considered.

## 5.2 Statistical Foundations of Classification

Classification deals with the probability theory. The underlying idea in pattern classification is expressed by the Byes rule given below [DuHS01]

$$P(\omega_i \mid \mathbf{x}) = \frac{g(\mathbf{x} \mid \omega_i)P(\omega_i)}{g(\mathbf{x})}$$
$$g(\mathbf{x}) = \sum_{i=1}^{C} g(\mathbf{x} \mid \omega_i)P(\omega_i) \tag{5.1}$$

where $\omega_i$, $g(\mathbf{x} \mid \omega_i)$ and $P(\omega_i)$ are the class $i$, class-conditional probability density function (pdf) of $\mathbf{x}$ in class $i$, and the prior probability of class $i$, respectively, and $C$ is the number of classes. $P(\omega_i \mid \mathbf{x})$ is the posterior probability of class $i$, given the input vector (input sample) $\mathbf{x}$. It is worth discussing the Bayes rule a little further, as it forms the basis for other classification techniques.

The prior probabilities $P(\omega_i)$ simply, and roughly, determine the likelihood of occurrence of their respective classes. For example in a 2-class problem, where either of the two classes is equally likely to happen, the prior probabilities $P(\omega_1)$ and $P(\omega_2)$ are both equal to ½. It becomes apparent readily that prior probabilities are simply a digest of the past history of the events in a given system, and do not depend on the observations made on the current sample. The Bayes rule uses the extra information available in $\mathbf{x}$ to come up with a better estimation of the actual class of a given input than the prior probabilities. In fact the underlying idea is to improve the estimation provided by the

prior probabilities by incorporating the observations contained in the features. This is carried out by evaluating the probability density function of each class for the input sample presented. An input sample that has more resemblance to a specific class, produces a larger $g(\mathbf{x} \mid \omega_i)$ for that class, and as such results in a larger numerator in (5.1). It is instructive to demonstrate the procedure on a 2-class problem with a single feature. Figure 5.1 shows the pdfs of the feature $x$ in each of the two classes A and B. An input sample, with a feature value equal to $x^*$ has much more likelihood of belonging to class A than class B. With equal prior probabilities for both classes, the input sample will be assigned to class A.

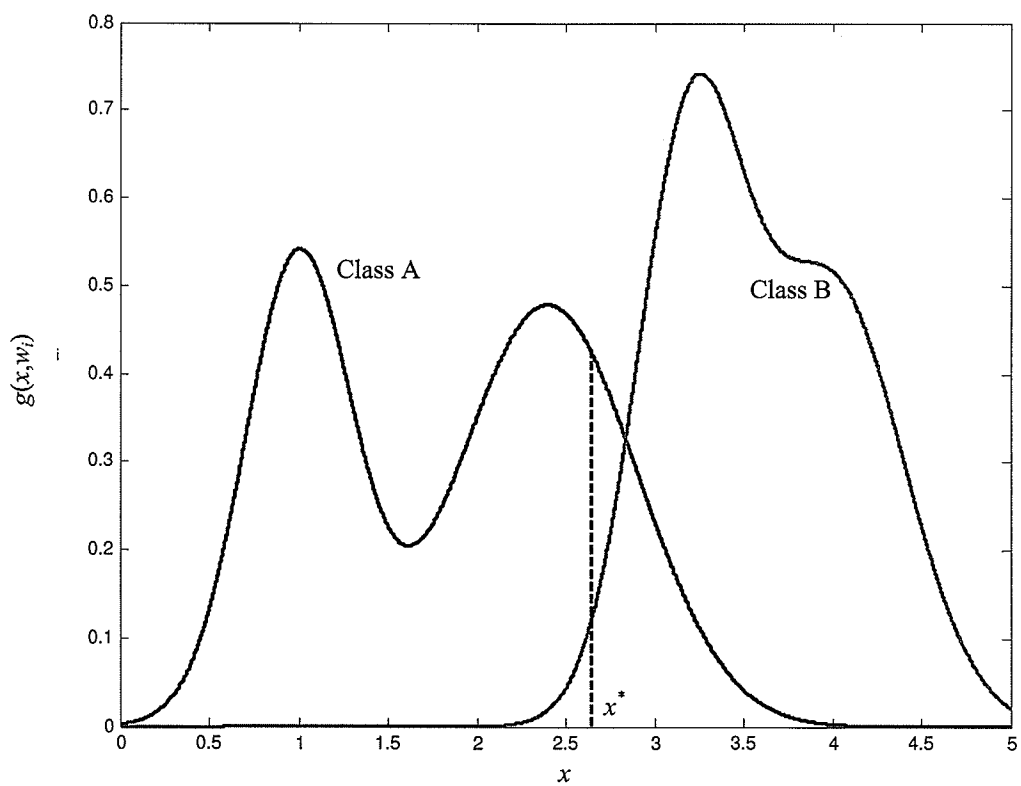


**Fig. 5.1** Decision-making in a two-class problem.

Since the denominator in (5.1) is the same for all classes, the decision-making process using the Bayes rule could be simplified as follows

Decide $\omega_i$ if

$$g(\mathbf{x} \mid \omega_i)P(\omega_i) > g(\mathbf{x} \mid \omega_j)P(\omega_j) \quad \forall i, i \neq j \tag{5.2}$$

Under circumstances where the classes are equally likely, the prior probabilities $P(\omega_i)$ could also be dropped. The Bayes rule is the most accurate method of determining the class of a given input (represented by the features contained in $\mathbf{x}$); however, in many cases, the class-conditional pdfs required in (5.2) are not available. Therefore, the Bayes rule can be applied only when either the pdfs are known explicitly or they can be estimated accurately.

In the following sections of this chapter, three classification methods will be discussed, namely the Bayes rule using the maximum-likelihood (ML), the nearest neighbor classifier ($k$-NN) and the Probabilistic Neural Networks (PNN). It will be shown that PNN and ML based methods, despite their visual differences, share roots in estimating the pdfs and using the Bayes rule.

## 5.3 The Method of Maximum-Likelihood (ML)

The method of *maximum-likelihood* (ML) is based on finding the parameters of a pdf with a given structure so that it best matches the true pdf (unknown) of the samples available. The pdfs estimated using the method of ML could be used in the Bayes rule. Note that

(i) the procedure requires a sufficiently large number of samples with known classes so that they can be used for determining the parameters of the pdf of each class. These samples are referred to as the training set; and

(ii) the method of ML assumes a given form for the pdfs, e.g. Gaussian, Poisson, and only determines the parameters of the given pdf.

If the training samples belonging to a specific class are $\{\mathbf{x}_1, \mathbf{x}_2, \cdots, \mathbf{x}_N\}$, the parameter set $\boldsymbol{\theta}$ of a pdf $g(\mathbf{x}, \boldsymbol{\theta})$ are estimated such that the following product is maximized

$$L(\boldsymbol{\theta}) = \prod_{i=1}^{N} g(\mathbf{x}_i, \boldsymbol{\theta}) \tag{5.3}$$

The rationale behind maximizing the function above is that a correctly identified pdf will generate higher values when samples of its respective class are presented to it. Therefore, by maximizing the function in Eq. 5.3, a suitable set of parameters for that class will be obtained. Since the form of the pdfs are assumed to be known, the problem is reduced to an ordinary maximization problem and can be solved using an optimization method. Further details about this method can be found in [DuHS01].

In many cases, the pdfs to be estimated are found to be mixtures of some underlying pdfs. For example, each of the pdfs shown in Fig. 5.1 are in fact combinations of two Gaussian pdfs. A typical 'mixture model' can be expressed as follows

$$G(\mathbf{x}) = \sum_{i=1}^{M} \pi_i g(\mathbf{x}, \boldsymbol{\theta}_i) \tag{5.4}$$

where $g(\mathbf{x}, \boldsymbol{\theta}_i)$ are the constituent pdfs, $\pi_i$ are the mixing factors and $M$ is the number of constituent models . The estimation of the parameters of such a mixture model (again with assumed forms for the underlying pdfs) involves determination of individual pdf

parameters ($\theta_i$) as well as the mixing factors. A similar optimization approach can be adopted for such cases as well [FiJa02].

## 5.4 The Nearest Neighbor Classifier (*k*-NN)

The *nearest neighbor classifier* (*k*-NN) is a simple, yet effective, classification method. Similar to the ML, this method is based on using a given number of training samples; however, unlike the previous method, where the training samples belonging to a certain class are treated as constituents of an overall pdf, the *k*-NN classifier treats them as individuals. In other words, while the training samples in an ML-based classifier do contribute to an overall pdf, which replaces the individual members, the *k*-NN relies on the individual samples directly in the decision-making process [DuHS01].

In simple terms, the *k*-NN classifier determines the class of a given sample by calculating its distance (using an appropriate measure) from its *k* closest neighbors in the training set. In a two-class problem, a 1-NN classifier will assign the input sample to the same class as that of the nearest neighbor.

Figure 5.2 shows a schematic diagram of a two-class problem (classes are denoted by circles and crosses). The input sample shown as X will be assigned to the class of crosses as its nearest neighbor belongs to that class (the Euclidian distance is used). The line segments shown on the graph represent the boundaries of an area around each sample, where a given input sample finds the enclosed point as its nearest neighbor.

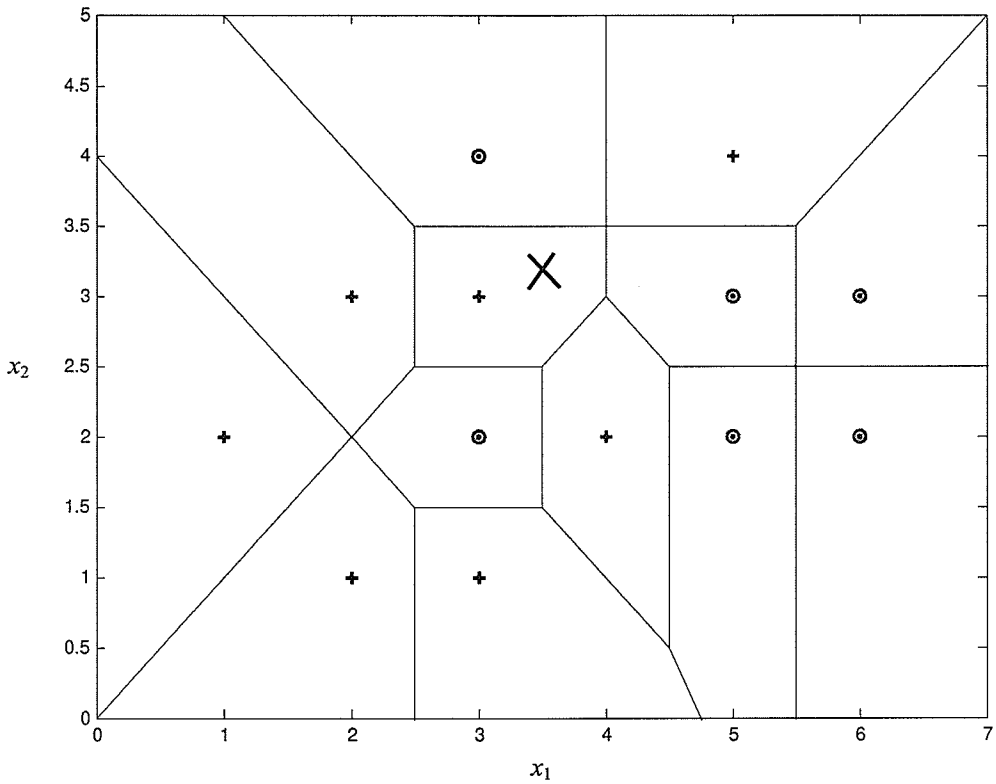


**Fig. 5.2** The nearest neighbor classification method.

It is evident that the 1-NN classifier gives any of the training set samples the possibility to determine the class of an unknown sample. The individual emphasis of the 1-NN classifier versus the cumulative approach of the ML-based methods is an important property that deserves careful attention.

To lower the significant impact of individual training samples on the outcome of the classifier, it is possible to include more than one neighbor in the decision-making process. For example in a two-class problem, it is possible to use a $k$-NN approach (with an odd $k$, to prevent ties). Under such cases, the winning class is the one that contains the majority of the $k$ nearest neighbors of the unknown sample. The $k$-NN ($k \neq 1$) classifier is a movement towards incorporating more than one training sample in the process of

decision making. Although more computationally demanding, a *k*-NN classifier does take into consideration the clusters of data that can be observed normally in many classification problems and lowers the impact of out-of-cluster samples in the final result.

One major benefit of the *k*-NN classifiers is the simplicity of implementation. The classifier requires no 'training' as the task of classification is done simply by calculating the distance, for example by the Euclidian distance, between the input sample and the training samples. This property makes the *k*-NN classifier a prime choice when the number of training samples is not sufficient to train other classifiers.

## 5.5 The Probabilistic Neural Networks (PNN)

The *probabilistic neural networks* (PNN) are classifiers that implement the Bayes rule; however, their training methodology is different from the ML-based approach described earlier.

It was mentioned that classification using the Bayes rule requires the pdfs of individual classes. The PNN is a mathematical representation of the Bayes rule and is trained so that the pdfs are obtained optimally.

Before proceeding to the concept of a PNN and its training procedure, a useful method of estimating a pdf, namely the Parzen method is presented.

### 5.5.1 Estimating a PDF Using the Parzen Method

A popular method for estimating a pdf was introduced by Parzen [Parz62]. According to this method, which is demonstrated first for a single-variable case, for a given class *k*

with $n_k$ training samples given by $x_r, r \in \{1,2,...,n_k\}$, the pdf can be estimated using the following expression

$$g_k(x) = \frac{1}{n_k \sigma} \sum_{r=1}^{n_k} W(\frac{x - x_r}{\sigma}) \tag{5.5}$$

where $g_k(x)$ is the estimated pdf, $\sigma$ is a scaling factor and $W(x)$ is a window function that satisfies the following conditions

1. $W(0) > W(x)\ \forall x$, and
2. $W(\pm\infty)$ approaches zero.

Note that for a given $x$, the pdf $g_k(x)$ first calculates the distance between this point and every one of the points of the training set. The distances are then normalized by $\sigma$ and passes through the window function $W$. For an input $x$ lying in close proximity to other training sample a large $g_k(x)$ will be obtained (according to condition 1 above); an input $x$ lying far from other data points (which is less likely to belong to class $k$) will have a small pdf evolution (see condition 2 above).

A good candidate for a window function is the Gaussian function given by

$$W(x) = \frac{1}{\sqrt{2\pi}} \exp(\frac{-x^2}{2}) \tag{5.6}$$

Note that the parameter $\sigma$ determines effectively the width of the window function used. In other words, larger values of $\sigma$ allow farther points to still contribute effectively to the

overall pdf. It is also worth noting that the use of a Gaussian window function is completely arbitrary and is not a necessary condition.

In multivariable cases, where the input sample has $p$ features, the estimation is expressed as follows

$$g_k(\mathbf{x}) = \frac{1}{n_k \sigma_1 \sigma_2 \cdots \sigma_p} \sum_{r=1}^{n_k} W\left(\frac{x_1 - x_{r,1}}{\sigma_1}, \frac{x_2 - x_{r,2}}{\sigma_2}, \cdots, \frac{x_1 - x_{r,p}}{\sigma_p}\right) \tag{5.7}$$

where $\mathbf{x} = (x_1, x_2, \cdots, x_p)$ is the input sample, and $\mathbf{x}_r = (x_{r,1}, x_{r,2}, \cdots, x_{r,p})$ is the $r$th sample in the training set.

The multivariable function $W$ can be assumed to have the following form

$$W(x_1, x_2, \cdots, x_p) = \prod_{i=1}^{p} W_i(x_i) \tag{5.8}$$

and with the choice of $W_i(x_i)$ to be as in (5.6), the expression for $p_k(\mathbf{x})$ will be as follows

$$g_k(\mathbf{x}) = \frac{1}{n_k \sigma_1 \sigma_2 \cdots \sigma_p} \sum_{r=1}^{n_k} \frac{1}{(\sqrt{2\pi})^p} \exp\left(-\sum_{i=1}^{p} \frac{(x_i - x_{r,i})^2}{2\sigma_i^2}\right) \tag{5.9}$$

which is simplified to

$$g_k(\mathbf{x}) = \frac{1}{n_k (\sigma_1 \sigma_2 \cdots \sigma_p)(\sqrt{2\pi})^p} \sum_{r=1}^{n_k} \exp\left(-\sum_{i=1}^{p} \frac{(x_i - x_{r,i})^2}{2\sigma_i^2}\right) \tag{5.10}$$

The problem of estimating the pdf, therefore, reduces to an optimal estimation of the $\sigma_i$ in (5.10).

In simple cases, the $\sigma_i$ parameters are sometimes assumed to equal; i.e., $\sigma_1 = \sigma_1 = \cdots = \sigma_p = \sigma$. The original PNN architecture used this simplified assumption; however, this is a limiting condition and poses a single spread on all the features. Improved PNNs use multiple spread parameters for the feature vector resulting in a better estimation of the underlying pdf [Mast95].

Choice of suitable values for the spread parameter(s) is an important task and has a profound impact on the performance of the classifier obtained using the estimated pdfs. To illustrate this, consider the training set shown in the *x-y* plane in Fig. 5.2(a). Note that the training set essentially consists of two clusters each with 4 points. The estimation of the pdf is shown for three sets of $[\sigma_x, \sigma_y]$ values. The estimation in Fig. 5.2(b) is for $[\sigma_x, \sigma_y]$=[0.2, 0.2] and it is evident that the narrow width of the window function has results in separation of the sample points and therefore the resulting pdf pertains to a *k*-NN classifier. This is because with a small window width, only the points that lie very close to a data point will be contributing to the total pdf evaluation, resulting in a loss of clusters in the overall pdf. The estimation with very large values of [2.2, 2.2] in Fig. 5.2(c) shows excessive smoothness in the estimated pdf. In other words, the pdf estimated using such large values suppresses the fact that the data effectively exists in two clusters (see Fig. 5.3(a)) and allows very far points to contribute almost equally as the points in a cluster. The estimation with well-selected values for $[\sigma_x, \sigma_y]$=[0.7, 0.7], as shown in Fig. 5.3(d), results in a pdf with adequate smoothness around each of the two clusters. Note that proper selection of the window widths, not only separates the clusters, but also identifies the cumulative impact training set samples within each cluster.

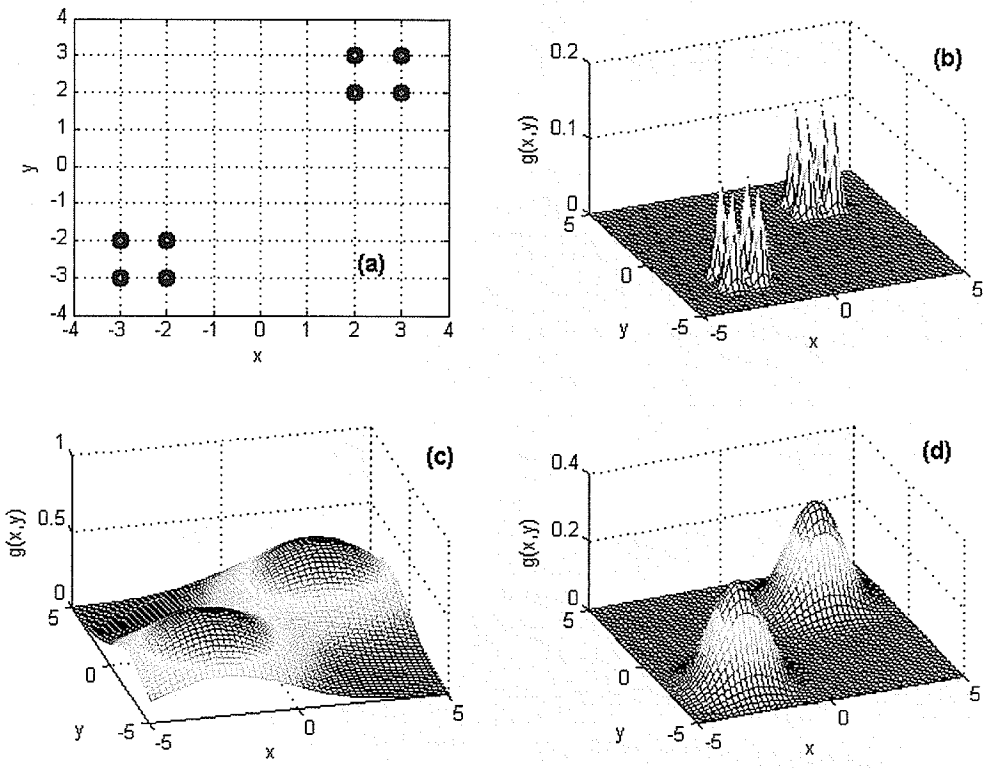


**Fig. 5.3** Effect of window width on Parzen pdf estimation.

## 5.5.2 The PNN Architecture

The PNN is essentially an implementation of the Bayes decision-making rule; however, it is possible to represent the overall procedure in the form of a multi-layer neural network as well [Spec88]. The PNN consists of 4 layer, namely the 'Input Layer', the 'Pattern layer', the 'Summation Layer', and the 'Output Layer'. These four layers are shown in Fig. 5.4 and their function is described in the following [Spec99].

The input layer consists of $p$ nodes corresponding to the number of features used. Therefore, when an input sample $\mathbf{x} = (x_1, x_2, \cdots, x_p)$ is presented to the network, each one of its components are assigned to its corresponding node in the input layer.

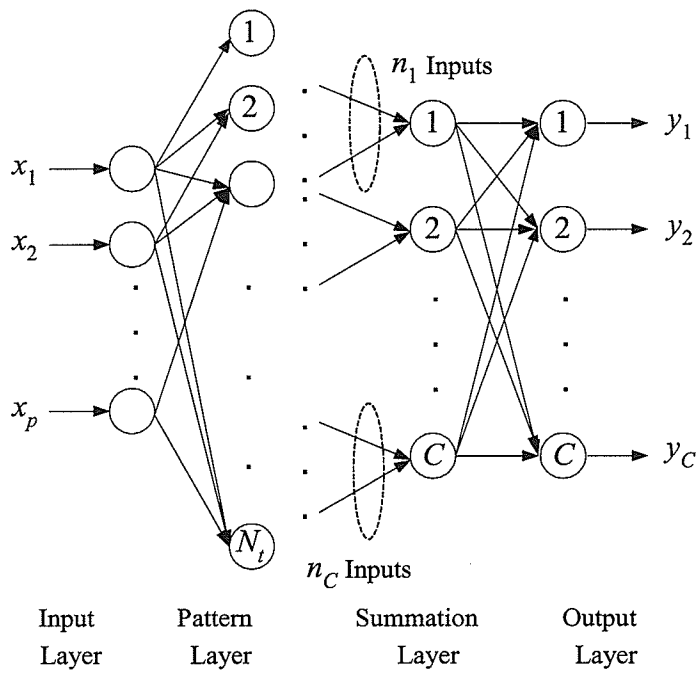


**Fig. 5.4** Structure of a PNN.

The pattern layer contains as many neurons as the number of training samples. If the number of training samples for class $k$ are denoted by $n_k$, and the total number of classes is denoted by $C$, the following expression holds

$$\sum_{i=1}^{C} n_i = N_t \tag{5.11}$$

where $N_t$ is the total number of training samples. Therefore the pattern layer of a PNN has $N_t$ neurons.

Each neuron in the pattern layer has two major functions. Firstly, it calculates the squared Euclidian distance between the input sample and its respective training sample and then passes the scaled result through the nonlinear window function according to

(5.9). The function of the pattern layer is therefore to calculate the expression $\exp(-\sum_{i=1}^{p}\frac{(x_i - x_{r,i})^2}{2\sigma_i^2})$ for each of the training set samples.

The summation layer has as many neurons as the number of classes, $C$. Each neuron receives its inputs from those neurons in the pattern layer that contain training samples belonging to that specific class. For example, the neuron number 2 in the summation layer receives $n_2$ inputs stemming from those neurons in the pattern layer that contain the $n_2$ samples belonging to class 2.

The output of the summation layer is the pdf evaluation of each class for the input sample. According to the Bayes rule, the input sample should be assigned to the class whose pdf evaluation (multiplied by the prior probability) is larger than the rest. The output layer is simply a decision-making engine with $C$ outputs. The output values $y_i$ are determined according to the following rule (assuming equal prior probabilities)

$$y_i = \begin{cases} 1 & \text{if } g_i(\mathbf{x}) > g_j(\mathbf{x})\ \forall j, j \neq i \\ 0 & \text{otherwise} \end{cases} \tag{5.12}$$

It is worth noting again that the architecture used for a PNN is simply an implementation of the Bayes rule with an embedded pdf estimation using the Parzen method.

### 5.5.3 Training of a PNN

Training of a PNN involves determination of the window-width parameters $\sigma_i$ optimally. Once a PNN is trained (its window widths estimated), it can be used as a classifier that essentially applies the Bayes rule. Essentially this is an optimization task

and therefore requires an objective function, whose minimization results in the optimal set of $\sigma_i$ parameters.

Suppose that an input sample **x** belonging to class $k$ is presented to the PNN; the $C$ outputs of the summation are indications of the pdf evaluations for their respective classes. In order to assess the relative significance of these evaluations, we use the following formula

$$q_i = \frac{u_i}{\sum_{j=1}^{C} u_j} \tag{5.13}$$

where $u_i$ is the output of the $i$th neuron in the summation layer. Note the under ideal circumstances, presentation of the sample described above (belonging to class $k$) should result in

$$q_k = 1 \text{ and } q_j = 0, j \neq k \tag{5.14}$$

With non-optimal $\sigma_i$ parameters, the $q_i$ values deviate from these ideal values. Such deviations can be used to form a suitable objective function whose minimization reduces the deviation of $q_i$ values thus yielding optimal $\sigma_i$. For a set of poorly selected $\sigma_i$ the deviation becomes larger, as the node corresponding to the true class of the input sample fails to produce a pdf evaluation significantly larger than the rest.

The objective function should include all of deviations for every sample in the training set. Therefore, for each sample **x** belonging to class $k$, a partial objective function is defined as follows

$$e(\mathbf{x}_i) = (1-q_k)^2 + \sum_{\substack{j=1 \\ j\neq k}}^{C} q_j^{\,2} \tag{5.15}$$

Note that for an $\sigma_i$ optimal set of parameters, the partial objective function of (5.15) will become very small (the absolutely lowest value for the expression in Eq. 5.15 is zero, which is obtained when $q_k = 1$ and $q_j = 0, j \neq k$), while non-optimal values for $\sigma_i$ result in large deviations and hence large $e(\mathbf{x}_i)$ values. The overall objective function, used for the minimization problem, is defined as follows

$$OF = \sum_{i=1}^{N_t} e(\mathbf{x}_i) \tag{5.16}$$

Optimization of the above objective function can be done using a nonlinear optimization algorithm, such as gradient-based optimization algorithms [Mast95].

There is a fundamental difference between the ML-based approach and the PNN in the way the pdfs are estimated. The ML-based approach estimates a pdf using only the samples belonging to that class. Also the parameters used in the pdf of a given class are independent of the parameters used in other pdfs. The PNN however, takes a unified approach and uses the same set of $\sigma_i$ parameters in all of the classes; the optimization setup is also comprehensive of all classes in that it aims at maximizing the contribution of the true class on each training sample and minimizing the contribution of other classes. The training complexity of the PNN is therefore, usually higher than the ML-based Bayes rule. Further details about the computational intensity of the three algorithms will be presented in the following chapters.

## 5.6 Chapter Summary

This chapter dealt with the methods that can be used for classification of various objects including transients in power systems. It was shown that the Bayes rule, which is the foundation of classification methods, requires such information as the class-conditional pdfs that are not available in most cases and as such methods are developed to estimate such pdfs.

Three classification methods, namely the Bayes rule using maximum-likelihood, the *k*-NN and the PNNs were discussed in detail. It was shown that these methods, despite their differences, are essentially estimations of the Bayes rule in the absence of readily available pdfs.

The Parzen method for estimating pdfs was introduced and it was shown that the PNN is an implementation of the Bayes rule with Parzen pdf estimation expressed in the frame of a neural network. An optimization objective function for the estimation of the parameters of a PNN was also developed.

The following chapter uses the mathematical foundation laid in the preceding chapters in the design of a comprehensive transient classification system. Design specifications and implementation are also presented.

# CHAPTER VI

# SYSTEM DESIGN AND IMPLEMENTATION

## 6.1 Introduction

The material presented in the previous chapters form the mathematical foundation of a system used for extraction of features from transients in a power system and their classification using the extracted features. In this chapter, details of the design of such a system will be presented. The chapter will also address the implementation procedures including the tools and techniques used for doing so.

This chapter is divided into three major sections, namely generation of samples of transients using simulation, feature extraction using VFDT and wavelet analyses, and implementation of classification methods.

## 6.2 Simulation of Transients in a Power System

As mentioned in Ch. 2, transients in a power system occur due to a large number of planned and unplanned causes, and they disturb the performance of a power system. Once a transient occurs, it disturbs the originally sinusoidal voltage and current waveforms by introducing various frequencies into the waveforms. Transients cover a wide frequency band ranging from a few Hertz (Hz) to several megahertz (MHz) and also tend to persist from a few microseconds (μs), e.g., switching transients, to several minutes, e.g., voltage instability, depending on their nature. The focus throughout this thesis is mainly on transients that can be categorized as short-term and mid-term

transients, which usually have frequency content in the order of kilohertz (kHz) and last for a few cycles of the power frequency.

Simulation of such transients involves precise modeling of the underlying electric network and solution of the resulting equations. In order to do so, it is possible to either use dedicated circuit simulation tools or develop a simulation program from scratch. Needless to say, the latter option requires not only much work, but also deep knowledge of and expertise in power systems that are beyond the scope of this project. Therefore, in this thesis simulation of transients in a power system has been tackled using a commercially available electromagnetic transient simulation program, namely the PSCAD/EMTDC® [EMTD03].

### 6.2.1 PSCAD/EMTDC® Transient Simulation Program

PSCAD/EMTDC is a time-domain electromagnetic transient simulation program developed by the Manitoba HVDC Research Center with close collaboration with the University of Manitoba. The program provides a fully interactive user interface and access to a library of various components used in electrical power systems. The user can select the desired components from the Master Library and place them on a draft page and make necessary connections between them. Upon completion of the circuit construction, the user can simulate the circuit and visually examine the results through graphs that can be generated as the simulation progresses.

The program also provides the user with the option of designing their specific custom components that are not available through the Master Library. Such a task is made possible through the Component Workshop, and is done by coding the function of the

new component in FORTRAN. Integration of the new component into the rest of the simulation case is done seamlessly and automatically by the program. Figure 6.1 shows a snapshot of the main screen of the program. The figure shows the main circuit schematic draft area as well as the control icons (at the top) and the quick access bars on the right-hand side. The control bar icons allow the user to run, pause or stop the simulation. Using the quick access bar icons, the user can select frequently-used elements such as resistors, capacitors, ground connection, and graphing tools. As shown the program can also generate graphs (two samples shown in the figure), which are drawn as the simulation progresses. Other parts of the program, such as the section shown on the left and the horizontal section at the bottom of the page, provide file and run-time management options.

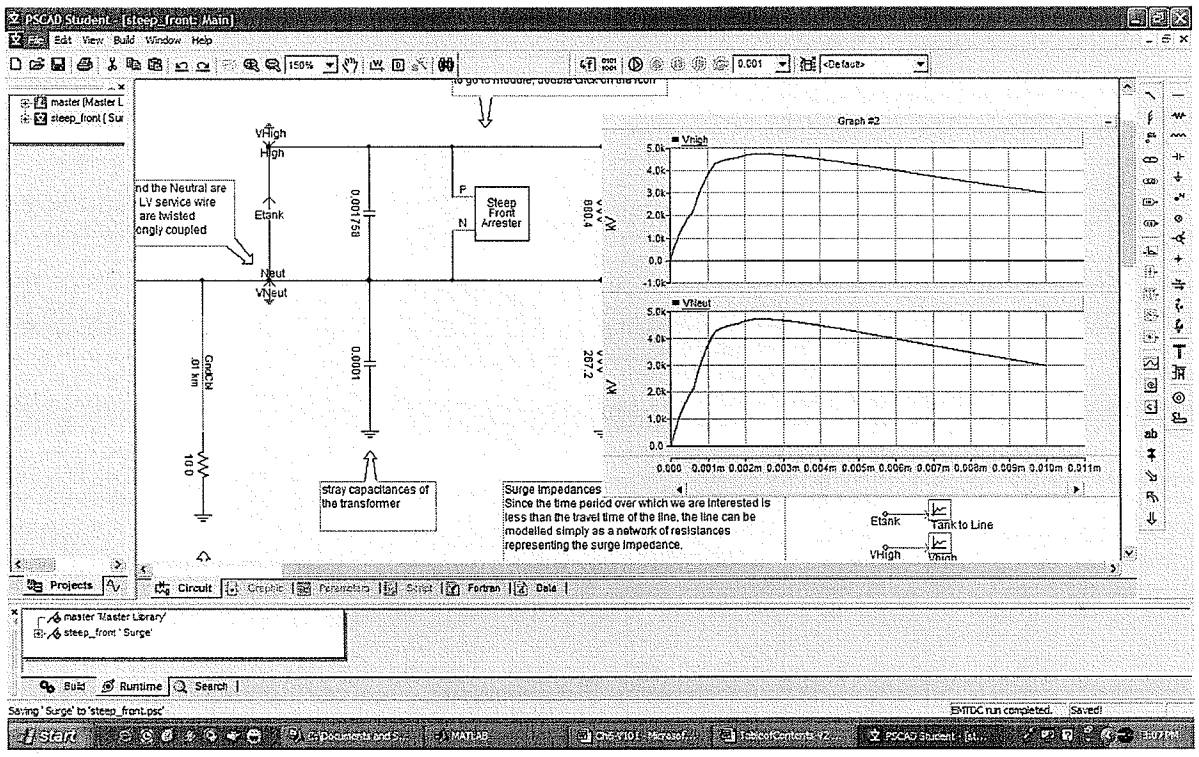


**Fig. 6.1** Snapshot of a simulation case in PSCAD/EMTDC.

## 6.2.2 Simulated Transients

Three types of power system transients, namely three-phase faults, capacitor swithcings and breaker operations have been simulated using the PSCAD/EMTDC program on a power system shown in Fig. 6.2.

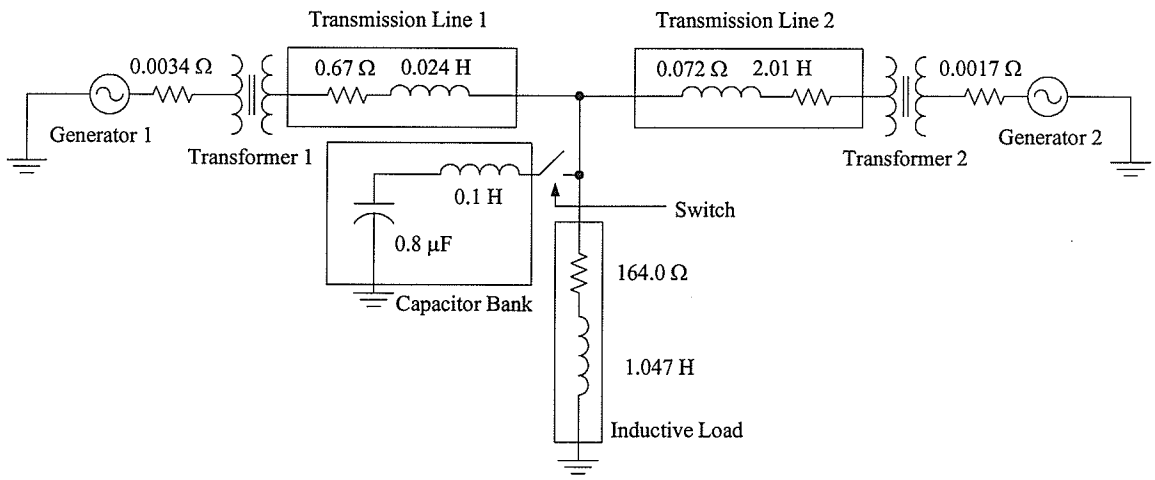


**Fig. 6.2** Schematic diagram of the power system under consideration. (After [GlSa87])

The diagram shown is a single-line representation of the three-phase system, with the other two phases identical to the phase shown. The system represents a simple power transmission network, in which two generating stations (generators 1 and 2) are connected through transmission lines to a load (the vertical branch in the middle). The transmission lines are represented by a simplified series RL model, which is used commonly in power system studies [GlSa87], [Kund95]. These elements show the total resistance and inductance of the line, and are influenced by factors such as line geometry, material, and frequency. Transmission lines are complex elements in a power system and their accurate modeling requires extensive studies, which are beyond the scope of this thesis [Kund95].

The load is represented using a series RL combination, and represents an inductive load, such as the majority of conventional residential and industrial loads. The numerical values shown on the schematic diagram of the network belong to the parameters of the transmission lines and generator equivalent impedances, and are in the typical ranges for such an apparatus [Kund95]. The LC branch shown in parallel with the load represents a switched capacitive branch (the inductance in series with the capacitor limits the current flow through the capacitor and serves a protection purpose) that can be connected (using the switch shown) to compensate partially the reactive power demand of the load. Such topologies for local generation of reactive power are employed commonly to lower the amount of reactive power flow through congested transmission lines and to release transmission capacity. The circuit is constructed in the simulation program and is used for simulation of samples of transients.

Selection of the number of samples to be simulated for each class is an important task. Since the number of recorded transients (from the Manitoba Hydro) was found to be fairly small, it was decided to keep the number of simulated transients low in order to make the methods to be developed still applicable to recorded transients. On the other hand, this number should be sufficiently large to allow estimation of pdfs (according to the central limit theorem). As a result, a total number of 120 sample transient waveforms have been simulated for each of the three classes of transients. Total simulation time is equal to 2.0 seconds, and each transient sample has a randomly (and uniformly) selected onset instant belonging to an interval of [0.6,1.0] seconds. This ensures that the transients are initiated only after the initial startup transient is over or after steady state is reached. Theses samples are used for the testing and training of the classifiers. For each class, a

total number of 40 samples are used for the training and the remaining 80 samples are used for the testing of the classifier. In practice, the number of recorded transients with identified causes (classes) was found to be very small (see Ch. 7); therefore, to assess the performance of the designed system with a small training set, only 40 samples/class are used for the training. Three sample waveforms from the transients simulated are shown in Fig. 6.3.

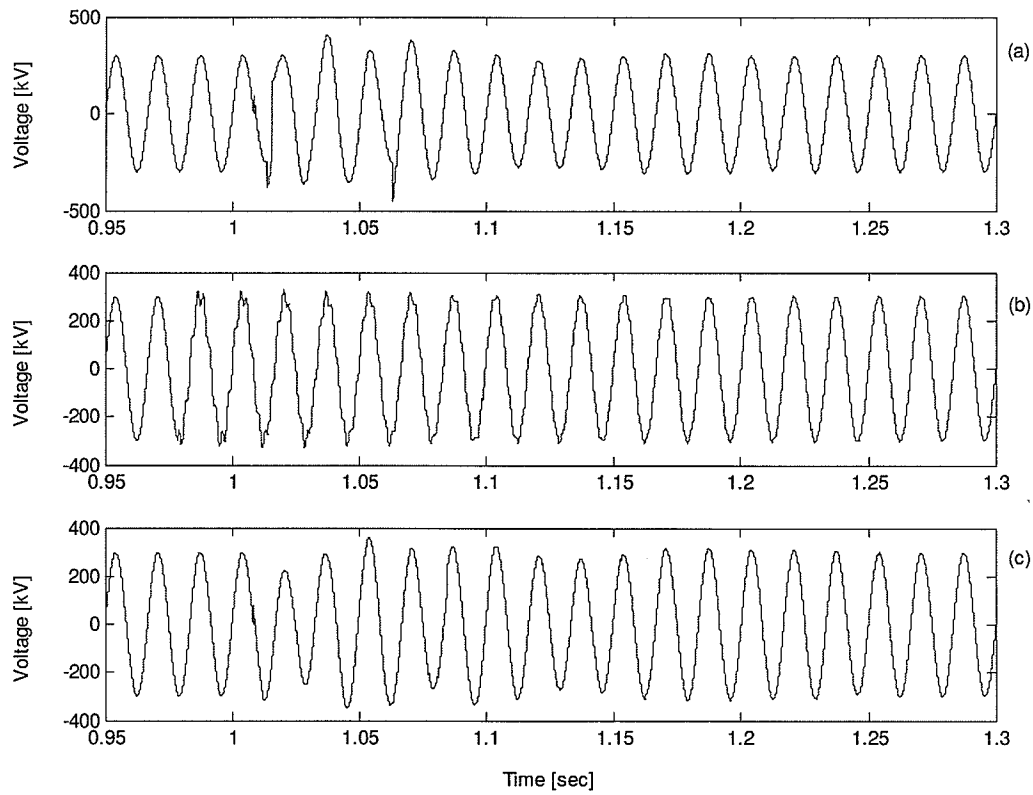


**Fig. 6.3** Samples of simulated transients.
(a) Breaker operation; (b) Capacitor switching; (c) Three-phase fault.

## 6.3 Segmentation of the Transient

The waveforms used in this thesis, either simulated or recorded, consist of two components: (i) the underlying sinusoidal component, and (ii) the superimpozed

transient. Extraction of features and the subsequent classification needs to be done only on the transient component. This is because in a practical setting, the process of feature extraction should be initiated only when a transient occurs. Therefore, it is necessary to use a monitory system whose role is to monitor the voltage (or current waveform) and to generate pulses at the start and end of the transient. Such a system would trigger the feature extraction engines only when a transient occurs and simplifies greatly the computational aspects of the overall system. A *phase-locked loop* (PLL) is such a system and it is, therefore, used as a segmentation block in this thesis.

### 6.3.1 PLL Application and Structure

In power systems, it is often necessary to extract the phase of a voltage waveform and use that as a reference. For example, in systems that involve power electronics, generation of firing pulses to controlled switches requires a reference phase angle that is obtained normally by using the output of a PLL locked to a given voltage waveform [Kund95]. A PLL is a system that generates a signal (e.g., a sine wave, or a sawtooth waveform) that follows exactly the variations of an externally supplied (sinusoidal) waveform. Any change in the external waveform characteristics, such as the frequency or phase shift, that can happen due to the operator command or presence of a transient is quickly traced by the PLL and the output is adjusted respectively.

Various PLL structures have been proposed that perform the same task, but have different characteristics [Rohd83]. In this thesis, a PLL structure shown in Fig. 6.4 is used because (i) it provides instantaneous detection of the onset of a transient, (ii) provides directly an error signal that is an indication of the superimpozed transients section and

(iii) uses generic building blocks (integrators and gains) that readily make implementation in the PSCAD/EMTDC possible. Moreover, it has been used extensively by other researchers and has been shown to be suitable for power system applications [KaMI00].

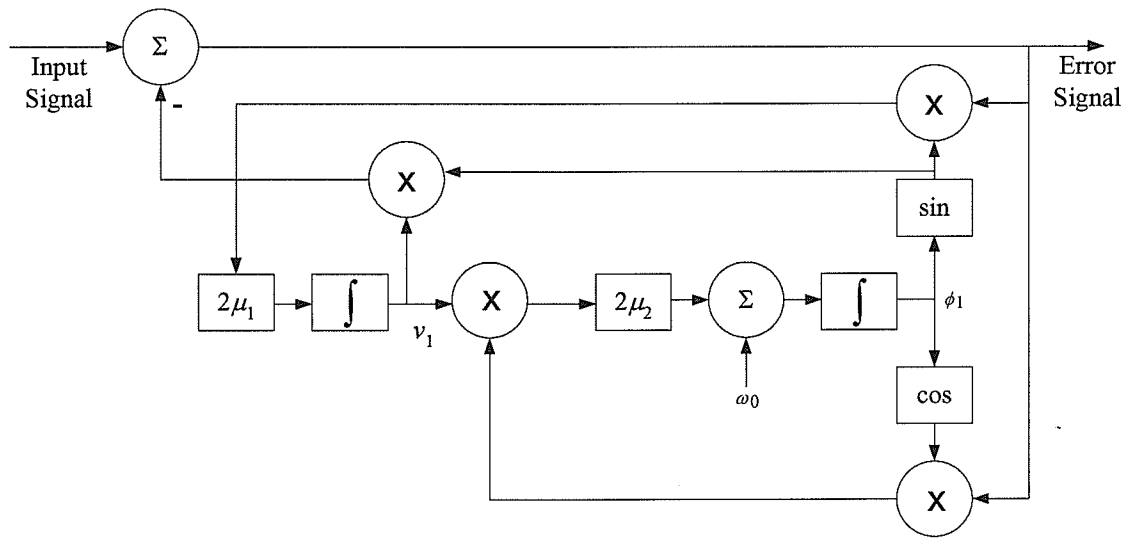


**Fig. 6.4** Schematic diagram of the PLL.

## 6.3.2 Analysis of the PLL Circuit

The PLL used is based on finding an estimation of the fundamental component of the input signal. When the input signal is void of transients, it will be a pure sine wave, with a constant frequency and amplitude of its fundamental component. Under such circumstances, the error signal $e(t)$ (which is the difference between the original and estimated signals) generated by the PLL will be equal to zero.

When a transient occurs, the underlying sine wave is superimpozed by a disturbance that distorts it, thus producing a nonzero error signal. The dynamic behaviour of the system is described as follows

$$\frac{dv_1}{dt} = 2\mu_1 \sin(\phi_1)e(t) \tag{6.1}$$

$$\frac{d\phi_1}{dt} = 2\mu_2 v_1 \cos(\phi_1)e(t) + \omega_0 \tag{6.2}$$

where the $v_1$ and $\phi_1$ are the estimated fundamental component amplitude and phase, respectively. The parameters $\mu_1$ and $\mu_2$ are adjustable gains that determine the speed of the operation of the PLL, and $\omega_0$ is the angular frequency of the input signal (fundamental component), which is equal to $2\pi \times 60 = 376.99\,\text{rad/sec}$ in the North American power system.

An important feature of the PLL described above is that following a transient, an error signal is generated immediately, which makes it adequate for real-time applications [KaMI00], where fast computations are necessary. Any change in the output of the PLL is an indication of a deviation from the original sine wave and could be used to initiate further analysis. In practice, deviations within a certain range are tolerated, and are not considered as transients. This range normally is equal to a ±5% interval around the nominal operating voltage, and is accepted normally by the power systems industry to be a safe boundary around the nominal values. Any deviation beyond this range is considered a transient that requires reaction. Using this concept, any PLL output beyond this limit is used in the subsequent feature extraction unit for identification of the true cause of the disturbance.

Figure 6.5 shows an example of a transient overvoltage along with the output of the PLL system. As shown, the PLL output is equal to zero prior to the occurrence of the

transient, which indicates that the PLL has been able to estimate correctly the underlying sine wave voltage. Following the onset of the transient, the output of the PLL extracts the imposed disturbance and provides it to the feature extraction unit.

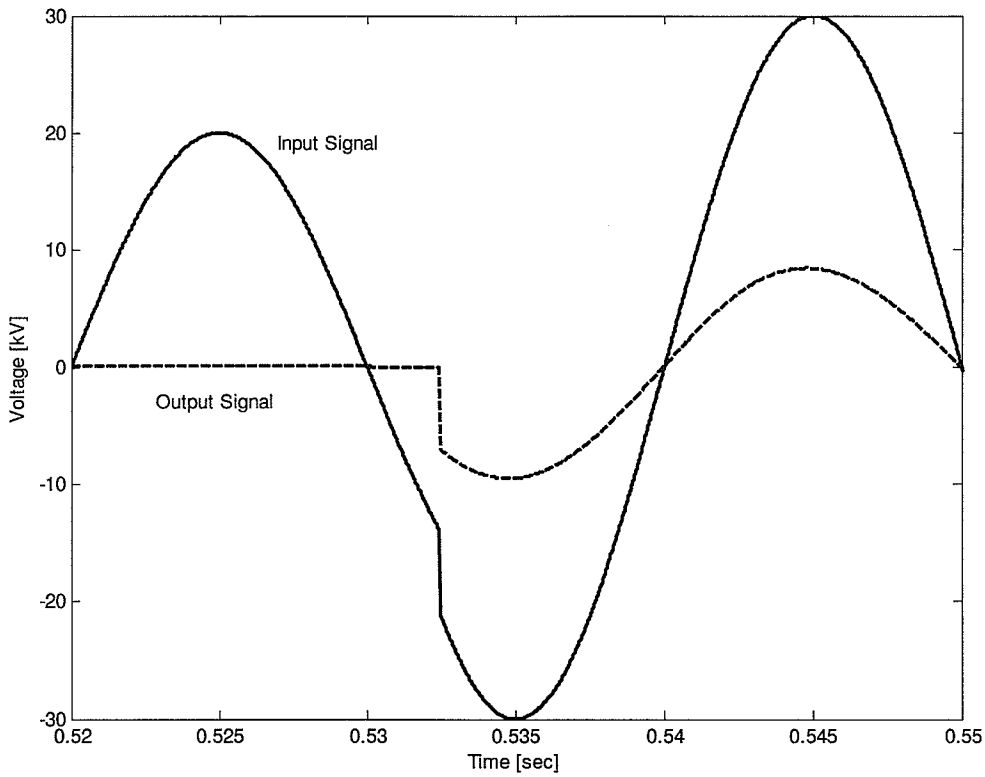


**Fig. 6.5** Samples of input and output waveforms of the PLL.
Solid line: the input waveform; Dotted line: the PLL output.

## 6.4 Feature Extraction

Transient waveforms, either simulated or recoded, contain a large number of samples, which makes them impractical to use as the input to a classifier. As noted in the preceding chapters, the VFDT and the wavelet transform are used in this thesis as the main methods for the extraction of a number of properties from the transients so that the essence of each waveform is represented by a few, convenient-to-analyze features. The

following presents the techniques used for the implementation of these two features extraction methods.

### 6.4.1 Implementation of the Wavelet Transform

The wavelet analysis was shown to be an effective method for characterizing signals with abrupt, short-term distortions, such as the transients in power systems. Doing so, however, involves several steps such as selection of a suitable mother wavelet, implementation of the transform and reduction of features. These steps are described in detail in the following.

#### 6.4.1.1 Choice of a Suitable Mother Wavelet

Selection of a suitable mother wavelet for a given application depends on a number of factors, including the type of the signals involved, the computational requirements of the algorithm, and the goals of the analysis to be carried out. Use of wavelets in the analysis of power systems has been considered by several researchers, and the pertinent literature shows a handful of mother wavelets used for this purpose [KiAg00], [BuBa03], [LiMo99], [HuHH99], [HuHs02]. The studies in this area have made important contributions to the development of advanced intelligent systems for the detection, characterization and classification of transients [Chen01], [KaMI00]; however, little insight has been provided as to what fundamental properties should be considered for the selection of a mother wavelet. In the following four subsections, important properties of a wavelet are presented that need to be considered before selecting a mother wavelet for the analysis of power system transients.

*Visual Similarity*

Wavelets are based on finding the correlation between the original waveform and shifted and scaled version of a short-duration wave called a mother wavelet. In this sense, it is obvious that the visual similarity between the signal and the original mother wavelet can be used as a simple, initial criterion for selecting a group of wavelets. It should be noted that the visual similarity is a very crude property and should not be relied on entirely, although in many publications it has been used solely for the selection of wavelets.

*Vanishing Wavelet Moments*

A wavelet is said to have $K$ vanishing moments if the following relation holds for all $k<K$

$$\int t^k f(t)dt = 0 \tag{6.1}$$

The vanishing moments relate to the order of function that can be approximated by the corresponding wavelet and also the level of compression that can be achieved through wavelet decomposition. For example, in the popular family of Daubechies wavelets (DB$n$), the number of vanishing moments for DB4 is equal to 2. For the analysis of highly transient signals with high complexity, wavelets with more vanishing moments are more suitable as they result in a more compact representation of the signals. However, there is always a trade-off between the performance and complexity that has to be resolved by the user. For example, more complex wavelets tend to be more

computationally intensive, which makes them less suitable for real-time applications where fast computations are required.

*Implementation and Computational Intensity*

It is very important to consider the implementation and computational complexity of an approach when selecting a mother wavelet for a given application. For example, wavelets with higher order filters (see Ch. 3) impose more intense computational complexity, and tend to be less suitable for real-time applications. In the analysis of power system transients, fast response is a major consideration as it directly affects the usefulness of the method in assisting the operator or the protection system to adopt the appropriate counter-measure. It is also important to make the storage and processing requirements as low as possible.

*Application-Related Aspects*

Apart from visual similarity, the number of vanishing wavelet moments and implementation and computational intensity, which can be used to limit the choices to a few mother wavelets, it is important to consider the actual performance of individual mother wavelets in the characterization of the transients. This is due to the variability of the transients in different power networks, depending on a large number of factors, including the physical properties of the underlying power network, proximity, and environmental aspects.

Due to this wide range of influential factors, which partially may not be known accurately, it is impractical to single out one specific wavelet that performs uniformly

well for all transients in all power networks and it is, therefore, important to consider the performance of a number of candidate wavelets (selected according to the criteria outlined above) to determine which one does perform better in practice.

Extensive literature survey, as well as personal experience with both simulated and recorded data, has led to the selection of DB4 wavelet for the analysis of transients in this thesis. This is because (i) power system transients, even the ones recorded in field, do not show an excessive level of complexity and as such higher order wavelets do not seem to be necessary, (ii) the performance of this wavelet has been considered versus other mother wavelets and no meaningful difference (neither in detection nor in characterization) has been identified [SaKT05] and (iii) the DB4 wavelet has been used by other researchers studying power systems transients and numerous publications exist that have used this wavelet [ChKi00], [MoKi97], [PiBh96], [MaAg01]; by selecting this mother wavelet, the results of the studies conducted in this research find more comparability with those of the researchers' and, therefore, provides the outcomes with further credibility in the community of peers.

#### 6.4.1.2 Feature Extraction from Wavelets

Wavelet analysis has been performed on both simulated and recorded transients and the first detail and approximation waveforms have been obtained. Although it is possible to continue the decomposition to include more stages, the results (as shown in the next chapter) have shown that the first level of detail and approximation is adequate. Careful consideration of a detail waveform shows that it still contains a large number of samples, although it contains almost half of the number of samples as in the original waveform. In other words, while the wavelet analysis is valuable in revealing important properties of

the transients, the outcome still needs further processing before it becomes suitable for use in a classifier.

To condense the information contained in a detail waveform $v_d(n)$ into a manageable number of features, the following formula is used

$$v_{rms^2} = \frac{1}{N}\sum_{i=1}^{N} v_d^2(n) \tag{6.2}$$

where $N$ is the total number of data points in the detail waveform (only the transient part is considered). Using this formula each detail waveform is condensed in only one feature that can be conveniently used in a classifier. In the next chapter, where experimental results are presented, it will be shown that the single feature extracted from the wavelet analysis of the transient provides invaluable assistance in the process of classification. An important objective of this thesis has been to develop methods that while being accurate use as few features as possible; the approach presented here is a major step towards realizing this objective (for a more detailed account of the savings obtained see the next and the final chapters of the thesis).

### 6.4.2 Implementation of the VFDT Analysis

Implementation of the VFDT approach is based on the formulation presented in Ch. 4. However, it is necessary to determine the appropriate window width and window displacement quantities to be used in the implementation of the VFDT. In addition, although the VFDT achieves a high compression ratio (by condensing the information in each window into a single fractal dimension), the output still contains a relatively large

number of data points, which are inconvenient to be used as features and as such feature reduction is still necessary. The following subsections address these important issues.

#### 6.4.2.1 Determination of the Window Width and Window displacement

Careful examination of the VFDT analysis reveals important aspects of the approach that will affect the quality of the features extracted using this method. The most important parameters that need to be determined carefully, are the window width $N_{ww}$ and the window displacement $N_{ws}$.

We note that the VFDT is based on calculating the variance fractal dimension of a signal in a number of windows along the signal. The data points contained in every window will be condensed into a single number, thus providing data compression. If the window width is too large, a large number of data points will be replaced with a single number; this is analogous to filtering the signal with a low-pass filter with a small pass band. The result of VFDT with an excessively large $N_{ww}$ is that the important properties of the signal will be surpassed by the presence of many other data points, and hence the high frequency data will be lost. On the other hand, a very small window width will not contain enough sample points to ensure proper estimation of the variance fractal dimension and will also result in computational complexity due to the large number of windows required to cover the signal.

The window displacement parameter controls the amount of overlap between adjacent windows. It can vary between 1 (maximum overlap) and $N_{ww}$ (no overalp). Apparently with maximum overlap, the computational intensity of the VFDT becomes overwhelming and the resulting trajectory will show significant correlation as the data points used for

calculation of the fractal dimension in the current window will heavily contribute to the dimension calculated in the next window. With no overlap (for $N_{ws} = N_{ww}$) each point is considered only once in the calculation of the fractal dimension and hence little correlation will be preserved.

To illustrate the impact of these two parameters, several variance fractal trajectories (corresponding to various combinations of $N_{ww}$ and $N_{ws}$) are presented below. The original signal whose VFDT is calculated is a transient caused by a lightning strike, and is shown in Fig. 6.6 (a). The signal is a sine wave that is interrupted severely by the lightning. A more detailed view of the interruption is also shown in Fig. 6.6 (b).

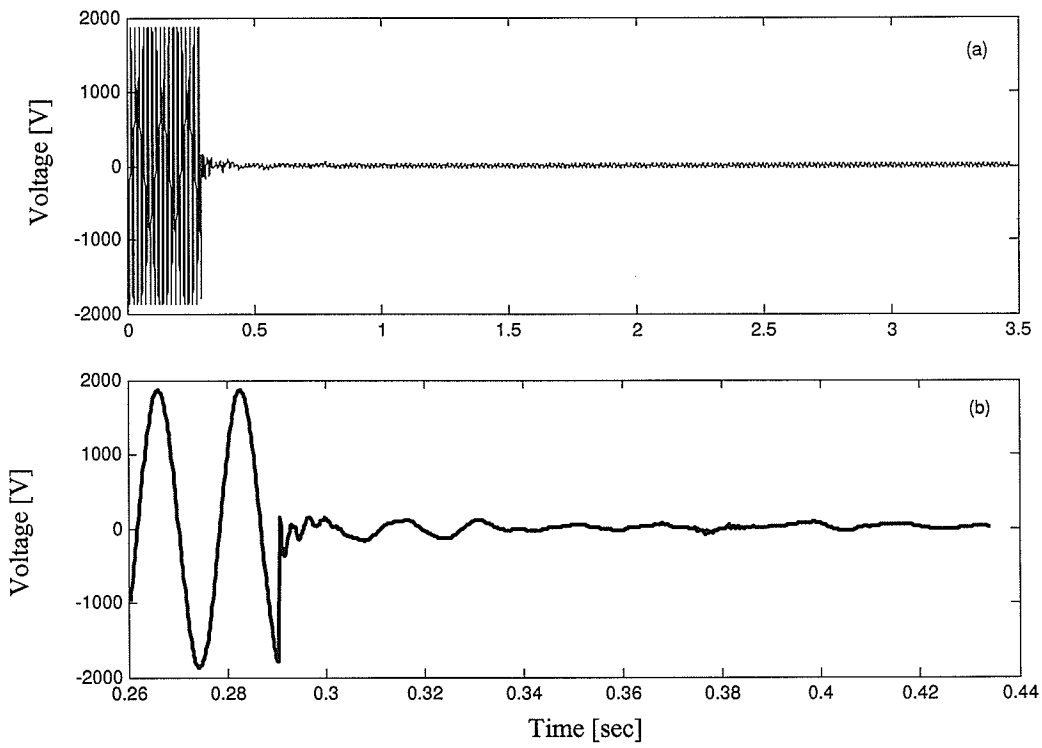


**Fig. 6.6** Transient caused by lightning strike.

In the following figures the VFDT of the signal is shown for various combinations of the window size and displacement parameters. As seen from these figures, VFDT with a relatively small window size (128 samples), as shown in Fig. 6.7, has a very fine resolution, and as such results in a low compression (large number of fractal dimensions). The excessively large window size of 2048 samples (Fig. 6.9) yields a very smooth VFDT with very few samples of fractal dimension, and as such suppresses the details of the transient. The suitably sized window width of 512 samples (Fig. 6.8) has enough number of samples of the fractal dimension in the trajectory it produces and is void of excessive details and is also capable of showing enough about the transient nature of the waveform.

The impact of the window displacement parameter is illustrated through Figs. 6.10 to 6.12. Figure 6.10 shows the VFDT with a window width of 512 samples and a window displacement of only 64 samples. As shown the trajectory possesses a great deal of detail resulting from significant overlap of successive windows. The two other trajectories with 256 (50% overlap) and 511 samples (minimum overlap) of window displacement show less detail. Figure 6.12 (with $N_{ws}$ = 511) shows inadequate detail of the transient portion and as such is not completely suitable for the characterization of complex transient nature of the signal.

Besides the resolution issues discussed above, it is important to consider the computational intensity of the method as well. Table 6.1 summarizes the results for such combinations, including the total number of fractal dimensions calculated and the processing time obtained on an Intel Centrino® 1.6 GHz machine with 512 Mb of RAM.

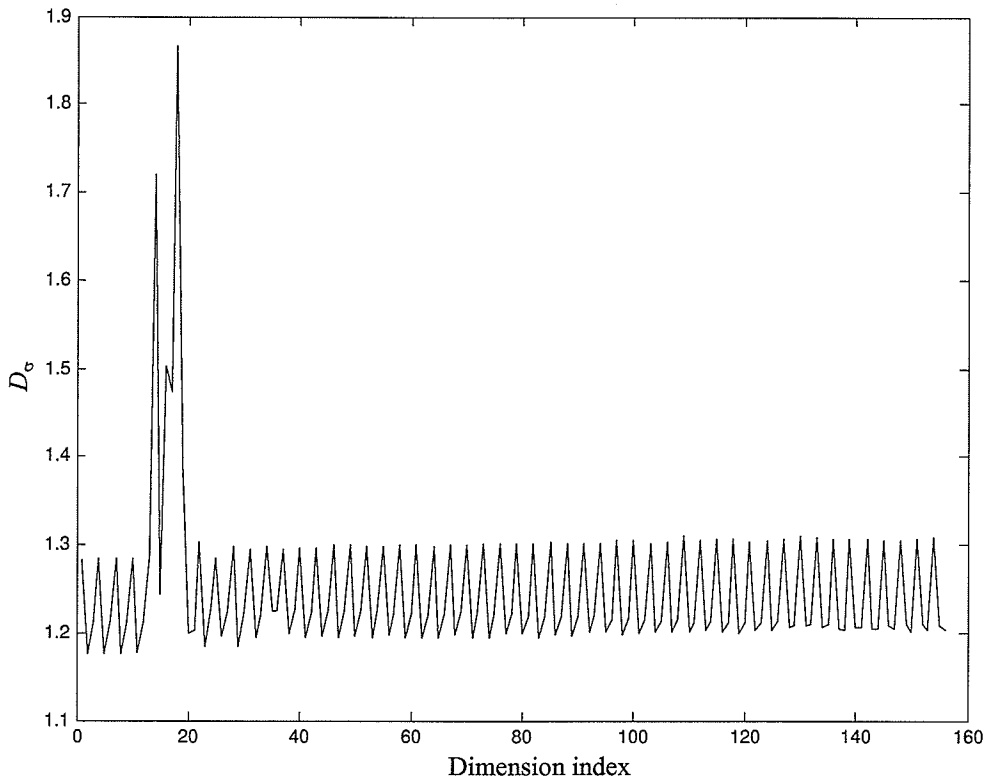


**Fig. 6.7** VFDT of the signal with $N_{ww}$ = 128 and $N_{ws}$ = 128 (no overalp).

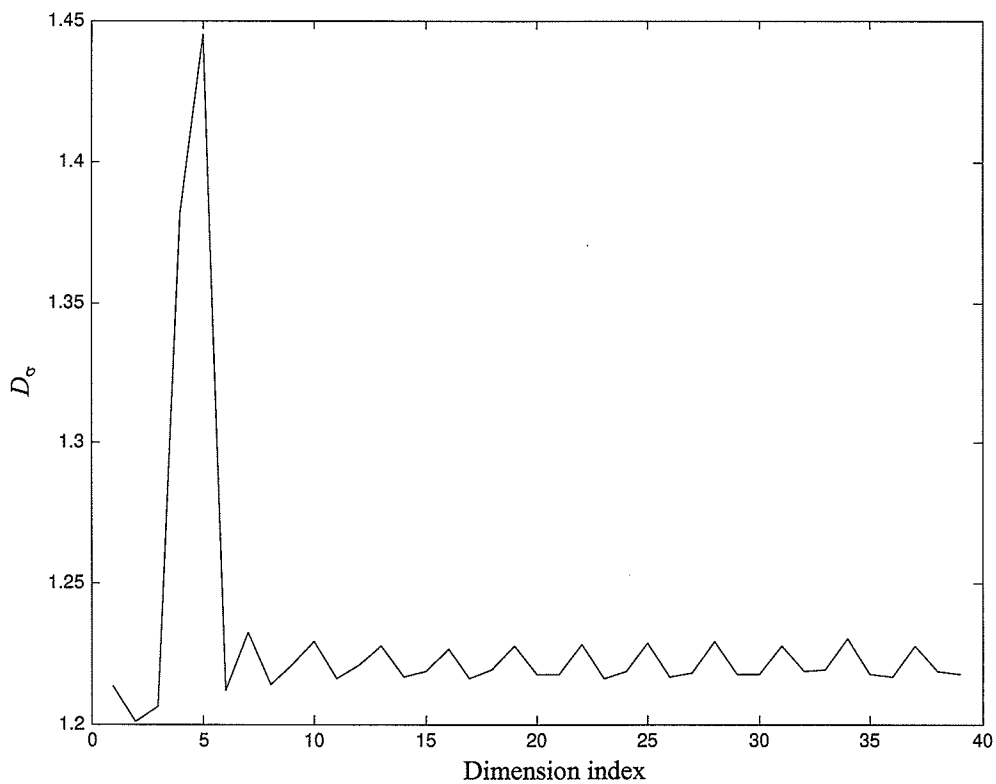


**Fig. 6.8** VFDT of the signal with $N_{ww}$ = 512 and $N_{ws}$ = 512 (no overalp).

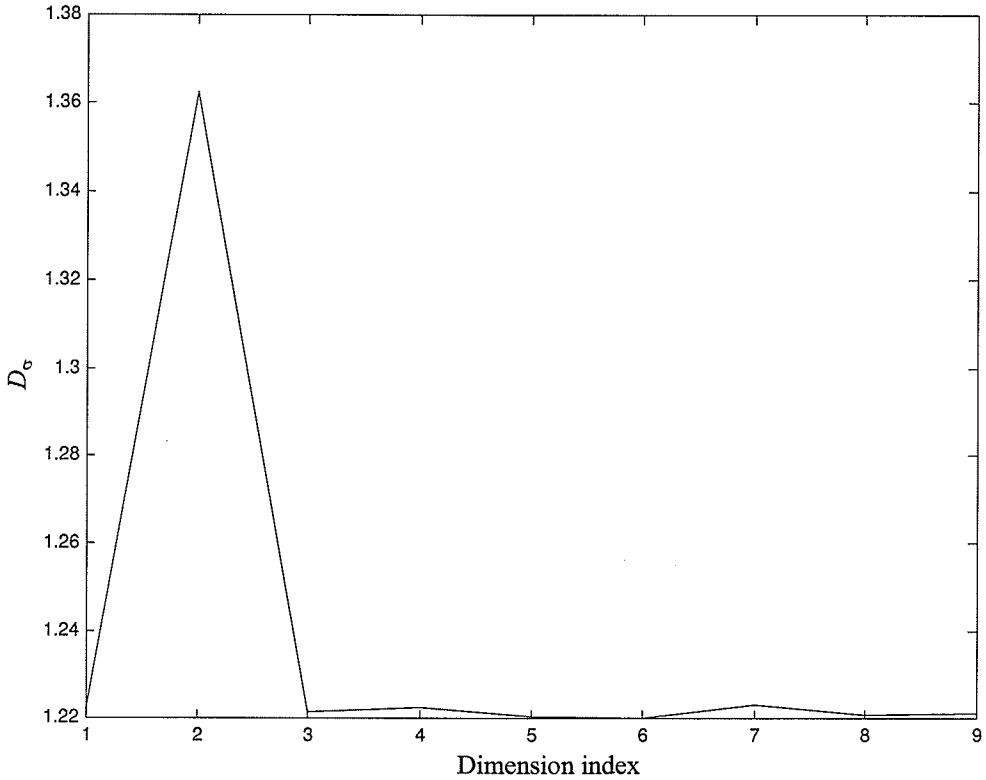


**Fig. 6.9** VFDT of the signal with $N_{ww}$ = 2048 and $N_{ws}$ = 2048 (no overalp).

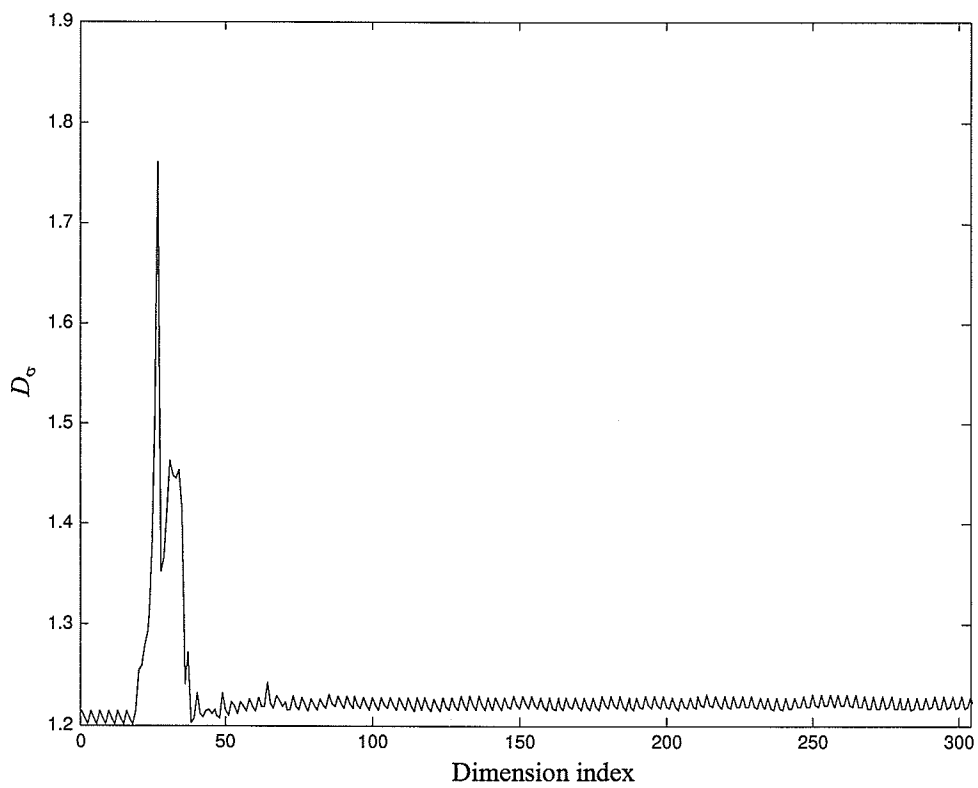


**Fig. 6.10** VFDT of the signal with $N_{ww}$ = 512 and $N_{ws}$ = 64.

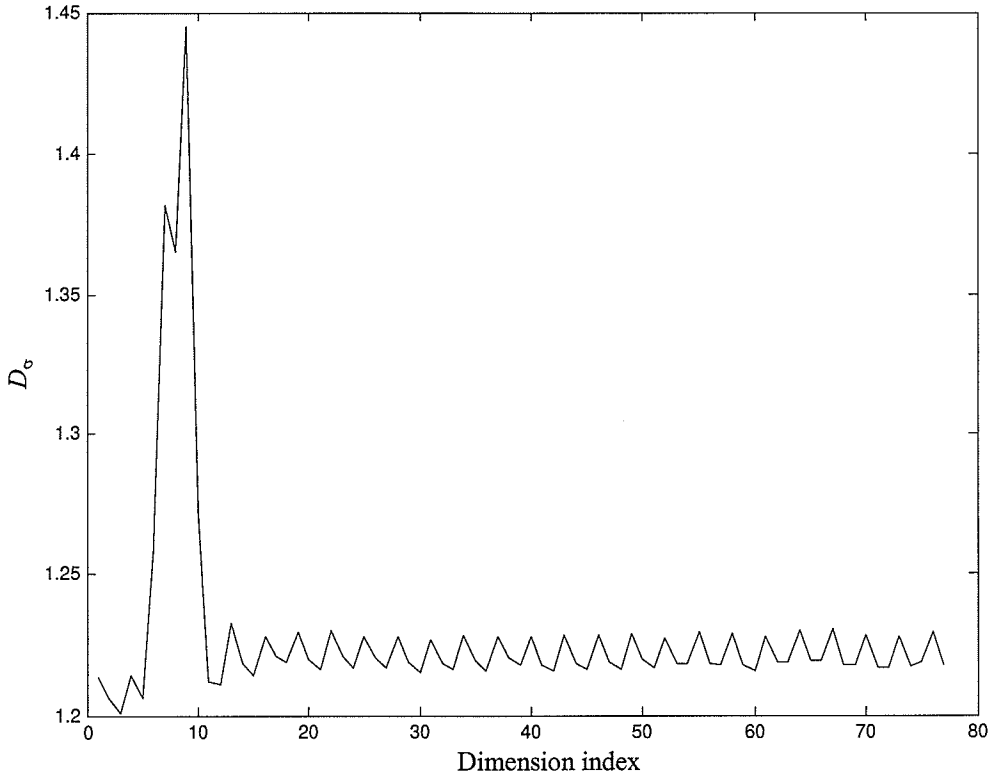


**Fig. 6.11** VFDT of the signal with $N_{ww}$ = 512 and $N_{ws}$ = 256.

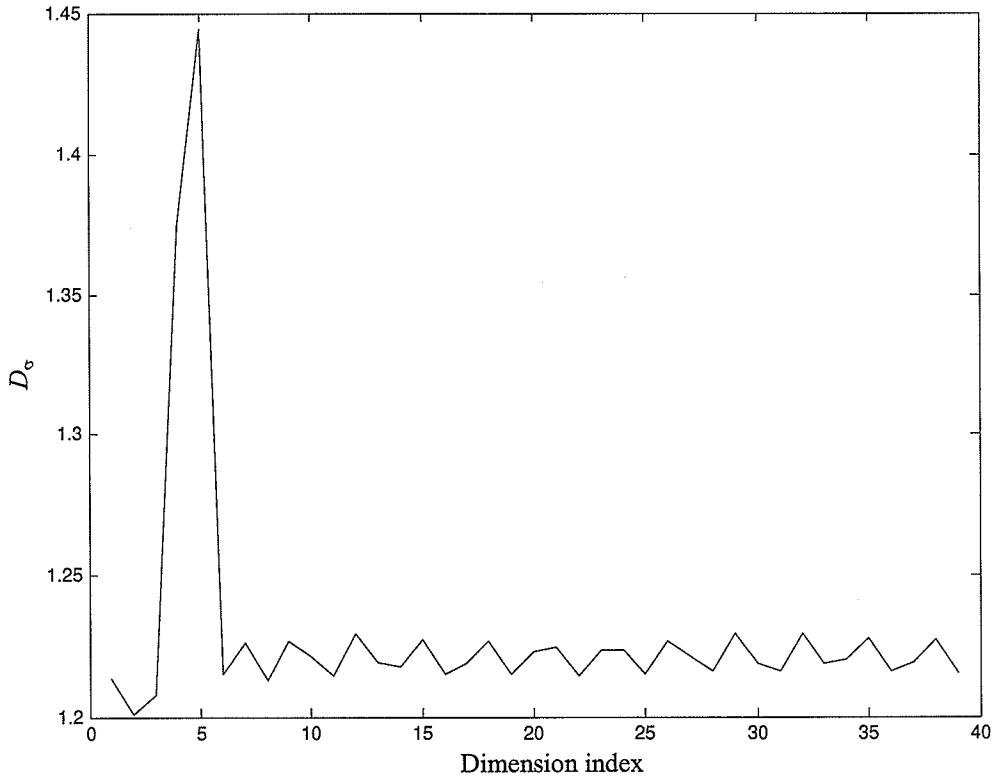


**Fig. 6.12** VFDT of the signal with $N_{ww}$ = 512 and $N_{ws}$ = 511.

**Table 6.1** Computational characteristics of the VFDT.

| Window Width ($N_{ww}$) | Window Displacement ($N_{ws}$) | Number of Dimensions ($N_d$) | Total Processing Time [sec] |
|---|---|---|---|
| 128 | 128 | 155 | < 0.02 |
| 512 | 512 | 38 | < 0.02 |
| 2048 | 2048 | 8 | < 0.02 |
| 512 | 64 | 304 | < 0.06 |
| 512 | 256 | 76 | < 0.03 |
| 512 | 511 | 38 | < 0.02 |

In the calculation of the VFDT of the transient signals (either simulated or recorded), the length of the signal varies depending on the duration of the transient. This poses a challenge as the number of samples within each waveform would vary. In order to overcome this and with consideration of the post-processing of the VFDT for extraction of feature (see below), a total number of 30 variance fractal dimensions were extracted from each transient. Since the sampling of signal is done at a relatively high rate (5760 for recorded data), the waveforms will have enough samples to allow for an accurate representation within each window. A window displacement of 50% is also considered for successive windows. This will eliminate excessive details and will reduce the computational intensity of the procedure while ensuring enough resolution for the final trajectory.

#### 6.4.2.2 Feature Extraction from VFDT

The VFDT analysis as described in Ch. 4 and the preceding section, compresses the data points in a signal into a number of fractal dimensions. Although this compression ratio is quite high, the fractal dimension trajectory so obtained still has a large number of components to make it inconvenient to be used as features.

In order to reduce the VFDT of each sample, a number of options have been developed and used in this thesis. The studies have confirmed that the extracted features (described in the following) do perform satisfactorily and can be good measures for distinguishing between various power system transients.

Although the distributions are not Gaussian, it was found that first and second moments could provide valuable information that can assist greatly in the classification process [SaKT04]. These moments are defined as follows

$$m_1 = \frac{1}{N_d}\sum_{i=1}^{N_d} f_d(i) \tag{6.3}$$

$$m_2 = \frac{1}{N_d}\sum_{i=1}^{N_d} (f_d(i) - m_1)^2 \tag{6.4}$$

where $m_1$ and $m_2$ are the first and second moments of the VFDT $f_d(t)$, and $N_d$ is the total number of values on the VFDT, each computed according to the algorithm described in Secs. 4.5 and 4.6.

Using these two features, it becomes possible to classify the transients in a power system; however, the performance of the classifier can be improved by combining the

two features obtained above with the feature obtained the wavelet analysis. The next chapter presents the numerical results obtained from individual feature extraction methods used as well as their combined features.

## 6.5 Implementation of the Classifier

The three types of classifiers described in the previous chapter are implemented and their performances are evaluated. The details about the implementation of the methods have been provided in Ch. 5. Although design of the classifiers such as the ML-based Bayes rule and the PNN is part of the overall system design, it is intentionally left to Ch. 7, since it will blend in more logically with the rest of the material in that chapter.

## 6.6 Overall System Layout

The mathematical foundations of the components of the overall system for detection, feature extraction and classification of transients in a power system have been described in the previous chapters. Their actual implementation details were given in this chapter. To be used as a suitable tool, these components need to be interconnected.

Figure 6.13 shows a schematic diagram of the overall system. It is seen that the PLL performs the segmentation of the transient and provides the feature extraction engine with its output. Feature extraction is done by two engines, namely the wavelet and the VFDT. The outputs of these two units are then condensed into a small number of features, which are then combined and used in a classifier. The output of the classifier is an indication of the underlying cause of the disturbance observed in the voltage waveform given to the system. Apart from the transient simulation done in the PSCAD, the remaining modules

of the system are coded in MATLAB. The developed source code has several modules that are shown, along with the code structures, in App. B.

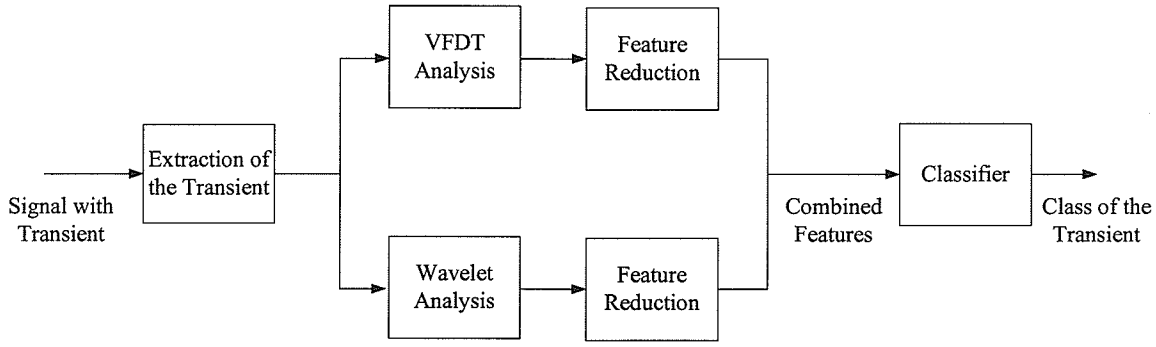


**Fig. 6.13** Schematic diagram of the overall system.

## 6.7 Chapter Summary

This chapter presented the details of the design of the overall feature extraction and classification system. The chapter discussed in detail the process of selection of a suitable mother wavelet as well as extraction of features from wavelet analysis. One level of wavelet decomposition is carried out on each transient signal using the DB4 wavelet. The RMS of resulting detail waveform is used as one of the features.

The chapter also discussed the implementation of the VFDT. In particular the selection of window width and window displacement parameters was discussed in detail. The VFDT analysis is done on each signal to yield a total of 30 variance fractal dimension (with a window displacement of 50%); the trajectory is then condensed into two features being the first and second moments of the trajectory. The two sets of features extracted from wavelet and VFDT analyses are combined and used in a classifier. The next chapter presents the experimental results obtained using simulated and recorded transients.

# CHAPTER VII

# EXPERIMENTAL RESULTS AND DISCUSSION

## 7.1 Introduction

Following the mathematical description of the feature extraction and classification methods, as well as a description of the design of the overall system presented in the previous chapter, this chapter presents the experimental results obtained by applying the tools and techniques to both simulated and recorded transients, and also provides technical discussion on the results and their significance.

The chapter is organized into two major sections: (i) the simulated transients and (ii) recorded transients. For each section, feature extraction details and classification results are presented.

## 7.2 Experimental Results Using Simulated Transients

Simulated transient waveforms are obtained using the PSCAD/EMTDC program. The simulated transients include samples from three types of disturbances, namely three-phase faults, capacitor switchings and breaker operations. A total of 120 samples are generated for each class, of which 40 samples are used for training and the remaining 80 are used for testing the classifier. Feature extraction from these transients is carried out using both wavelets and the variance fractal dimension trajectory, VFDT.

In the following subsections, classification results using the ML-based Bayes rule for each of these two sets of features are presented. It is followed by the results obtained using combined features and the classification results using the PNN.

### 7.2.1 ML-Based Classification Using the VFDT Features

The VFDT for each of the 40 training samples from each class is computed, and the results are then condensed into two features being the first and second moments of the trajectory of variance fractal dimensions, resulting in two features per sample.

The ML-based Bayes rule, as described earlier, intends to fit a pdf to the features so obtained. Since there are two features for each sample from the three classes, there are a total of 6 pdfs to be fitted. Parts (a) of Figs. 7.1 to 7.6 show the histograms of the features in each class. An important consideration in generation of such histograms is number of bins used. While use of too few bins would result in an overly smooth graph, too many bins can introduce excessive detail. Both such cases will affect adversely the estimation of underlying pdfs. The histograms shown have been obtained using 10 bins, which in this case provides sufficient resolution.

The next step after generation of data histograms is the estimation of pdfs. The histograms of Figs. 7.1 to 7.6 show that the underlying distributions are often multimodal, and are not single Gaussians. In order to use the ML-based Bayes rule, one needs to assume known forms for the underlying pdfs; as such, we have attempted to model these distributions using a combination of local Gaussian pdfs. This is because a Gaussian distribution is identified by only two parameters and its higher order moments are equal to zero, thus making the estimation convenient. The estimated pdfs are shown in parts (b) of Figs. 7.1 to 7.6. The classification results obtained using these pdfs confirm the suitability of this assumption. Estimation of the parameters of the underlying pdfs involves an iterative optimization that maximizes the objective function given in Eq. (5.4). Table 7.1 summarizes the starting and final parameters of the estimated pdfs. It is

important to know that the estimation method provides the user with a great deal of flexibility in terms of the number of underlying pdfs for each mixture model; however, it is important to select as few such pdfs as possible (while ensuring proper accuracy) to prevent over-fitting of the data. This concept is in conformity with the well-known Occam's Razor principle [Bish95]. The estimated pdfs are subsequently used in the Bayes rule to assign an input sample with a given set of features (obtained using VDFT) to one of the three classes of the simulated data.

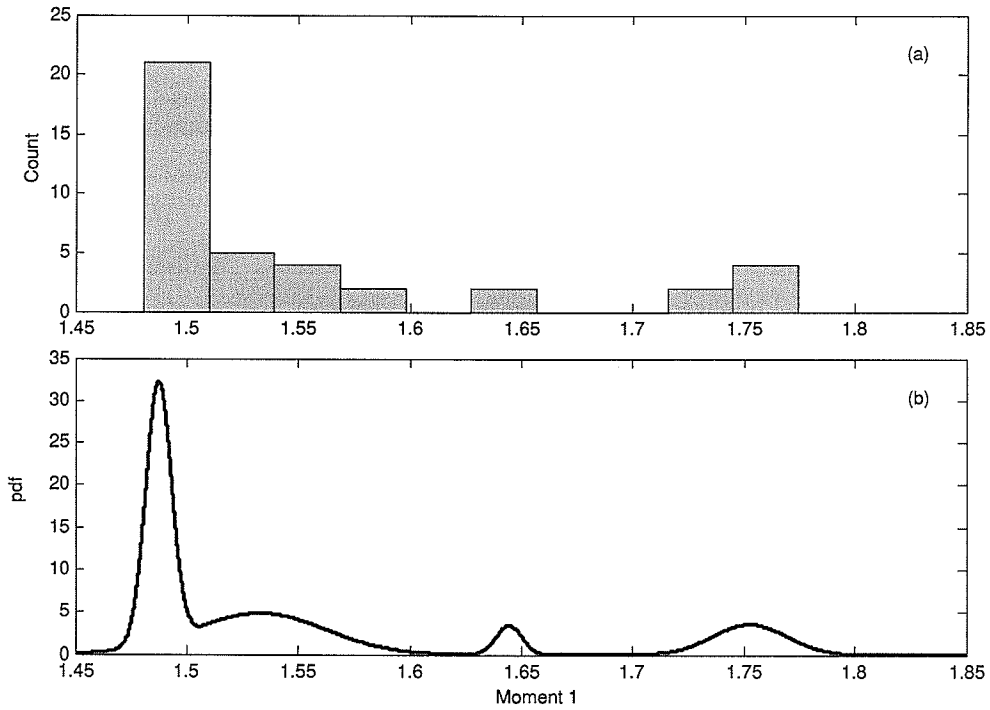


**Fig. 7.1** PDF estimation for feature moment 1 in the class of capacitor switchings. (a) Histogram of the data; (b) Estimated pdf.

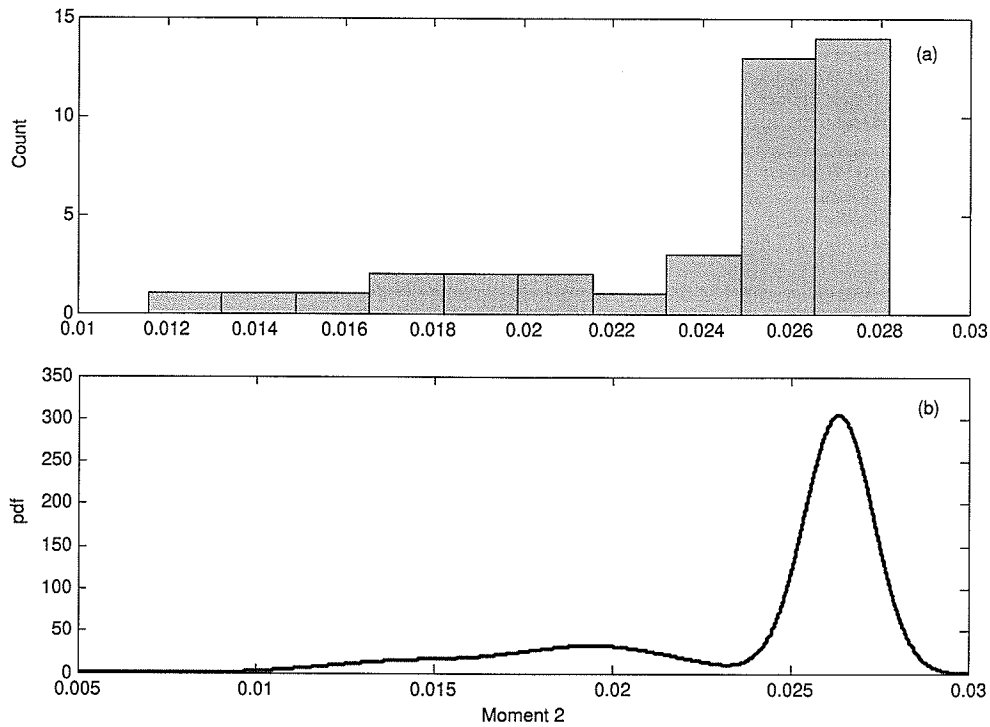


**Fig. 7.2** PDF estimation for feature moment 2 in the class of capacitor switchings. (a) Histogram of the data; (b) Estimated pdf.

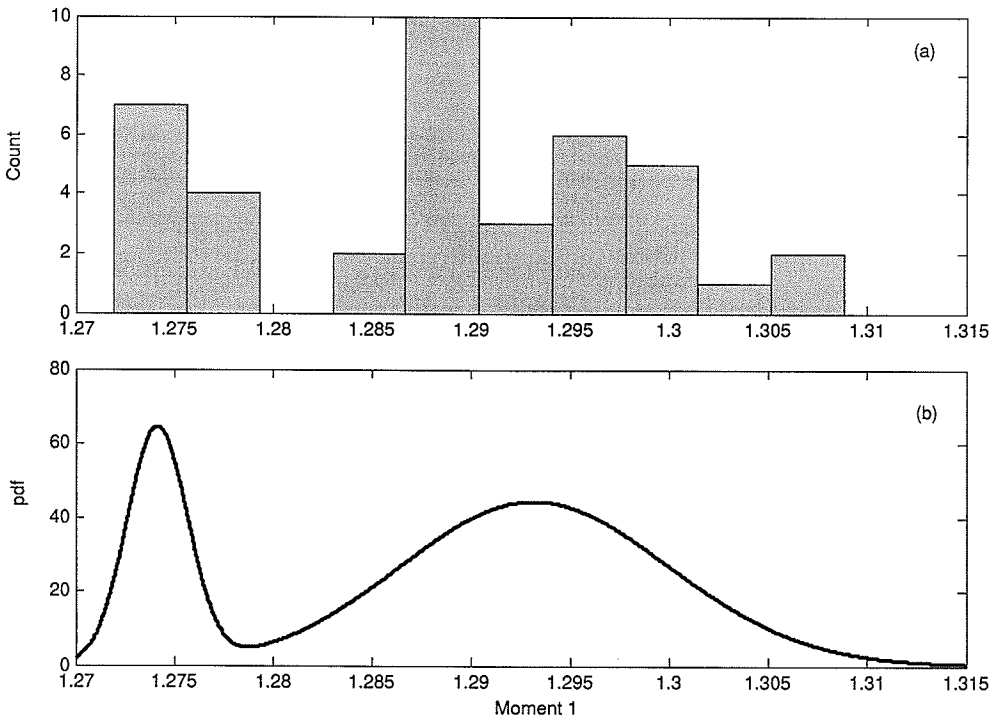


**Fig. 7.3** PDF estimation for feature moment 1 in the class of faults. (a) Histogram of the data; (b) Estimated pdf.

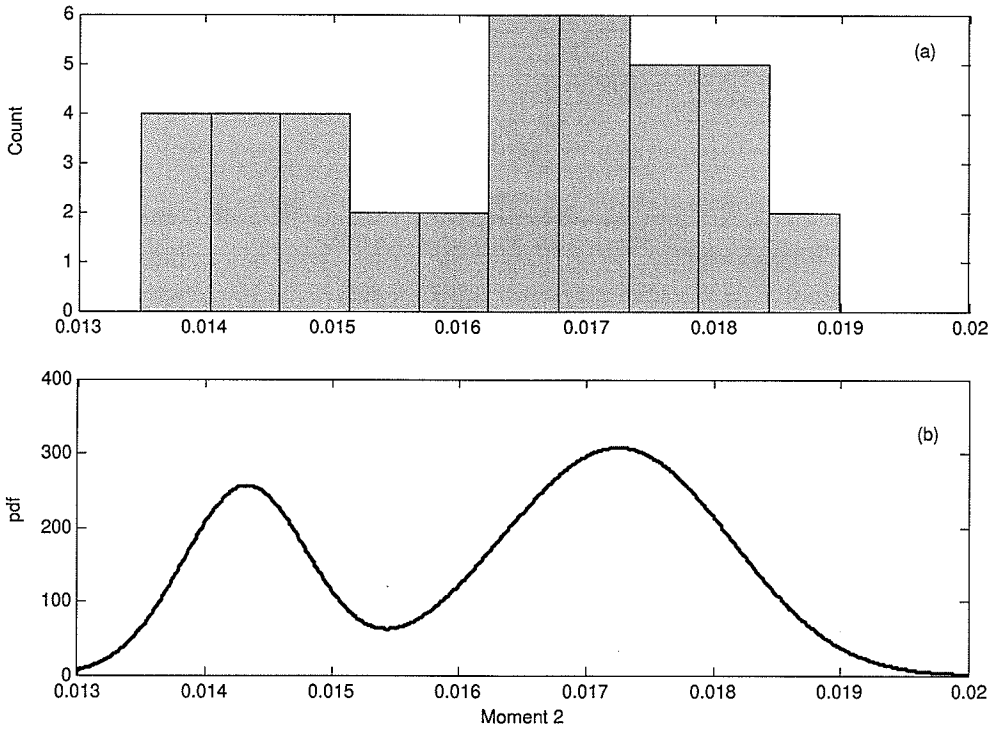


**Fig. 7.4** PDF estimation for feature moment 2 in the class of faults.
(a) Histogram of the data; (b) Estimated pdf.

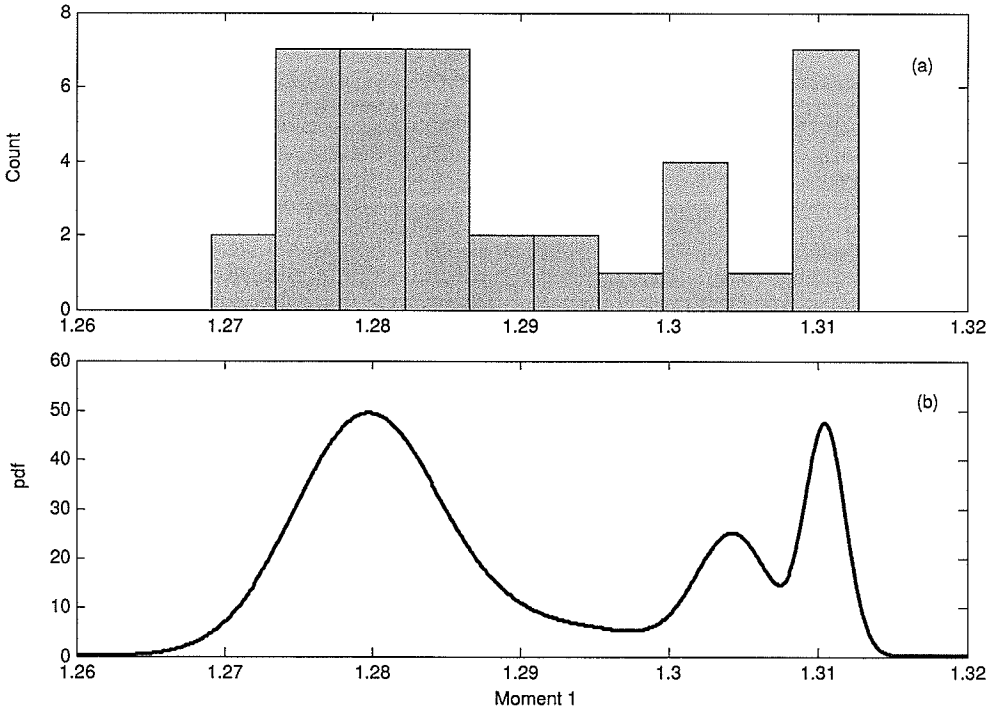


**Fig. 7.5** PDF estimation for feature moment 1 in the class of breaker operations.
(a) Histogram of the data; (b) Estimated pdf.

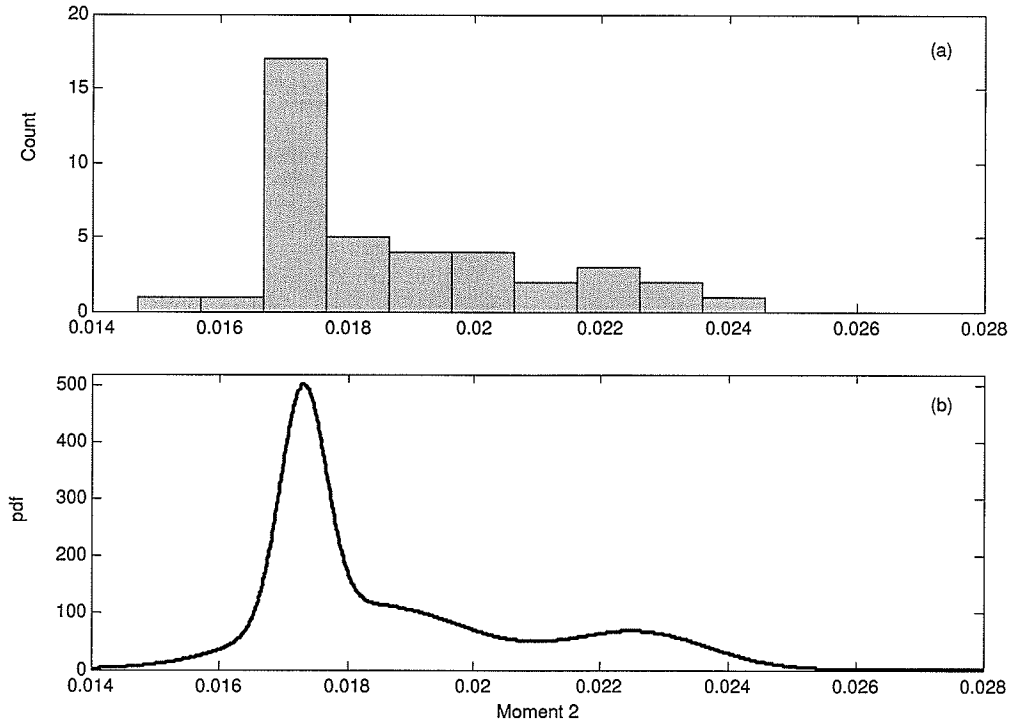


**Fig. 7.6** PDF estimation for feature moment 2 in the class of breaker operations. (a) Histogram of the data; (b) Estimated pdf.

The parameters listed in Table 7.1 are obtained using the 40 training samples from each class. For testing the performance of the ML-based Bayes classifier the remaining 80 samples from each class are used. Upon presentation of each testing sample the corresponding class-conditional pdfs are calculated and the class with the highest probability is chosen as the winner and the input sample is assigned its label. Note that we have assumed equal prior probabilities for each of the three respective classes.

**Table 7.1** Parameters estimated using the maximum likelihood (VFDT features).

| Class/Feature Identifier | | Initial Parameters | Final Parameters |
|---|---|---|---|
| Capacitor Switching | Moment 1 | **m** = [1.5 1.55 1.65 1.75]<br>**σ** = [0.01 0.02 0.01 0.01]<br>**π** = [0.5 0.25 0.1 0.15] | **m** = [1.49 1.53 1.64 1.75]<br>**σ** = [0.0057 0.029 0.0058 0.0167]<br>**π** = [0.44 0.357 0.0499 0.15] |
| | Moment 2 | **m** = [0.014 0.019 0.026]<br>**σ** = [0.002 0.002 0.003]<br>**π** = [0.15 0.15 0.7] | **m** = [0.0141 0.0196 0.0264]<br>**σ** = [0.0022 0.0023 0.000973]<br>**π** = [0.073 0.18 0.74] |
| Faults | Moment 1 | **m** = [1.27 1.29 1.295 1.305]<br>**σ** = [0.01 0.01 0.02 0.01]<br>**π** = [0.25 0.5 0.15 0.10] | **m** = [1.274 1.29 1.294 1.297]<br>**σ** = [0.0015 0.006 0.007 0.0072]<br>**π** = [0.246 0.52 0.122 0.108] |
| | Moment 2 | **m** = [0.0145 0.0168 0.018]<br>**σ** = [0.002 0.001 0.001]<br>**π** = [0.25 0.5 0.25] | **m** = [0.014 0.01696 0.0177]<br>**σ** = [0.0005 0.00084 0.0007]<br>**π** = [0.317 0.445 0.24] |
| Breaker Operations | Moment 1 | **m** = [1.28 1.295 1.305 1.31]<br>**σ** = [0.02 0.01 0.005 0.005]<br>**π** = [0.65 0.15 0.1 0.1] | **m** = [1.279 1.292 1.30 1.31]<br>**σ** = [0.0049 0.008 0.0028 0.0014]<br>**π** = [0.581 0.12 0.143 0.157] |
| | Moment 2 | **m** = [0.015 0.016 0.019 0.022]<br>**σ** = [0.001 0.001 0.001 0.001]<br>**π** = [0.2 0.4 0.2 0.2] | **m** = [0.017 0.0173 0.0184 0.023]<br>**σ** = [0.36 0.362 1.55 1.1]$\times 10^{-3}$<br>**π** = [0.125 0.25 0.44 0.182] |

Table 7.2 shows the summary of the classification results obtained by using the features obtained from the VFDT analysis and the ML-based Bayes rule. For each entry the total number of features along with their percentage share is given.

**Table 7.2** Classification results for the VFDT features using the Bayes rule.

| **Test Sample Class** | **Assigned Class** | | |
|---|---|---|---|
| | Capacitor Switching | Faults | Breaker Operations |
| Capacitor Switching | **80 (100%)** | 0 (0%) | 0 (0%) |
| Faults | 0 (0%) | **71 (88.75%)** | 9 (11.25%) |
| Breaker Operations | 0 (0%) | 20 (25%) | **60 (75%)** |

The results presented in Table 7.2 show that the VFDT-based features have been able to separate completely the class of capacitor switching transients from the remaining two classes. However, the classes of faults and breaker operations show some error, indicated by the misclassification of some of their samples into the other class. In order to visualize the case, it is instructive to consider Fig. 7.7, which shows the training samples in the moment 1-moment 2 plane. As shown the class of capacitor switching is separated entirely from the other classes, which show overlap.

VFDT-based features are not the only features available to us for classification. Wavelet analysis also provides us with means for classification. In the following subsection we firstly consider the performance of wavelet analysis on its own and then examine the performance of combined features.

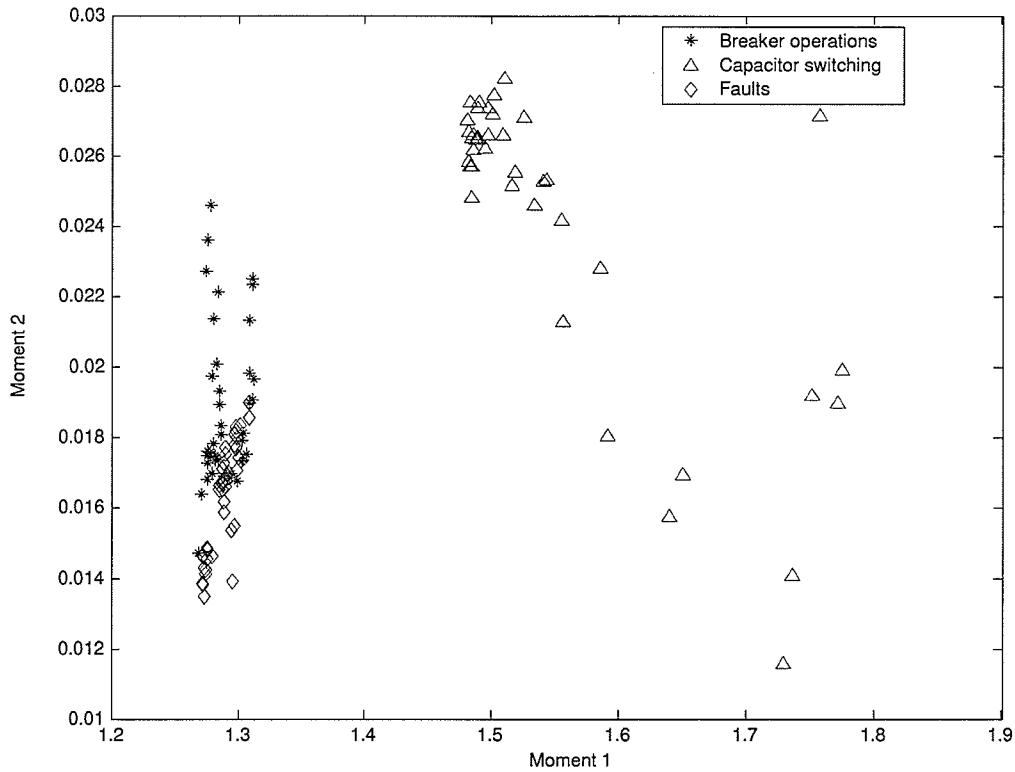


**Fig. 7.7** Spread of features obtained using VFDT.

### 7.2.2 ML-Based Classification Using the Wavelet Feature

Since there was only one feature extracted from the wavelet analysis of simulated data, classification of the three types of simulated classes only requires three pdfs to be estimated for implementation of the Bayes rule. Following the same procedure as in the previous section for VFDT features, we start by examining the histograms of the training samples and then use the ML-based mixture model approach to fit pdfs.

Figures 7.8 to 7.10 show the histograms of the wavelet-based features along with the estimated pdfs. The initial parameters as well as final parameters for the pdf estimation are listed in Table 7.3.

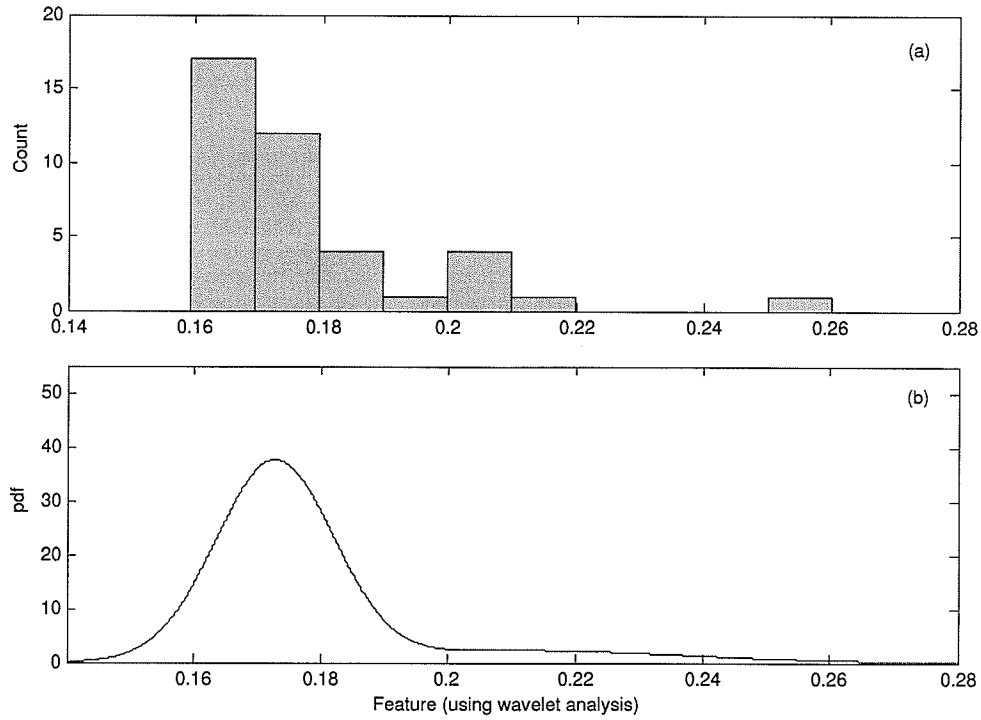


**Fig. 7.8** PDF estimation for the wavelet feature in the class of capacitor switching. (a) Histogram of the data; (b) Estimated pdf.

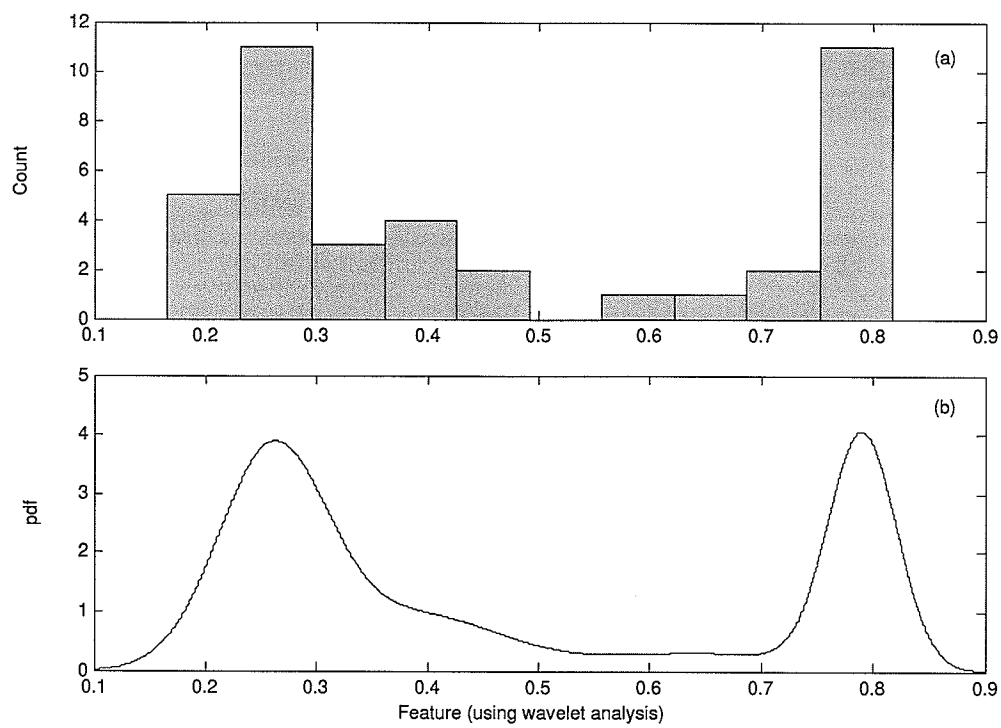


**Fig. 7.9** PDF estimation for the wavelet feature in the class of faults. (b) Histogram of the data; (b) Estimated pdf.

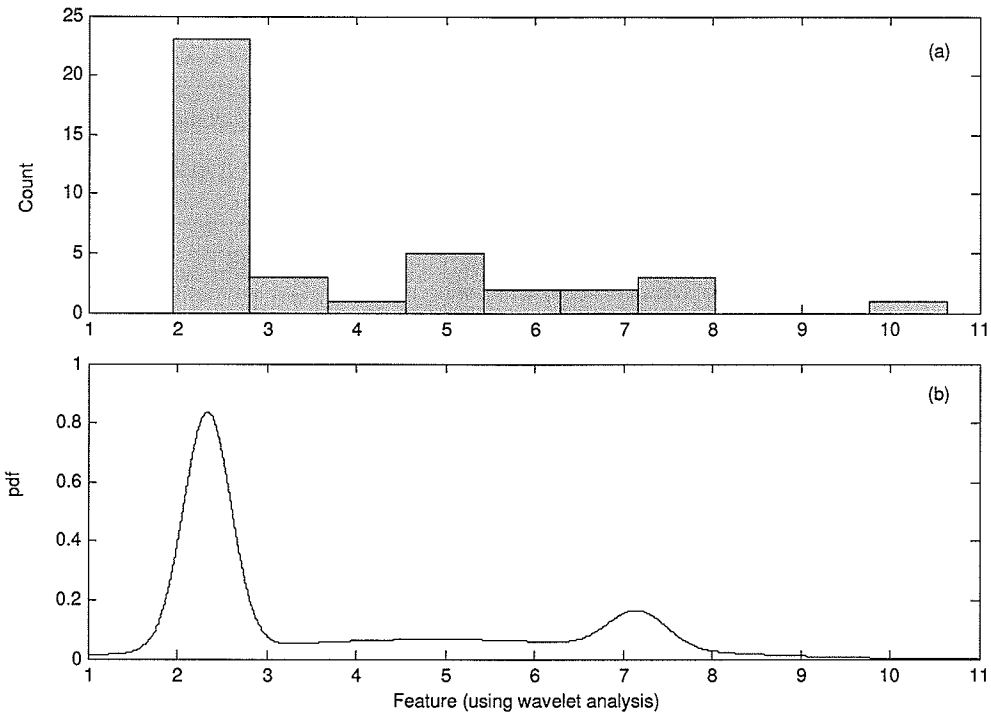


**Fig. 7.10** PDF estimation for the wavelet feature in the class of breaker operations. (a) Histogram of the data; (b) Estimated pdf.

**Table 7.3** Parameters estimated using the maximum likelihood (wavelet feature).

| Class Identifier | Initial Parameters | Final Parameters |
|---|---|---|
| Capacitor Switching | $\mathbf{m}$ = [0.17 0.21 0.25]<br>$\boldsymbol{\sigma}$ = [0.02 0.02 0.001]<br>$\boldsymbol{\pi}$ = [0.8 0.15 0.05] | $\mathbf{m}$ = [0.173 0.212 0.26]<br>$\boldsymbol{\sigma}$ = [0.009 0.026 $10^{-8}$]<br>$\boldsymbol{\pi}$ = [0.856 0.145 $2\times10^{-8}$] |
| Faults | $\mathbf{m}$ = [0.25 0.4 0.65 0.75]<br>$\boldsymbol{\sigma}$ = [0.08 0.08 0.05 0.02]<br>$\boldsymbol{\pi}$ = [0.4 0.2 0.1 0.3] | $\mathbf{m}$ = [0.26 0.391 0.646 0.79]<br>$\boldsymbol{\sigma}$ = [0.048 0.079 0.0878 0.03]<br>$\boldsymbol{\pi}$ = [0.443 0.186 0.067 0.30] |
| Breaker Operations | $\mathbf{m}$ = [2.5 5.0 7.0]<br>$\boldsymbol{\sigma}$ = [0.1 1.0 0.5]<br>$\boldsymbol{\pi}$ = [0.7 0.15 0.15] | $\mathbf{m}$ = [2.34 4.93 7.17]<br>$\boldsymbol{\sigma}$ = [0.265 2.13 0.325]<br>$\boldsymbol{\pi}$ = [0.536 0.366 0.1037] |

Bayes rule classification using the feature obtained from the wavelet analysis yields the results contained in Table 7.4. Note that similar to the VFDT approach, 40 samples are used for training and the remaining 80 samples are used for testing.

**Table 7.4** Classification results for the wavelet feature using the Bayes rule.

| **Test Sample Class** | **Assigned Class** | | |
|---|---|---|---|
| | Capacitor Switching | Faults | Breaker Operations |
| Capacitor switching | **77 (96.25%)** | 3 (3.75%) | 0 (0%) |
| Faults | 6 (7.5%) | **74 (92.5%)** | 0 (0%) |
| Breaker Operations | 0 (0%) | 0 (0%) | **80 (100%)** |

Table 7.4 contains important information about the performance of the wavelet analysis in classification of the three types of simulated transients. As shown the analysis is capable of separating completely the class of breaker operations from the other two classes. The classes of capacitor switchings and faults also show very good level of separation but still have some small overlap. It is also important to note that the wavelet analysis has been able to remove the overlap between the faults and breaker operations observed in VFDT analysis (see Table 7.2). In other words, it seems that the wavelet and VFDT analyses can be used cooperatively in a classifier, which takes advantage of both methods to remove as much overlap among the classes as possible.

The following subsection presents the classification results of the combined features using the ML-based Bayes rule.

### 7.2.3 ML-Based Classification Using Combined Features

Examination of the experimental results of the previous sections suggests that combination of the features obtained using VFDT and wavelet analyses could improve potentially the correct classification rate by removing the overlap areas observed in individual sets.

The new input vector, which combines the two features form the VFDT with the single feature from wavelet analysis, has the following form.

$$\mathbf{x} = [\text{first moment from VFDT, second moment from VFDT, feature from wavelet}] \quad (7.1)$$

Upon presentation of this combined feature to the classifier, the overall pdf is calculated and the one with the largest numerical evaluation is chosen as the winner. Table 7.5 shows the classification results using the combined features in an ML-based Bayes classifier.

**Table 7.5** Classification results for the combined features using the Bayes rule.

| **Test Sample Class** | **Assigned Class** | | |
|---|---|---|---|
| | Capacitor Switching | Faults | Breaker Operations |
| Capacitor Switching | **80 (100%)** | 0 (0%) | 0 (0%) |
| Faults | 0 (0%) | **80 (100%)** | 0 (0%) |
| Breaker Operations | 0 (0%) | 0 (0%) | **80 (100%)** |

### 7.2.4 Discussion on the ML-Based Bayes Rule for Simulated Data

The experimental results presented in the previous subsections addressed the performance of the ML-based Bayes rule in classification of simulated data. The two signal analysis methods used for feature extraction, namely the VFDT and the wavelets, each characterize the transient signal from a different standpoint, and that is the reason why combination of the two sets of features obtained using these methods results in such a high correct classification rate.

Besides the merit of the features used, it is very important to consider the classification method itself too. The ML-based Bayes rule provides a very convenient method for training a good classifier. The training time, which is the time required for optimizing the pdf parameters, is very short and the optimization completes in a fraction of a second. The method also provides flexibility in terms of adjusting the complexity of the pdfs and allows for derivation of low-order models conforming with the Occam's razor rule.

The important point when using the ML-based method is to ensure that enough training samples are available so that the underlying pdf can be accurately estimated. This is however, a limitation on a wide variety of classifiers.

### 7.2.5 Classification of Simulated Transients Using a PNN

As mentioned earlier in our discussion of classification methods, a probabilistic neural network is an implementation of the Bayes rule with the Parzen pdf estimation embedded in it. The beauty of a PNN is in the fact that depending on the selection of the window-width parameter(s) it can resemble anything ranging from a nearest neighbor

classifier to overly smooth pdfs. The challenge in using a PNN is to find suitably optimal values for these window-width parameters. PNNs have been used by Chen [Chen01] for the classification of power system transients. Although we have been able to obtain a very high correct-classification rate using the previously presented ML-based Bayes rule, it is worthwhile to consider the PNN option as it provides us with opportunity to (i) assess the performance of our approach to that of the previous work, and (ii) compare the performance with that of the ML-based Bayes rule, which can prove to be useful in advising the user as to which method has superior performance in the task given.

We will follow the same approach as presented earlier for the combined features, and will use 40 samples from each class for the training and 80 samples per class for the testing of the classifier. Table 7.6 shows a summary of the training phase of the PNN, including the starting and final values of the window-width parameters.

**Table 7.6** Data for the training phase of a PNN.

| **Initial Values of the Window-Widths ($\sigma_1$, $\sigma_2$, $\sigma_3$)** | | |
|---|---|---|
| 0.05 | 0.1 | 0.2 |
| **Final Values of the Window-Widths ($\sigma_1$, $\sigma_2$, $\sigma_3$)** | | |
| 0.001378 | 0.089746 | 0.189898 |

| **Total Calculation Time [sec]** | **Number of Iterations** |
|---|---|
| 316.4 | 95 |

The training of the PNN is done in 316.4 seconds (see Table 7.6) on an Intel Centrino 1.6 GHz processor with 512 Mb of RAM. In order to ease the burden of the optimization of the window-widths, the input data (features) have been normalized by their mean values. This causes the values to be numerically comparable, thus improving the numerical stability of the optimization algorithm. Tables 7.7 and 7.8 show the PNN classification results for both the training and testing sets.

**Table 7.7** PNN classification results for the training set.

| **Test Sample Class** | **Assigned Class** | | |
|---|---|---|---|
| | Capacitor Switching | Faults | Breaker Operations |
| Capacitor Switching | **39 (97.5%)** | 1 (2.5%) | 0 (0%) |
| Faults | 0 (0%) | **37 (92.5%)** | 3 (7.5%) |
| Breaker Operations | 0 (0%) | 2 (5%) | **38 (95%)** |

**Table 7.8** PNN classification results for the testing set.

| **Test Sample Class** | **Assigned Class** | | |
|---|---|---|---|
| | Capacitor Switching | Faults | Breaker Operations |
| Capacitor Switching | **73 (91.25%)** | 4 (5%) | 3 (3.75%) |
| Faults | 0 (0%) | **72 (90%)** | 8 (10%) |
| Breaker Operations | 2 (2.5%) | 10 (12.5%) | **68 (85%)** |

### 7.2.6 Discussion on the PNN Classification of Simulated Data

The PNN, as discussed in Ch. 5, is a unified approach to classification. Using the Parzen pdf estimation method, it estimates the underlying pdfs in a classification problem and implements it as a neural network.

The experimental results reported before do reveal important properties of PNN classifiers. As shown a PNN needs a fairly burdensome training, which in our case took more than five minutes. In comparison to the ML-based Bayes rule, which as indicated before takes only a fraction of a second to optimize, this longer training time is a serious drawback. Another important observation is that despite significant computational intensity during its training, the PNN still fails to produce as accurate results as the ML-based Bayes rule. This could be explained by nothing that the PNN imposes the same window-width for each of the features in all classes involved. In the ML-based Bayes rule method, each feature in each class has a different distribution; however, the PNN assumes that a given feature has the same $\sigma$ in all classes, which does not necessarily hold in all cases. The optimization carried out during the training, aims at finding a suitable value for each $\sigma$ so that the best tradeoff is achieved; however, this tradeoff can sometimes result in a loss of accuracy. For example, the feature 'moment 1' obtained from the VFDT analysis does not show the same scattering in the three classes of transients (see Fig. 7.7).

In other research works in this area, PNNs have been used for the classification of transients in power systems [Chen01]. The experimental results presented in that work show slightly higher classification rates; however, the training set in that work has had

much more samples than the training set in this work and also it had a different set of samples from different classes of transients; besides the classification in that work was carried out using 60 features, which is by far larger than the number of features used here. As mentioned earlier, the number of training samples are selected intentionally fairly low to comply with the lack of an abundant training set in practice.

Despite its less accurate performance in this work, PNNs do provide a powerful means for classification of patterns where a large number of features are used. In such cases, the ML-based Bayes rule requires an overly large number of pdfs to be estimated that can potentially reduce the classification performance; however, the PNN is a convenient, easy to implement method especially if the training set has an adequately large number of samples.

## 7.3 Experimental Results Using Recorded Transients

The experimental results obtained using the simulated data provide a confidence level as to how effective our methods will be when applied to data obtained using field measurement. The overall design of the power system transient detection, characterization and classification unit has been done on simulated data, which is safe, fairly accurate and inexpensive to obtain. However, the final stage of the design will focus naturally on its performance on real data. Further adjustments and modifications will be introduced as necessary.

The recorded data used in this research has been obtained from Manitoba Hydro. The data belongs to the Manitoba Hydro system at various locations and different times of the year. Hydro has several recording facilities that record the transients in the system;

however, labeling of the data has been started recently and as such the volume of the labeled recoded data available to the researchers is not very high. Besides, a large number of transients are caused by severe weather conditions and in the absence of such extreme cases some specific types of transients may not have more than a few occurrences. This also puts further limitations on the training samples in our experimentation with real data.

Table 7.9 shows a summary of the recorded data made available by the Manitoba Hydro, including the type and number of samples of each transient. The sampling frequency used for recording the transients is equal to 5760 Hz.

**Table 7.9** Recorded transients obtained from Manitoba Hydro.

| Type of Transient | Number of Samples |
|---|---|
| Bird | 24 |
| Lightning | 15 |
| Storm | 12 |
| Switching | 5 |
| Mis-Operation (No Fault) | 2 |

Figures 7.11 (a-e) shows samples of recorded transients. In the following, we consider the feature extraction and classification of these recorded data. Of special interest will be the selection of features and also selection of an appropriate feature extraction method.

### 7.3.1 Extraction of Features from Recorded Transients

The simulated data used in the previous sections was created for three classes of transients that are different from the real data obtained. Careful consideration of the recorded transients reveals that the number of samples available in the classes of mis-operation and switching is inadequately small so that development of a pdf for these classes becomes impossible. In other words, the insufficient number of samples in these two classes does not permit the distribution of other samples in this class to be discovered. Therefore, any attempt for establishment of a feature extraction method and the subsequent classification using such data will be pointless. Our focus will therefore be on the remaining three classes; i.e., bird, lightning and storm.

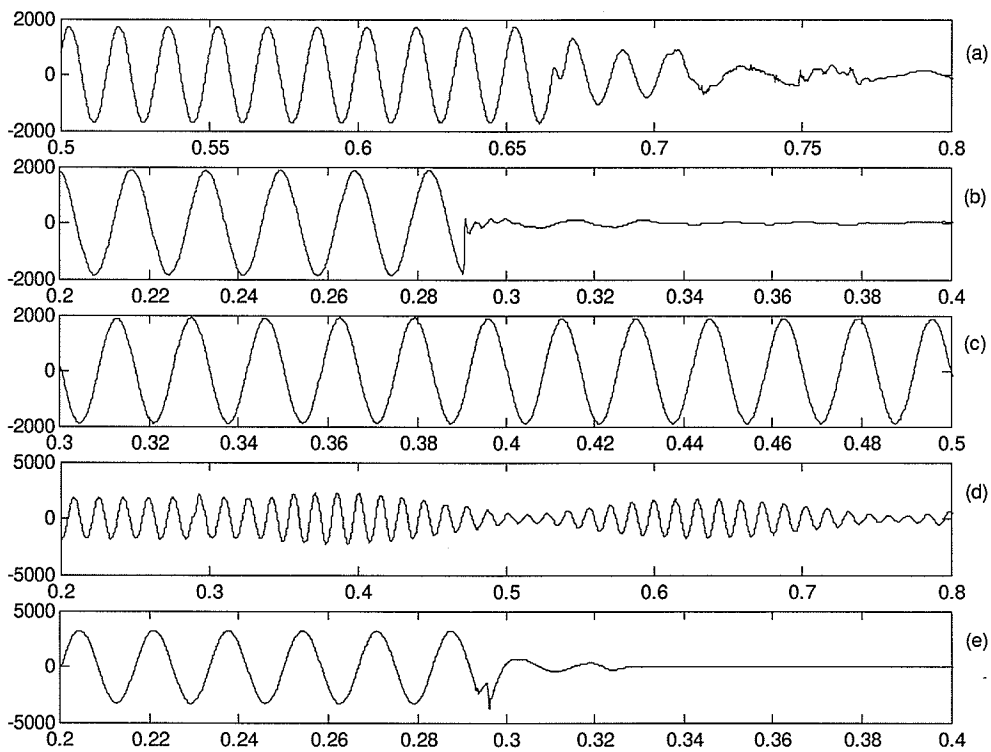


**Fig. 7.11** Samples of recorded transients.
(a) Bird; (b) Lightning; (c) Storm; (d) Mis-operation; (e) Switching.

The three classes mentioned above have marginally enough number of samples to make an initial attempt for classification possible. Further examination of the transients in this class also reveals that the class of storms represents a totally distinguishable pattern from the other two classes. Transients in this class are characterized by having small variations in the voltage magnitude and the distortion is mainly affecting the harmonic content of the waveform. Such distinguishable patterns make separation of the class of storm very straightforward, and as such the challenge remains on how the transients caused by bird or lightning strike can be separated.

Since the classes of recorded data are different from the classes of simulated data, it is always intriguing to re-consider the feature extraction in order to ensure that features that are most readily accessible have been considered as well. At first sight, it is observed that the transients caused by lightning and bird strikes cause significant changes in the voltage levels. It therefore seems reasonable to consider the variations of the power through the line due to the changes in the voltage to see how viable it could be to be used as a feature. Although the load characteristics are essential in the power delivered to them, initially, we can assume that average power is proportional to the square of the voltage. Figure 7.12 shows the variations of the *average power* during the transient caused by a bird striking the line. The average power signal (i) has by far fewer samples than the original signal, as the samples in every period of the waveform are condensed in a single number, and (ii) has much smoother variations due to the integration involved.

Despite these properties, the average power waveform fails to act as suitable feature, because (i) calculation of the average power is done over a period and as such a considerably large amount of delay is introduced, which makes the overall scheme unfit

for real-time applications, (ii) the averaging involved does eliminate some of the important details of the waveform that makes classification very difficult. For example note that the average power for the classes of bird and lightning strikes will not be different completely as both classes present a quick interruption of the voltage following the transient.

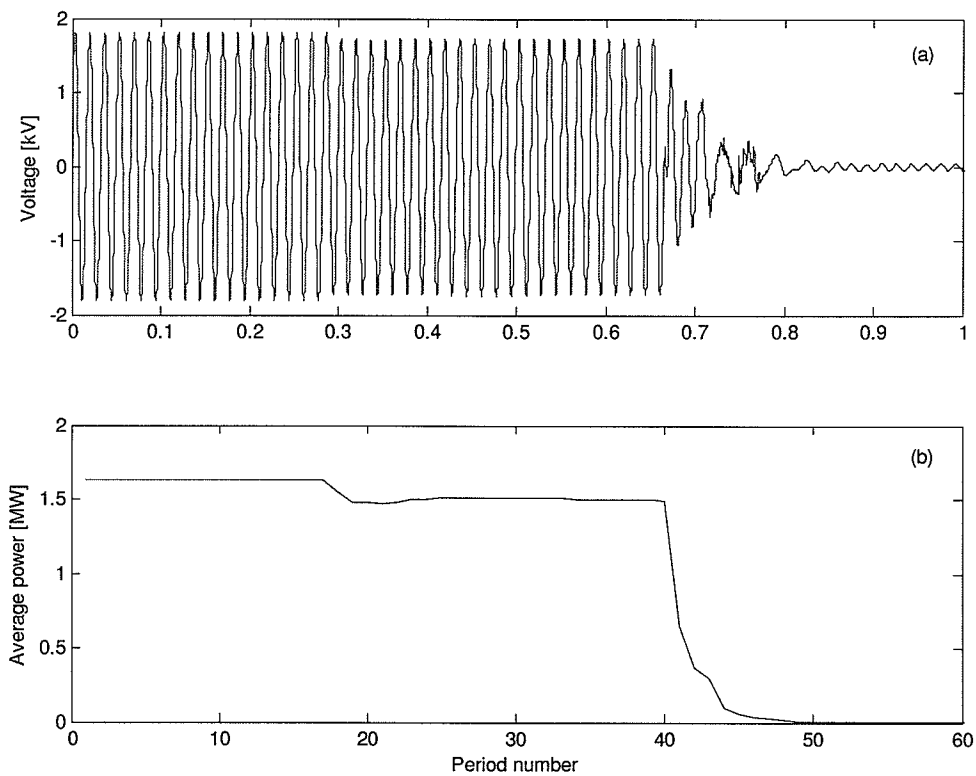


**Fig. 7.12** Average power variations.
(a) Transient waveform; (b) Average power waveform.

Although the average power does not seem to be a suitable feature, other physical properties of transients could be considered. To extract as much information from the physical properties of signal as possible, we considered two other factors: the initial voltage and the duration of the transient. Figure 7.13 shows how these two indices are

calculated for a typical waveform in the two classes of interest. Table 7.10 shows statistical properties of these two indices in the classes of bird and lighting strikes.

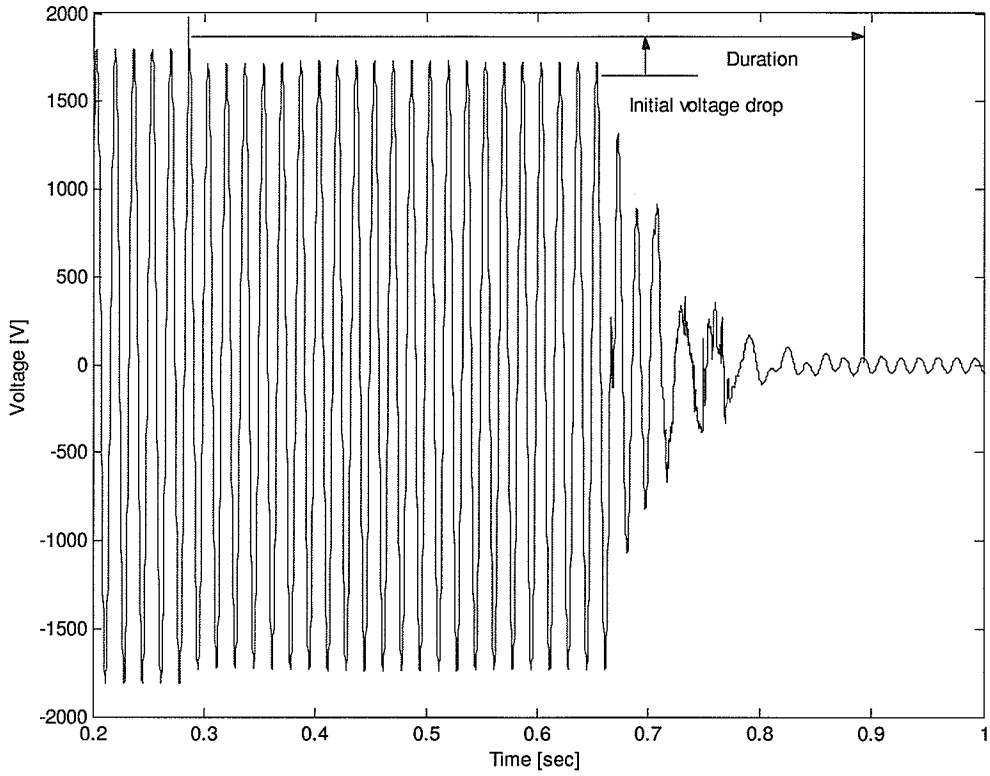


**Fig. 7.13** Calculation of duration of and initial voltage drop caused by a transient.

**Table 7.10** Statistical properties of the duration and initial voltage drop.

| Class/Feature Identifier | | Min | Max | Mean |
|---|---|---|---|---|
| **Bird** | Initial Voltage Drop [V] | 10 | 300 | 97.08 |
| | Duration [sec] | 0.38 | 0.82 | 0.63 |
| **Lightning** | Initial Voltage Drop [V] | 10 | 1700 | 499 |
| | Duration [sec] | 0.17 | 0.78 | 0.45 |

Distribution of these two features is shown in Fig. 7.14. As shown these physical features can partially separate the two classes despite the fact the overall trend of transients in these two classes are very similar. Another important observation in Fig. 7.14 is that the transients in the class of bird tend to be slower (with longer durations) and less severe (in terms of the initial voltage drop) than those caused by the lightning strike. Such observations agree with intuitive impressions that suggest lightings should be typically faster and more severe than bird strikes.

It should also be mentioned that the same features could also be extracted for the class of storms. This class is characterized by having very small voltage drops and very long durations (with a mean duration of 1.66 sec), which once again confirms that this class is entirely separable from the two classes of bird and lightning strikes.

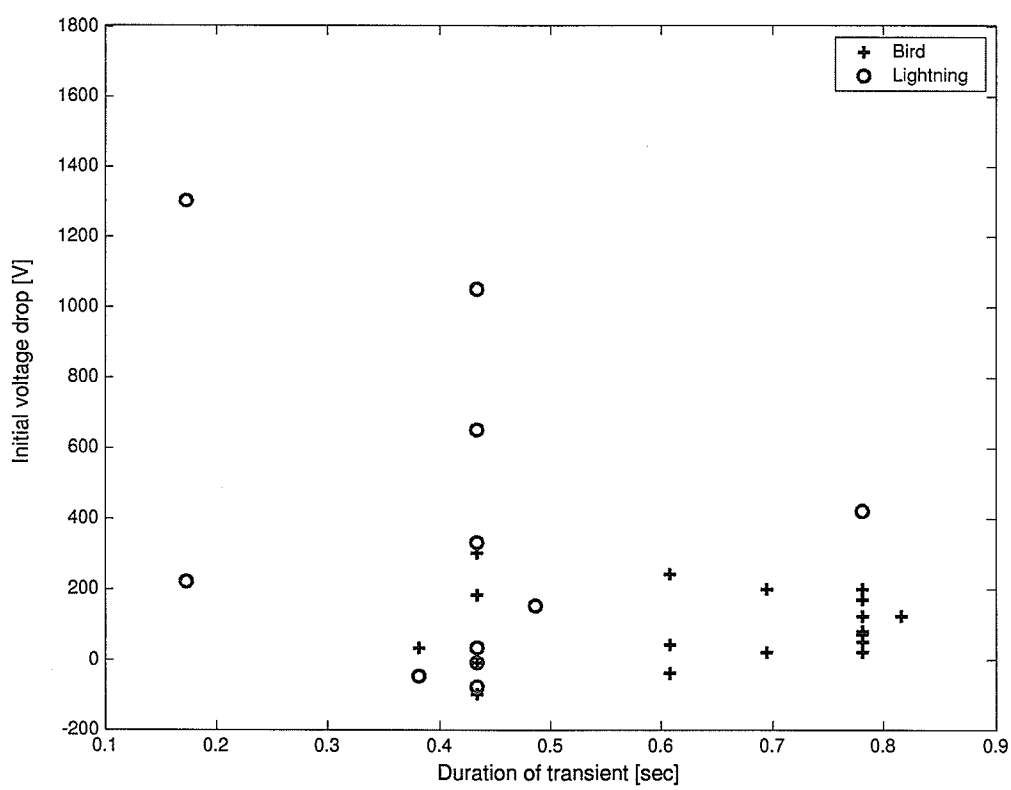


**Fig. 7.14** Distribution of the physical samples for the classes of bird and lightning.

The two physical features extracted are successful partially in separating the two most challenging classes of the recorded data; however, it is observed that the two classes still have some overlap, which contributes to the classification error. To improve the performance of classification, it is necessary to add other features that can contribute further to the separation of samples (see below for numerical results). Experimental results using these combined approaches are reported in the following section.

### 7.3.2 Classification of Recorded Transients

The methods presented in Ch. 6 are suitable techniques for classification of patterns based on features extracted from samples. Despite their similar function, which is assignment of an input sample to a given class, they possess different properties that make them suitable for only a limited number of classification problems. In other words, selection of a classification method should only be done with careful consideration of properties of the underlying problem as well as capabilities of the method itself.

In general, the ML-based Bayes rule and the PNN are aimed at estimating the pdfs of the underlying classes, and this is done through analysis of the distribution of samples belonging to each class. The procedure therefore, requires a certain amount of input data before an accurate estimation of the pdf could be obtained. The recorded data in this research, as indicated in Table 7.9, has very limited number of samples per class, which is insufficiently low for estimation of the pdfs, thus making the ML-based Bayes rule and the PNN impractical options.

A feasible method for pattern classification when the number of samples is not large enough to make estimation of parameters possible is the nearest neighbor classification

method. Since individual samples have enough contribution in the final decision-making process, the 1-NN classifier can provide a more reliable means for classification in the presence of a small training set. In the following, classification results of the recorded data for various combinations of features are reported. It should be noted that since the number of samples in the classes of mis-operation and switching transients are extremely small, the performance of the classifier is not tested for them as such numerical values could be misleading drastically.

The procedure for testing is similar to a PNN, where a given sample is expected to be identified by its peers belonging to the same class. Therefore, testing happens for all 24 samples of the class of birds and 12 samples of the class of lightning. As before, the features are normalized by their mean to yield a more numerically well-posed condition.

**Table 7.11** 1-NN classification results for voltage drop and duration used as features.

| **Test Sample Class** | **Assigned Class** | | |
|---|---|---|---|
| | Bird | Lightning | Unclassified (tie) |
| Bird | **16 (66.67%)** | 4 (16.67%) | 4 (16.67%) |
| Lightning | 6 (40%) | **9 (60%)** | 0 (0%) |

As shown the physical features cannot provide desirable separation between the classes. This is the main incentive why advanced signal analysis techniques, such as the VFDT and wavelet analyses presented in previous chapters, should be used to enhance the performance of our classifier.

**Table 7.12** 1-NN classification results for VFDT-moment 1, voltage drop and duration used as features.

| Test Sample Class | Assigned Class | | |
|---|---|---|---|
| | Bird | Lightning | Unclassified (tie) |
| Bird | **20 (83.33%)** | 4 (16.67%) | 0 (0%) |
| Lightning | 6 (40%) | **9 (60%)** | 0 (0%) |

**Table 7.13** 1-NN classification results for VFDT-moment 1, VFDT-moment 2, voltage drop and duration used as features.

| Test Sample Class | Assigned Class | | |
|---|---|---|---|
| | Bird | Lightning | Unclassified (tie) |
| Bird | **20 (83.33%)** | 4 (16.67%) | 0 (0%) |
| Lightning | 6 (40%) | **9 (60%)** | 0 (0%) |

Since the VFDT-moment 2 does not improve the results, it is not used along with the wavelet-based feature, whose results are in Table 7.14.

**Table 7.14** 1-NN classification results for wavelet-rms, VFDT-moment 1, voltage drop and duration used as features.

| Test Sample Class | Assigned Class | | |
|---|---|---|---|
| | Bird | Lightning | Unclassified (tie) |
| Bird | **21 (87.5%)** | 3 (12.5%) | 0 (0%) |
| Lightning | 4 (26.67%) | **11 (73.33%)** | 0 (0%) |

### 7.3.3 Discussion on the Feature Extraction and Classification of Recorded Data

The recorded data of transients in the Manitoba Hydro system proved to be an interesting and important portion of this research project. We discussed how physical properties of transients could assist us in the task of classification; however, improvement of the performance does require advanced signal processing techniques, such as the ones developed throughout the previous chapters. Examination of the experimental results obtained reveals that the classification rate for recorded data is lower than the simulated ones. The main reason for this is the fact that the number of samples of recorded data is very low, thus making the estimation of the underlying distributions almost impossible. The nearest neighbor classifier used performs appreciably higher for the class of bird-caused transients, as this class has a larger number of samples, which increases the chance of correct estimation.

Another issue that plays an important role in the classification is the quality of the samples. Since the recorded data have a very high signal to noise ratio (SNR), they are used directly for feature extraction. Analysis of the sensitivity to white and coloured noise has been reported in previous work and confirms that the developed methods are robust in noisy environment [Chen00]. The recorded data obtained from Manitoba Hydro is labeled according to the cause of transients observed in the network. In a power system protection setting, such labeling does not yield much valuable information as it does not provide the operator or the protection systems with an indication whether the transient is due to a severe event that requires immediate attention or by a planned operation that will affect transiently the system voltage and current waveforms. For example, in a practical power system protection scheme, separation of the two classes of birds and lightings (as

done here) has little practical significance, as both events have caused service interruption. In other words, a better scheme for labeling will be to determine whether a transient is an indication of a low-risk or a high-risk event so that proper remedial action could be initiated.

Despite the above-mentioned issues, the feature extraction and classification methods used demonstrate reasonably high performance, which can be improved by using larger training sets.

## 7.4 Chapter Summary

This chapter dealt with the experimental results obtained using the mathematical tools developed for extraction of features and classification of transients in power systems. The chapter included a comprehensive treatment of the simulated data as well as the results obtained using the developed techniques on the real transient recordings obtained from Manitoba Hydro.

The experimental results presented throughout this chapter do prove the suitability of our methods for correct classification of transients. It was shown that the ML-based Bayes rule and the PNN are suitable options when the training data set has enough number of samples to ensure proper estimation of the underlying pdfs. It was also shown that the PNN had slightly lower performance in classification than the Bayes rule; however it is a prime option is classification of pattern that have large number of samples, as it has a fairly straightforward training phase and typically has good performance.

Our experiments with the recorded data showed that physical properties of waveforms can sometimes be used in classification; however, improvement of the performance necessitates their combination with the features obtained using advanced signal analysis techniques.

It was also observed that the nearest neighbor classifier is a feasible option in classification cases where the size of the training set is inadequate for methods based on pdf estimation. The impact of the size and quality of the training set was demonstrated by the higher classification rate in the class of birds as this class had a larger number of training samples.

# CHAPTER VIII

# CONCLUSIONS AND RECOMMENDATIONS

## 8.1 Conclusions

The objective of the research undertaken through this project was to develop new techniques and to improve existing methods for extraction of features and classification of transients in power systems. Such a system can be an essential part of an intelligent power system protection scheme, and can significantly contribute towards improvement of the quality of electric power delivery, by increasing the accuracy of the protection system in identifying the true cause of transients and reducing their adverse impact.

The approach adopted for the development of such a system, was to use firstly simulated transient waveforms, and subsequently to use recorded transients obtained from Manitoba Hydro. The overall system has two major components, namely the feature extraction and the classification units.

### 8.1.1 Feature Extraction

Wavelet and multifractal analyses were used to extract features from simulated transients. These two methods offer excellent capability for characterizing complex non-stationary signals, such as transients in power systems. Wavelet analysis can provide a multi-resolution image of the signal that adapts itself to the varying complexity of signals and provides invaluable information about the frequency and time content of transients. The thesis discussed, in detail, the major aspects that need to be taken into consideration for selection of a mother wavelet. In particular, DB4 wavelet family was implemented

using a filter bank structure and was used for characterization of transients. One level of detail was derived from the transient waveforms and was then condensed into its RMS value, which was used as one of the features in the classifier.

Another signal analysis tool, namely the variance fractal dimension trajectory (VFDT) was used in conjunction with wavelets for improvement of the quality of the features extracted. In total, 30 overlapping windows (with 50% overlap) were selected along the transient portion of the waveform. The trajectory of the variance fractal dimensions calculated was condensed subsequently into two features, namely the first and second moments of the dimensions.

Selection of these two techniques has enabled us to characterize the transient signals from two different, yet complementary, points of view, which gives this study conducted a leading edge over other studies in this area.

For both wavelet and multifractal analyses, a preceding phase-locked loop (PLL) was deployed to extract the transient section of the waveform. As a result of these two techniques, a total of three features were extracted from each simulated transient. From the total number of 360 simulated transients for the three classes of capacitor switchings, faults and breaker operations, 120 (40 per class) samples were used for training of two classifiers: an ML-based Bayes rule and a PNN.

### 8.1.2 Classification

The ML-based Bayes rule produced an average accuracy of 82.92% with the VFDT-based features, an average accuracy of 96.25% with the wavelet features and 100% with

the combined features. The PNN yielded an average accuracy of 95% with the training set and 88.75% with the testing set of data.

The lower accuracy of the PNN could be attributed to the single window-width parameter that is imposed on each feature in various classes. Although different features still have different window-widths, this still could restrict the accuracy of estimation. Although the ML-based Bayes rule could produce results of higher accuracy, users should be cautioned about the growing computational burden of this method, when the number of features or number of classes increases. Under such circumstances, the number of pdfs to be estimated grows so large that makes the task of pdf estimation very inconvenient. For such cases, a more viable approach will be to use the PNNs, which provide more convenience in training.

Once the algorithms were tested and verified on the simulated data, their performance was considered on the recorded data as well. Unfortunately the recoded data obtained from Manitoba Hydro had very few samples in most of the 5 classes, such that any extrapolation using classification techniques would be premature at this stage.

The three classes with the largest number of features were the transients caused by bird and lightning strikes and storms. The class of storm had completely distinguishable features that made it completely separable from the remaining two classes. The challenge therefore was in classifying the samples from the bird and lightning transients. The treatment started with examination of physical features, namely the duration and initial voltage drop, and was then supplemented by features extracted from VFDT and wavelets. The viable option for classification cases where inadequate samples exist to enable

estimation of pdfs is the *k*-NN. Classification resulted in an average accuracy of 64.1% with the physical features, 74.36% with the physical and VFDT features and 82% with the physical features along with wavelet and VFDT features.

Careful examination of the results reveals that the results of classification are less accurate for the class of lightning, which has by far fewer samples than the class of bird, thus making estimation very difficult.

With consideration of the effectiveness of the methods developed and significance of the results, it could be concluded that the objectives of the research project are fully met. The following section summarizes the most notable contributions of the thesis.

## 8.2 Thesis Contributions

The thesis has made several important contributions to its respective area, including:

a) A rich library of simulated transient was created using the PSCAD/EMTDC transient simulation program. The simulated transients are faithful replicas of actual transients in a real power system; the set of simulated transients can serve as a reliable resource for further studies involving power system transients;

b) Segmentation of the transient section of a waveform has been done successfully using a phase lock loop (PLL) module;

c) The VFDT method has been implemented successfully for extraction of suitable features from transients;

d) A comprehensive study of influential properties of various mother wavelets has been done, which sheds light on the important issues of selection of a suitable wavelet family for transients in power systems;

e) Wavelet transform of power system transients has been conducted successfully;

f) Feature reduction has been successfully done, with significant improvement over previous works in this area (the work by Chen [Chen01] used a total of 60 features for classification);

g) Three different classifiers have been implemented and used for classification of transients and comparative studies have been made;

h) Classification has been done using various combinations of features providing a quantitative measure of the effectiveness of individual features in characterizing transients;

i) Recorded transients have been used for the verification of the effectiveness of the algorithms for feature extraction along with the 1-NN classifier;

## 8.3 Recommendations for Future Work

Although the research conducted and reported in this thesis has resulted in favorable outcomes, the topic could greatly benefit from further research and development in the areas recommended below:

a) Recorded transients, feature extraction and their classification require further consideration before practically applicable outcomes could be obtained; therefore, further research is deemed to be necessary on real data;

b) Communication with Manitoba Hydro and other utilities could improve the manner in which transients are recorded and labeled;

c) The theoretical work in the area seems to have reached enough maturity to allow focusing on the development of a practical hardware setup for using the recorder information for the purpose of feature extraction and classification. Such a system can be used ultimately as an integral part of an intelligent protection system;

d) Development of a user-friendly interface between the computational engines for feature extraction and classification can enhance the ease with which the studies can be conducted.

# REFERENCES

[Bish95] C. M. Bishop, *Neural Networks for Pattern Recognition*. New York, NY: Oxford University Press, 1995, 504 pp.

[BuBa03] K. L. Butler-Puurry and M. Bagriyanik, "Characterization of transients in transformers using discrete wavelet transforms," *IEEE Trans. on Power Systems*, vol. 18, no. 2, pp. 648-656, May 2003.

[Chen01] J. Chen, "Classification of transients in power system," *M. Sc. Thesis*. Winnipeg, MB: Department of Electrical and Computer Engineering, University of Manitoba, 2001, 201 pp.

[ChKi00] J. Chen and W. Kinsner, "Multifractal analysis of transients in power systems," *Proc. IEEE 2000 Canadian Conference on Electrical and Computer Engineering,* CCECE 00 (Halifax, NS, Canada; May 7-10, 2000), vol. 1, pp. 307-311.

[Daub92] I. Daubechies, *Ten Lectures on Wavelets*. Philadelphia, PA: Capital City, 1992, 376 pp.

[DuHS01] R. O. Duda, P. E. Hart, and D. G. Stork, *Pattern Classification*. New York, NY: Wiley Interscience, 2001 (2nd ed.), 680 pp.

[EMTD03] *EMTDC Users' Guide*. Winnipeg, MB: Manitoba HVDC Research Center, 2003, 154 pp.

[FiJa02] M. A. T. Figueiredo, and A. K. Jain, "Unsupervised learning of finite mixture models," *IEEE Trans. on Pattern Analysis and Machine Intelligence*, vol. 24, no. 3, pp. 381-396, March 2002.

[GlSa87] J. D. Glover and M. Sarma, *Power System Analysis and Design*. Boston, MA, PWS Publishers, 1987, 450 pp.

[HuHH99] S. J. Huang, C. T. Hsieh, and C. L. Huang, "Application of Morlet wavelet to supervise power system disturbances," *IEEE Trans. on Power Systems*, vol. 14, no. 1, pp. 235-241, January 1999.

[HuHs02] S. J. Huang and C. T. Hsieh, "Coiflet wavelet transform applied to inspect power system disturbance-generated signals," *IEEE Trans. on Aerospace and Electronic Systems*, vol. 38, no. 1, pp. 204-210, January 2002.

[KaMI00] M. Karimi, H. Mokhtari, and M. R. Iravani, "Wavelet based on-line disturbance detection for power quality applications," *IEEE Trans. on Power Systems*, vol. 15, no. 4, pp. 1212-1220, October 2000.

[KiAg00] C. H. Kim and R. Aggarwal, "Wavelet transform in power systems, Part 1: General introduction to the wavelet transforms," *Power Engineering Journal*, vol. 14, no. 2, pp. 81-87, April 2000.

[KiAg01] C. H. Kim and R. Aggarwal, "Wavelet transform in power systems, Part 2: Examples of application to actual power system transients," *Power Engineering Journal*, vol. 15, no. 4, pp. 193-202, August 2001.

[Kins94a] W. Kinsner, "Fractal dimensions: morphological, entropy, spectrum, and variance classes," *Technical Report*, DEL 94-4. Winnipeg, MB: Department of Electrical and Computer Engineering, University of Manitoba, May 1994, 146 pp.

[Kins94b] W. Kinsner, "Batch and real-time computation of a fractal dimensions based on variance of a time series," *Technical Report*, DEL 94-6. Winnipeg, MB: Department of Electrical and Computer Engineering, University of Manitoba, May 1994, 22 pp.

[Kins95] W. Kinsner, "Self similarity: Fractals, chaos, scaling and their applications," *Technical Report*, DEL 95-2. Winnipeg, MB: Department of Electrical and Computer Engineering, University of Manitoba, January 1995, 113 pp.

[Kund95] P. S. Kundur, *Power System Stability and Control.* New York, NY: McGrawHill, 1995, 1176 pp.

[LiMo99] T. B. Littler and D. J. Morrow, "Wavelets for the analysis and compression of power system disturbances," *IEEE Trans. on Power Delivery*, vol. 14, no. 2, pp. 358-364, April 1999.

[MaAg01] P. L. Mao and R. K. Aggarwal, "A Novel approach to the classification of transient phenomena in power transformers using combined wavelet transform and neural network," *IEEE Trans. on Power Delivery*, vol. 16, no. 4, pp. 654-660, October 2001.

[Mall99] S. G. Mallat, *A Tour of Signal Processing*. San Diego, CA: Academic Press, 1999, 557 pp.

[Mand82] B.B. Mandelbrot, *The Fractal Geometry of Nature*. New York, NY: W. H. Freeman, 1982, 465 pp.

[Mast95] T. Masters, *Advanced Algorithms for Neural Networks: A C++ Sourcebook.* New York, NY: John Wiley & Sons, 1995, 448 pp.

[MaVa68] B. B. Mandelbrot and J. W. Van Ness, "Fractional Brownian motions, fractional noises and applications," *SIAM Rev.*, vol. 10, no. 4, pp. 422-437, 1968.

[MoKi97] F. Mo and W. Kinsner, "Wavelet modeling of transients in power systems," *Proc. IEEE 1997 Can. Conf. on Communications, Power and Computing* (Winnipeg, MB, Canada; May 22-23, 1997), pp. 132-137.

[Parz62] E. Parzen, "On estimation of a probability density function and mode," *Annual of Mathematical Statistics*, vol. 33, no. 3, pp. 1065-1076, September 1962.

[PaSa98] S. K. Pandey and L. Satish, "Multiresolution signal decomposition: a new tool for fault detection in power transformers during impulse tests," *IEEE Trans. on Power Delivery*, vol. 13, no. 4, pp. 1194-1200, October 1998.

[PeJS92] H. O. Peitgen, H. Jürgens, and D. Saupe, *Chaos and Fractals: New Frontiers of Science*. New York, NY: Springer-Verlag, 1992, 984 pp.

[PiBh96] P. Pillay and A. Bhattacharjee, "Application of wavelets to model short-term power system disturbances," *IEEE Trans. on Power Systems*, vol. 11, no. 4, pp. 2031-2037, November 1996.

[Rohd83] U. L. Rohde, *Digital PLL Frequency Synthesizers: Theory and Design.* Englewood Cliffs, NJ: Prentice Hall, 1983, 494 pp.

[SaKT04] L. Safavian, W. Kinsner, and H. Turanli, "Classification of transients in power systems using multifractal analysis," *Proc. IEEE 2004 Canadian Conference on Electrical and Computer Engineering,* CCECE 04 (Niagara Falls, ON, Canada; May 2-5, 2004), vol.3, pp. 1445-1448.

[SaKT05] L. Safavian, W. Kinsner, and H. Turanli, "A quantitative compression of different mother wavelets for characterizing transients in power systems," *Proc. IEEE 2005 Canadian Conference on Electrical and Computer Engineering,* CCECE 05 (Saskatoon, SK, Canada; May 1-4, 2005), pp. 1435-1438.

[SaPG97] S. Santoso, E. J. Powers, and W. M. Grady, "Power quality disturbance data compression using wavelet transform methods," *IEEE Trans. on Power Delivery*, vol. 12, no. 2, pp. 1250-1257, July 1997.

[SaSu98] T. K. Sarkar and C. Su, "A tutorial on wavelet from an electrical engineering perspective, Part 2: The continuous case," *IEEE Antennas and Propagation Magazine*, vol. 40, no. 6, pp. 36-49, December 1998.

[Shaw97] D. B. Shaw, "Classification of transmitter transients using fractal measures and probabilistic neural networks," *M. Sc. Thesis*. Winnipeg, MB: Department of Electrical and Computer Engineering, University of Manitoba, 1997, 375 pp.

[Spec88] D. F. Specht, "Probabilistic neural networks for classification, mapping or associative memory," *Proc. IEEE Intern. Conf. Neural Networks*, vol. 1, pp. 525-532, July 1988.

[Spec99] D. F. Specht, " Probabilistic neural networks," *Neural Networks*, vol. 3, pp. 109-118, 1990.

[SPGH96] S. Santoso, E. J. Powers, W. M. Grady, and P. Hofmann, " Power quality assessment via wavelet transform analysis," *IEEE Trans. on Power Delivery*, vol. 11, no. 2, pp. 924-930, April 1996.

[SSAS98] T. K. Sarkar, C. Su, R. Adve, M. Salazar-Palma, L. Garcia-Castillo, and R. R. Boix, "A tutorial on wavelet from an electrical engineering perspective, Part 1: Discrete wavelet techniques," *IEEE Antennas and Propagation Magazine*, vol. 40, no. 5, pp. 49-70, October 1998.

[Yous03] O. A. S. Youssef, "Online applications of wavelet transforms to power system relaying," *IEEE Trans. on Power Delivery*, vol. 18, no. 4, pp. 1158-1165, October 2003.

# APPENDIX A

# UP-SAMPLING AND DOWN-SAMPLING IN Z-DOMAIN

In the filter bank implementation of wavelets, up-sampling and down-sampling operators are used. It is necessary to know the input/output relationships for these two operations in the $z$-domain in order to determine the output of the filter bank in terms of the input and filters.

## A.1 Down-Sampling of a Discrete Signal

When a discrete signal is down-sampled (by a factor of two in this case), the resulting decimated signal includes alternative samples of the original one. In mathematical expressions, we have

$$y(n) = x(2n) \tag{A.1}$$

where x(n) and y(n) are the original and decimated signal, repetitively.

In $z$-domain the above expressions can be written as

$$\begin{aligned} Y(z) &= \sum_{n} z^{-n} y(n) \\ &= \sum_{m \text{ even}} z^{-m/2} x(m) \\ &= \sum_{m \text{ even}} z^{-m/2} x(m) \\ &= \sum_{m} \frac{x(m)}{2} (1 + (-1)^m) z^{-m/2} \\ &= \frac{1}{2} (X(\sqrt{z}) + X(-\sqrt{z})) \end{aligned} \tag{A.2}$$

Down-sampling occurs at every level of wavelet decomposition following the filtering of the original signal using appropriately designed low-pass and high-pass filters.

## A.2 Up-Sampling of a Discrete Signal

Up-sampling of a discrete signal can be done by inserting zeros in between alternatives samples of the original signal. Mathematically, this can be expressed as

$$y(n) = x(\frac{n}{2}) \tag{A.3}$$

In the $z$-domain the expression becomes

$$\begin{aligned} Y(z) &= \sum_n z^{-n} y(n) \\ &= \sum_n z^{-m} x(\frac{n}{2}) \\ &= \sum_n z^{-2n} x(n) \\ &= X(z^2) \end{aligned} \tag{A.4}$$

The up-sampling operator is used in the reconstruction of wavelet transform.

# APPENDIX B

# CODE STRUCTURE AND SOURCE CODE

## B.1 Code Structure for the Simulated Data

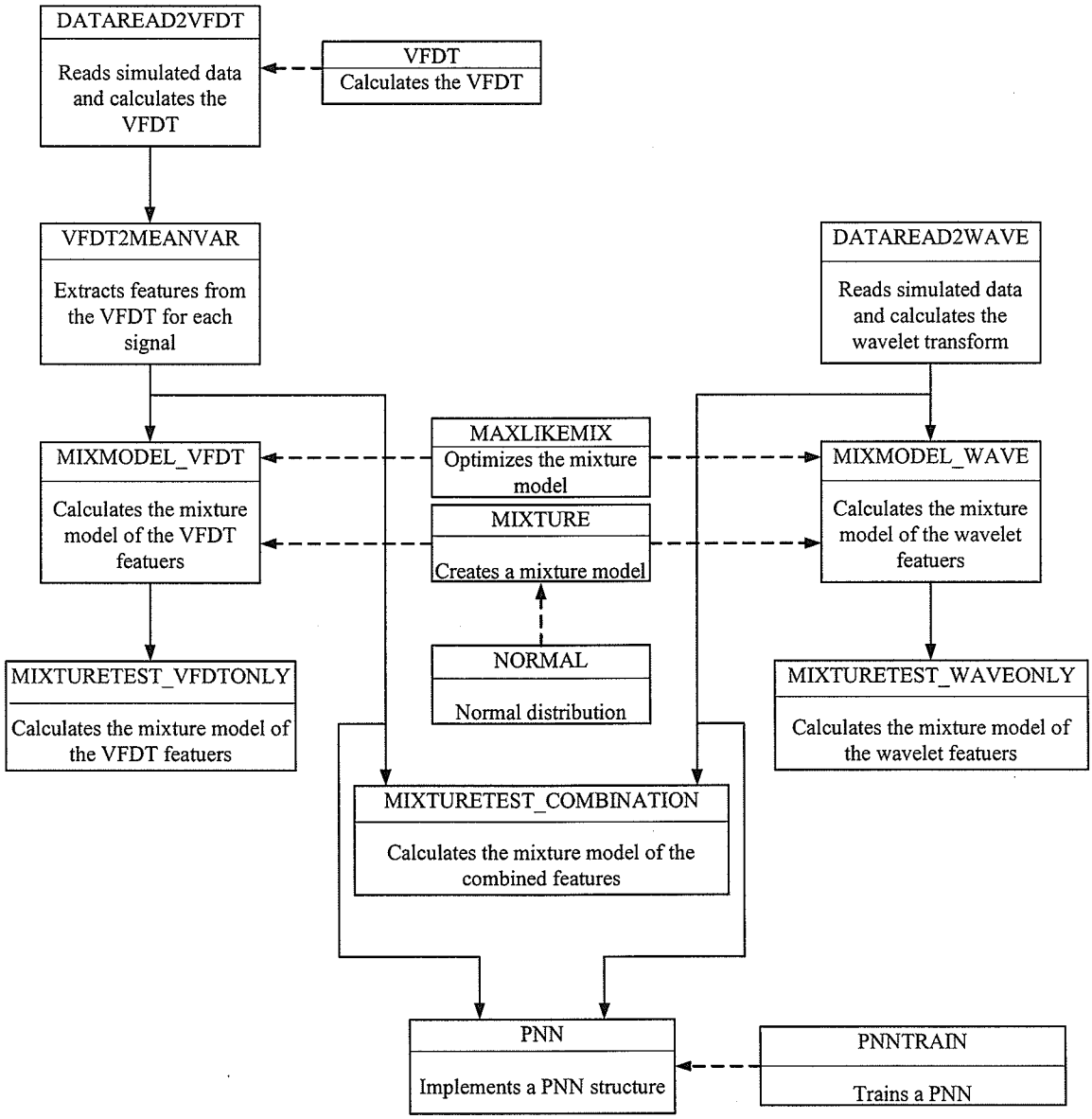

The code developed for the simulated data is based on the algorithms for feature extraction using the variance fractal dimension trajectory (Secs. 4.4 and 6.4.2) and DB4 wavelet (Secs. 3.3 and 6.4.2.2), and classification using the ML-based Bayes rule (Secs. 5.3 and 7.2.1), and probabilistic neural networks (Secs. 5.5 and 7.2.5). Simulated data (obtained using transient simulation of the sample network (see Sec. 6.2.2) in the PSCAD/EMTDC) are read into the MATLAB environment for feature extraction (using DATAREAD2VFDT and DATAREAD2WAVE scripts) as described in Chs. 3 and 4. Extraction of the first and second moments from the VFDT is done by the script VFDT2MEANVAR, as described in Sec. 6.4.2.2.

Classification of the samples can be done using either the ML-based Bayes rule or the PNN. It could involve either or both of the VFDT-based and wavelet-based features. ML_based Bayes rule (see Ch. 5) for the VFDT-based features are done using MIXMODEL_VFDT and MIXTURETEST_VFDTONLY (as described in Sec. 7.2.1). The same is done using MIXMODEL_WAVE and MIXTURETEST_WAVEONLY for the wavelet-based features (as described in Sec.7.2.2). Bayes rule for the combined features are used in the MIXTURETEST_COMBINATION. The PNN classifier (see Ch. 5) uses only the combined features and is implemented in the function PNN, which uses PNNTRAIN for the training of the classifier.

## B.2 Code Structure for the Recorded Data

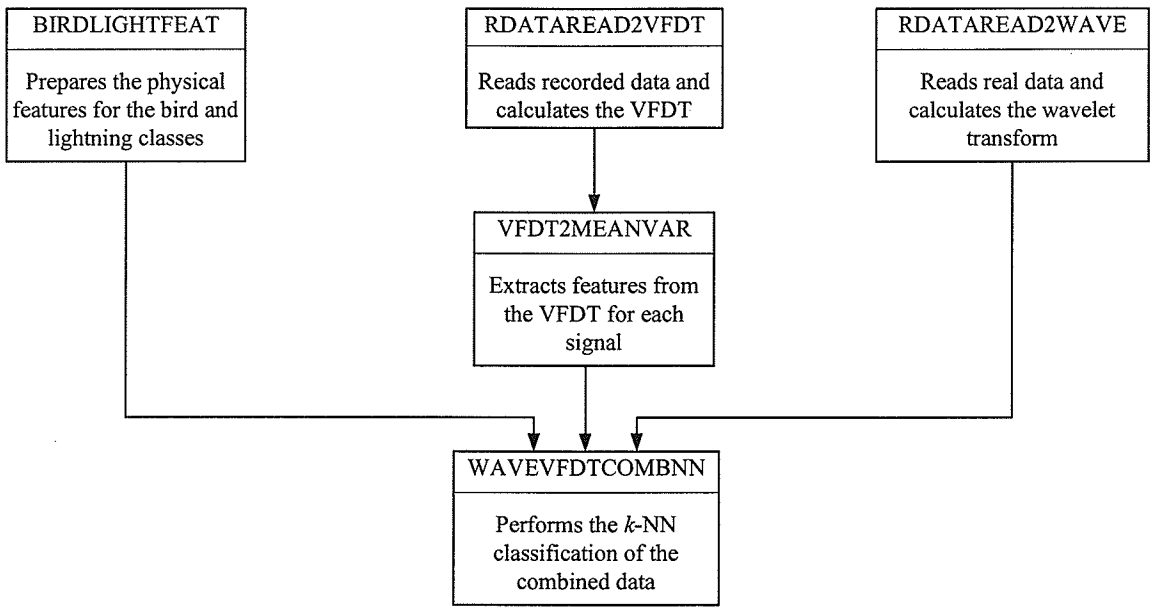


The source code for processing of the recorded transients uses physical features, as described in Sec. 7.3.1 (declared in BIRDLIGHTFEAT), VFDT-based features (obtained using RDATAREAD2VFDT and VFDT2MEANVAR), and wavelet-based features (obtained using RDATARED2WAVE). The combined features are used in a *k*-NN classifier (see Secs. 5.4 and 7.3.2) implemented in WAVEVFDTCOMBNN, in which selection of the type of combination is also permitted.

## B.3 Script DATAREAD2VFDT

```
% Script file DATAREAD2VFDT
% Input: File extension corresponding to a given class of simulated data.
% Output: The VFDT of the signal.
% Function: This script reads the simulated data and calculates its VFDT.
for j = 1 : 9
   eval(['signal = load("e:\000' num2str(j) '.brk");']);
   brk_vfdt(j , :) = vfdt(signal);
   clear signal
   j = j + 1;
end

for j = 10 : 99
   eval(['signal = load("e:\00' num2str(j) '.brk");']);
   brk_vfdt(j , :) = vfdt(signal);
   clear signal
   j = j + 1;
end

for j = 100 : 120
   eval(['signal = load("e:\0' num2str(j) '.brk");']);
   brk_vfdt(j , :) = vfdt(signal);
   clear signal
   j = j + 1;
end

% The three matrices generated by this script (you need to run it three
% times each time with the proper names for matrices), should be saved in a
% .mat file named VFDT_3class.
```

## B.4 Script VFDT2MEANVAR

```
% Script VFDT2MEANVAR
% Input: The .mat file containing the VFDT of all simulated signals.
% Output: The VFDT-based features for each sample (the .mat file vfdtfeatures).
% Function: This script loads the .mat file VFDT_3class. The .mat file contains three
% matrices: cap_vfdt, flt_vfdt and brk_vfdt, each with 120 rows and 30
% columns, being 30 fractal dimensions for 120 samples of each transient type.
%
% This script also calculates the mean and variance of each row and stores
% the results in respective matrices.

load VFDT_3class

for i = 1:120,
   mean_vfdt_cap(i) = mean(cap_vfdt(i, :));    % mean of the VFDT for class cap
   mean_vfdt_flt(i) = mean(flt_vfdt(i, :));    % mean of the VFDT for class flt
   mean_vfdt_brk(i) = mean(brk_vfdt(i, :));    % mean of the VFDT for class brk
end

for i = 1:120
   var_vfdt_cap(i) = mean(cap_vfdt(i, :).^2);  % E{x^2} for class cap
   var_vfdt_flt(i) = mean(flt_vfdt(i, :).^2);  % E{x^2} for class flt
   var_vfdt_brk(i) = mean(brk_vfdt(i, :).^2);  % E{x^2} for class brk
end

for i = 1:120
   var_vfdt_cap(i) = var_vfdt_cap(i) - mean_vfdt_cap(i)^2;  % E{x^2}-(E{x})^2 = var(x) for class cap
   var_vfdt_flt(i) = var_vfdt_flt(i) - mean_vfdt_flt(i)^2;  % E{x^2}-(E{x})^2 = var(x) for class flt
   var_vfdt_brk(i) = var_vfdt_brk(i) - mean_vfdt_brk(i)^2;  % E{x^2}-(E{x})^2 = var(x) for class brk
end

plot(mean_vfdt_cap, var_vfdt_cap, 'o', mean_vfdt_flt, var_vfdt_flt, '*', mean_vfdt_brk, var_vfdt_brk, '+')
legend('Capacitor switching', 'Faults', 'Breaker operation')
xlabel('Mean'), ylabel('Variance')

save vfdtfeatures mean_vfdt_cap var_vfdt_cap mean_vfdt_flt var_vfdt_flt mean_vfdt_brk var_vfdt_brk

%clear all
```

## B.5 Function VFDT

```
% Function VFDT
% Input: signal whose VFDT is to be calculated.
% Output: The VFDT of the signal.
% Function: The function reads in a given signal and calculates its VFDT.
function feature = vfdt(signal);

k1 = 1;
k2 = 6;
k_total = k2 - k1 + 1;
E = 1;

signal = signal( : , 2);
le = length(signal);

if mod(le,31) == 0
   le = le - 1;
end

shift_window = floor(le / 31);
window_width = floor(shift_window * 2);

last_location = le - window_width;
dimension_number = last_location / shift_window;

m = 1;
for L=1 : shift_window : last_location
  for k = k1 : k2
    sum1 = 0;
    sum2 = 0;
    nk = 2^k;
    NK = window_width - nk;
    for n = 1 : NK
      dB = signal(L+n+nk) - signal(L+n);
      sum1 = sum1 + dB * dB;
      sum2 = sum2 + dB;
    end
    varB(k) = sum1 - (sum2 *sum2) / NK;
    varB(k) = varB(k) / (NK -1);
    varB(k) = log2(varB(k));
    X(k) = k;
    Y(k) = varB(k);
  end

  s1 = 0;
  s2 = 0;
  s3 = 0;
  s4 = 0;
  for i = k1 : k2
    s1 = s1 + X(i) * Y(i);
    s2 = s2 + X(i);
    s3 = s3 + Y(i);
    s4 = s4 + X(i) * X(i);
  end
```

```
  s = (k_total *s1 - s2 *s3) / (k_total *s4 - s2 * s2);
  H = s / 2;
  D(m) = E + 1 - H;
  m = m + 1;
end

feature = D;
```

## B.6 Script MIXMODEL_VFDT

```
% Script MIXMODEL_VFDT
% Input: The VFDT features of the simulated data.
% Output: The mixture model for the VFDT-based features.
% Function: This script is used to develop the mixture model of the
% simulated data for the VFDT-based features. The outputs are the mean,
% variance and proportions of the mixture components.

%clear all, close all, clc

% load the data file and calculate the mean and var features
vfdt2meanvar;

% visualize the data (only the portion used for training, which is the
% first 40 samples is used)
figure(1), subplot(211), hist(mean_vfdt_cap(1:40), 10), title('Mean for Cap'),
subplot(212), hist(var_vfdt_cap(1:40), 10), title('Var for Cap'),
figure(2), subplot(211), hist(mean_vfdt_flt(1:40), 10), title('Mean for flt'),
subplot(212), hist(var_vfdt_flt(1:40), 10), title('Var for flt'),
figure(3), subplot(211), hist(mean_vfdt_brk(1:40), 10), title('Mean for Brk'),
subplot(212), hist(var_vfdt_brk(1:40), 10), title('Var for Brk'),

kmax = 12;
% estimate the parameters of the mean in the class of Cap
[ M_MC, S_MC, P_MC] = maxlikemix( mean_vfdt_cap(1:40), 4, [1.5 1.55 1.65 1.75], [0.01 0.02 0.01
0.01].^2, [0.5 0.25 0.1 0.15], kmax);
% estimate the parameters of the var in the class of Cap
[ M_VC, S_VC, P_VC] = maxlikemix( var_vfdt_cap(1:40), 3, [0.014 0.019 0.026], [0.002 0.002 0.003].^2,
[0.15 0.15 0.7], kmax);

% estimate the parameters of the mean in the class of Flt
[ M_MF, S_MF, P_MF] = maxlikemix( mean_vfdt_flt(1:40), 4, [1.273 1.287 1.295 1.305], [0.01 0.01 0.02
0.01].^2, [0.25 0.5 0.15 0.10], kmax);
% estimate the parameters of the mean in the class of Flt
[ M_VF, S_VF, P_VF] = maxlikemix( var_vfdt_flt(1:40), 3, [0.0145 0.0168 0.018], [0.002 0.001 0.001].^2,
[0.25 0.5 0.25], kmax);

% estimate the parameters of the mean in the class of Brk
[ M_MB, S_MB, P_MB] = maxlikemix( mean_vfdt_brk(1:40), 4, [1.28 1.295 1.305 1.31], [0.02 0.01 0.005
0.005].^2, [0.65 0.15 0.1 0.1], kmax);
% estimate the parameters of the var in the class of Brk
[ M_VB, S_VB, P_VB] = maxlikemix( var_vfdt_brk(1:40), 4, [0.015 0.015 0.019 0.022], [0.001 0.001
0.001 0.001].^2, [0.2 0.4 0.2 0.2], kmax);


x1 = 1.45:0.00001:1.85;
mean_cap_est = mixture( x1, P_MC(kmax, :), M_MC(kmax, :), S_MC(kmax, :));

x2 = 0.005:0.000001:0.03;
var_cap_est = mixture( x2, P_VC( kmax, :), M_VC( kmax, :), S_VC( kmax, :));

x3 = 1.27:0.00001:1.315;
mean_flt_est = mixture( x3, P_MF( kmax, :), M_MF( kmax, :), S_MF( kmax, :));
```

```
x4 = 0.013:0.00001:0.02;
var_flt_est = mixture( x4, P_VF( kmax, :), M_VF( kmax, :), S_VF( kmax, :));

x5 = 1.26:0.0001:1.32;
mean_brk_est = mixture( x5, P_MB( kmax, :), M_MB( kmax, :), S_MB( kmax, :));

x6 = 0.014:0.00001:0.028;
var_brk_est = mixture( x6, P_VB( kmax, :), M_VB( kmax, :), S_VB( kmax, :));

figure(4), subplot(211), hist( mean_vfdt_cap(1:40), 10), subplot(212), plot( x1, mean_cap_est), axis( [min(
x1) max( x1) 0 55])
figure(5), subplot(211), hist( var_vfdt_cap(1:40), 10), subplot(212), plot( x2, var_cap_est), axis( [min( x2)
max( x2) 0 350])

figure(6), subplot(211), hist( mean_vfdt_flt(1:40), 10), subplot(212), plot( x3, mean_flt_est), axis( [min(
x3) max( x3) 0 180])
figure(7), subplot(211), hist( var_vfdt_flt(1:40), 10), subplot(212), plot( x4, var_flt_est), axis( [min( x4)
max( x4) 0 400])

figure(8), subplot(211), hist( mean_vfdt_brk(1:40), 10), subplot(212), plot( x5, mean_brk_est), axis( [min(
x5) max( x5) 0 60])
figure(9), subplot(211), hist( var_vfdt_brk(1:40), 10), subplot(212), plot( x6, var_brk_est), axis( [min( x6)
max( x6) 0 450])

save mixmodelvfdt M_MC S_MC P_MC M_VC S_VC P_VC M_MF S_MF P_MF M_VF S_VF P_VF
M_MB S_MB P_MB M_VB S_VB P_VB

%clear all
```

## B.7 Script MIXTURETEST_VFDTONLY

```
% Script MIXTURETEST_VFDTONLY
% Input: The mixture model of the VFDT-based features.
% Output: The respective class of the input samples.
% Function: This script is used to test the mixture model obtained for either the
% training or the test set of data. The inputs to the script are the mixture
% model parameters obtained using the script mixmodel.m
% The output is a vector whose elements show the classes assigned.

% The Bayes Rule
% we use the first 300 samples (200 samples already used for training) to test the rule
% w1: fault
% w2: cap sw.

clear all, close all, clc

load vfdtfeatures
load mixmodelvfdt
% The data to be tested
xt = [mean_vfdt_brk(41:120); var_vfdt_brk(41:120)];

[kmax, m] = size(P_MC);

classofx = [];

for i = 1:80,
 P_X_w1 = mixture(xt(1, i), P_MF(kmax, :), M_MF(kmax, :), S_MF(kmax, :)) * ...
    mixture(xt( 2, i), P_VF(kmax, :), M_VF(kmax, :), S_VF(kmax, :));

 P_X_w2 = mixture(xt(1, i), P_MC(kmax, :), M_MC(kmax, :), S_MC(kmax, :)) * ...
    mixture(xt(2, i), P_VC(kmax, :), M_VC(kmax, :), S_VC(kmax, :));

 P_X_w3 = mixture(xt(1, i), P_MB(kmax, :), M_MB(kmax, :), S_MB(kmax, :)) * ...
    mixture(xt(2, i), P_VB(kmax, :), M_VB(kmax, :), S_VB(kmax, :));

  if ( P_X_w1 > P_X_w2 & P_X_w1 > P_X_w3)
     classofx(i) = 1;
  end

  if ( P_X_w2 > P_X_w1 & P_X_w2 > P_X_w3)
     classofx(i) = 2;
  end

  if ( P_X_w3 > P_X_w1 & P_X_w3 > P_X_w2)
     classofx(i) = 3;
  end

end

classofx
```

## B.8 Function MICTURE

```
% Function MIXTURE
% Input: The mean, variance, proportions and input values.
% Output: The mixture pdf evaluation.
% Function: The function implements a mixture model pdf.
function y = mixture( x, P, M, S)
% This function generates a mixture pdf of proportions P,
% menas M and variance S.
% It evaluates the mixture model at x
G = length( P); % number of mixture pdfs

y = 0;
for i = 1: G,
  y = y + P( i) * normal( x, M( i), sqrt( S( i)));
end
```

## B.9 Function NORMAL

```
% Function NORMAL
% Input: Input, mean and variance.
% Output: The pdf evaluation.
% Function: The function implements a normal pdf.
function y = normal( x, m, s)
y = 1/(sqrt(2*pi)*s)*exp(-(x-m).^2/(2*s^2));
```

## B.10 Function MAXLIKEMIX

```
% Function: MAXLIKEMIX
% Input: The initial guess values for the mixture model.
% Output: The optimized values of the mixture model.

function [ M, S, P] = maxlikemix( x, g, m, s, p, kmax)
% This m-file finds the parameters of a mixture model using the method of
% maximum likelihood.
%
% [ M, S, P] = maxlikemix( x, g, m, s, p, kmax)
% x: the samples
% g: the number of Gaussians
% p: initial guess for mixing proportions
% m: initial guess for the means
% s: initial guess for the variances (not standard deviations!)
% kmax: maximum number of iterations
%
% M: the final values of the mean values
% S: the final values of the var values
% P: the final values of mixing proportions

n = length( x);     % number of samples in x

k = 1;    % iteration number
M = m;
P = p;
S = s;
```

```
while k<kmax
  for i = 1:n,
    den = 0;
    for l = 1:g,
      den = den + normal( x(i), M( k, l), sqrt(S( k, l))) * P( k, l);
    end
    for j = 1:g,
      W( i, j) = normal( x(i), M( k, j), sqrt(S(k, j))) * P( k, j) / den;
    end
  end
  % update p, m, s
  for j = 1:g,
    P( k+1, j) = 1/n * sum( W( :, j));
    den = 0;
    for i = 1:n,
      den = den + W( i, j) * x(i);
    end
    M( k+1, j) = 1/(n*P( k+1, j)) * den;
    den = 0;
    for i = 1:n,
      den = den + W( i, j) * ( x(i) - M( k+1, j))^2;
    end
    S( k+1, j) = 1/(n*P( k+1, j)) * den;
  end
    k = k+1;
 end
 %end
```

## B.11 Script DATAREAD2WAVE

```
% Script DATAREAD2WAVE
% Input: The simulated data.
% Output: The wavelet analysis.
% Function: This script reads the transient data into MATLAB and submits them for
% wavelet analysis. The results are stored in three matrices, one
% corresponding to each class.
%
% The wavelet analysis is carried out to yield the first detail
% coefficients of the signal. They are then squared and averaged and used s
% features. So each waveforms is distilled into only one feature.
%
% the file extensions are (.cap) for capacitor switching, (.flt) for faults
% and (.brk) for breaker operations.
% For each class, a total number of 120 samples are used.

for j = 1 : 9
   eval(['signal = load("e:\000' num2str(j) '.cap");']);

   signal = signal( : , 2);
   [C , L] = wavedec(signal, 3 , 'db4');
   cD1 = detcoef(C , L , 1);
   cap_D1(j, :) = mean(cD1.^2);

   clear signal C L cD1
   j = j + 1;
end

for j = 10 : 99
   eval(['signal = load("e:\00' num2str(j) '.cap");']);

   signal = signal( : , 2);
   [C , L] = wavedec(signal, 3 , 'db4');
   cD1 = detcoef(C , L , 1);
   cap_D1(j, :) = mean(cD1.^2);

   clear signal C L cD1
   j = j + 1;
end

for j = 100 : 120
   eval(['signal = load("e:\0' num2str(j) '.cap");']);
   signal = signal( : , 2);
   [C , L] = wavedec(signal, 3 , 'db4');
   cD1 = detcoef(C , L , 1);
   cap_D1(j, :) = mean(cD1.^2);

   clear signal C L cD1
   j = j + 1;
end

% The three matrices generated by this script (you need to run it three
% times each time with the proper names for matrices), should be saved in a
% .mat file named Wavelet_3class.
```

## B.12 Script MIXMODEL_WAVE

```
% Script MIXMODEL_WAVE
% Input: The wavelet-based features.
% Output: The mixture model based on the wavelet features.
% Function: The script uses the features obtained using wavelet analysis to
% establish an ML-based mixture model for the data.

clear all, close all, clc
% load the data file that contains the wavelet data
load Wavelet_3class

% The loaded file cntains three vectors: brk_D1, cap_D1, flt_D1

% visualize the data (only the portion used for training, which is the
% first 40 samples is used)
figure(1), hist(cap_D1(1:40), 10), title('Data for Cap'),

figure(2), hist(flt_D1(1:40), 10), title('Data for flt'),

figure(3), hist(brk_D1(1:40), 10), title('Data for Brk'),

kmax = 3;
% estimate the parameters of the class of Cap
[ M_C, S_C, P_C] = maxlikemix(cap_D1(1:40), 3, [0.17 0.21 0.25], [0.02 0.02 0.001].^2, [0.8 0.15 0.05],
kmax);

% estimate the parameters of the class of Flt
[ M_F, S_F, P_F] = maxlikemix(flt_D1(1:40), 4, [0.25 0.4 0.65 0.75], [0.08 0.08 0.05 0.02].^2, [0.4 0.2 0.1
0.3], kmax);

% estimate the parameters of the class of Brk
[ M_B, S_B, P_B] = maxlikemix(brk_D1(1:40), 3, [2.5 5.0 7.0], [0.1 1.0 0.5].^2, [0.7 0.15 0.15], kmax);

% Plot the hostograms and the estimated PDFs
x1 = 0.14:0.000001:0.28;
cap_est = mixture( x1, P_C(kmax, :), M_C(kmax, :), S_C(kmax, :));

x2 = 0.1:0.000001:0.9;
flt_est = mixture( x2, P_F( kmax, :), M_F( kmax, :), S_F( kmax, :));

x3 = 1.0:0.00001:11.0;
brk_est = mixture( x3, P_B( kmax, :), M_B( kmax, :), S_B( kmax, :));

figure(4), subplot(211), hist(cap_D1(1:40), 10), subplot(212), plot(x1, cap_est), axis( [min( x1) max( x1) 0
55])

figure(5), subplot(211), hist(flt_D1(1:40), 10), subplot(212), plot(x2, flt_est), axis( [min( x2) max( x2) 0
5])

figure(6), subplot(211), hist(brk_D1(1:40), 10), subplot(212), plot(x3, brk_est), axis( [min( x3) max( x3) 0
1])

save mixmodelwave M_C S_C P_C M_F S_F P_F M_B S_B P_B
%clear all
```

## B.13 Script MIXTURETEST_WAVEONLY

```
% Script MIXTURETEST_WAVEONLY
% Input: The mixture model of the wavelet-based features.
% Output: The corresponding class of the input sample.

% The Bayes Rule
% we use the first 120 samples (40 samples already used for training) to test the rule
% w1: fault
% w2: cap sw.
% w3: breaker op.
clear all, close all, clc

load mixmodelwave
load Wavelet_3class

% The data to be tested
xt = [brk_D1(41:120)];

[kmax, m] = size(P_C);

classofx = [];

for i = 1:80,
 P_X_w1 = mixture(xt(i), P_F(kmax, :), M_F(kmax, :), S_F(kmax, :));

 P_X_w2 = mixture(xt(i), P_C(kmax, :), M_C(kmax, :), S_C(kmax, :));

 P_X_w3 = mixture(xt(i), P_B(kmax, :), M_B(kmax, :), S_B(kmax, :));

  if ( P_X_w1 > P_X_w2 & P_X_w1 > P_X_w3)
     classofx(i) = 1;
  end

  if ( P_X_w2 > P_X_w1 & P_X_w2 > P_X_w3)
     classofx(i) = 2;
  end

  if ( P_X_w3 > P_X_w1 & P_X_w3 > P_X_w2)
     classofx(i) = 3;
  end

end

classofx
```

## B.14 Script MIXTURETEST_COMBINATION

```
% Script: MIXTURETEST_COMBINATION
% Input: The mixture models of VFDT and wavelet features.
% Output:
% This script is used to test the mixture model obtained for either the
% training or the test set of data.
% The MIXTURE models obtained for the VFDT and wavelet data are used
% together.
%
% Input:
% mixmodelvfdt.mat and mixmodelwave.mat --> for the mixture models
% vfdtfeatures and Wavelet_3class for the data
clear all, close all, clc

load mixmodelvfdt
load mixmodelwave
load vfdtfeatures
load Wavelet_3class

% The data to be tested is the combination of the features
xt = [mean_vfdt_brk(41:120); var_vfdt_brk(41:120); brk_D1(41:120)'];

[k1, m] = size(P_MC);
[k2, m] = size(M_C);

classofx = [];

for i = 1:80,
 P_X_w1 = mixture(xt(1, i), P_MF(k1, :), M_MF(k1, :), S_MF(k1, :)) * ...
    mixture(xt(2, i), P_VF(k1, :), M_VF(k1, :), S_VF(k1, :)) * ...
    mixture(xt(3, i), P_F(k2, :), M_F(k2, :), S_F(k2, :));

 P_X_w2 = mixture(xt(1, i), P_MC(k1, :), M_MC(k1, :), S_MC(k1, :)) * ...
    mixture(xt(2, i), P_VC(k1, :), M_VC(k1, :), S_VC(k1, :)) * ...
    mixture(xt(3, i), P_C(k2, :), M_C(k2, :), S_C(k2, :));

 P_X_w3 = mixture(xt(1, i), P_MB(k1, :), M_MB(k1, :), S_MB(k1, :)) * ...
    mixture(xt(2, i), P_VB(k1, :), M_VB(k1, :), S_VB(k1, :)) * ...
    mixture(xt(3, i), P_B(k2, :), M_B(k2, :), S_B(k2, :));

  if ( P_X_w1 > P_X_w2 & P_X_w1 > P_X_w3)
     classofx(i) = 1;
  end

  if ( P_X_w2 > P_X_w1 & P_X_w2 > P_X_w3)
     classofx(i) = 2;
  end

  if ( P_X_w3 > P_X_w1 & P_X_w3 > P_X_w2)
     classofx(i) = 3;
  end

end
classofx
```

## B.15 Function PNN

```
% Function PNN
% Input: The input sample, sigma, trainings set and sample numbers.
% Output: The resulting output of a PNN using the parameters given in the
% input.
function g = pnn(x, sig, trset, n)
% function g = pnn(x, sig, trset, n)
%
% g = output vector -- has C elements. The largest element indicates the
% class of the input vector.
% x = input vector -- has p elements.
% sig = vector of the sigms -- has p elements.
% trset = training set -- contains the training set samples. Training
% samples are given as row vectors of length p each.
% n = vector of the number of training samples per class -- has C elements.

% Step 1: calculate the distance of the input vector x to the individual members of the training set.
% Step 2: apply the kernel function to the distances.
% Step 3: Do the summation for individual classes.

[N, p] =size(trset); % N = total number of training samples; p = number of features.
C = length( n); % total number of classes

for i = 1:N
   % calculate the distance between the input vector and the training
   % samples
   D(i) = euclidian(x, trset(i,:), sig);
end

% offset is the index number that shows the start of the samples in the
% trset vector
offset = 0;

for k = 1:C
   g(k) = 0;
   for r = 1:n(k)
      g(k) = g(k) + exp(-D(r+offset)/2.0);
   end
   g(k) = g(k)/n(k);
   offset = offset + n(k); % increment offset to shift it to the next bacth
end

function d = euclidian(x, vec, sig)
% d = distance between the vectors x and vec.
% x = vector one -- has p elements
% vec = vector two -- has p elements
% sig = vector of sigmas -- has p elements

p = length(x);
d = 0;

for i = 1:p
   d = d + ((x(i)-vec(i))/sig(i))^2;
end
```

## B.16 Function PNNTRAIN

```
% Function PNNTRAIN
% Input: The initial guess values for the sigma, as well as the training
% set and other optimization parameters.
% Output: The optimal sigma values.
function optsigma = pnntrain(insig, trset, n, ds, alpha, epsil)
% function optsigma = pnntrain(insig, trset, n, ds, alpha, epsil)
%
% optsigma = vector for the optimized sigma values -- has p elements
% insig = vector for the initial sigma values -- has p elements
% trset = training set -- contains the training set samples. Training
% samples are given as row vectors of length p each.
% n = vector of the number of training samples per class -- has C elements.
% ds = percent change in the sigmas for derivative calculation
% alpha = initial step length
% epsil = termination criterion

% Note: gradient-based optimization (with numerically evaluated
% derivatives) is used.
tic
p = length(insig); % number of features
C = length(n);  % number of classes

tempsig = insig;
%tempsig = insig.^2;

magder = 1; % initialize the magnitude of the gradient so that we enter the while loop
LC = 0; % loop counter

while (magder > epsil && LC <= 95)
   % Step 1) find the derivatives
   for i = 1:p
      sigplus = tempsig;
      sigplus(i) = sigplus(i) * (1+ds/100);
      sigminus = tempsig;
      sigminus(i) = sigminus(i) * (1-ds/100);
      %deriv(i) = (objf(sigplus.^2, trset, n) - objf(sigminus.^2, trset, n)) / (2*tempsig(i)*ds/100);
      deriv(i) = (objf(sigplus, trset, n) - objf(sigminus, trset, n)) / (2*tempsig(i)*ds/100);
   end
   % calculate the magnitude of the gradient vector
   magder = 0;
   for i = 1:p
      magder = magder + deriv(i)^2;
   end
   magder = sqrt(magder);
   deriv = deriv / magder; % normalize the derivative vector

   % Step 2: determine the step length in the opposite direction of the
   % gradient
   ak = alpha; % initialize the step length
   ak = findsteplength(tempsig, ak, deriv, trset, n);

   % Step 3: move along the direction with the step length just found
   tempsig = tempsig - ak*deriv;
```

```
  LC = LC + 1;
  info = [objf(tempsig, trset, n) LC tempsig]
end

optsigma = tempsig.^2;
toc
%==========================================================================
% The functions used in the algorithm are defined below.
%==========================================================================

function ise = objf(sig, trset, n)

% Note: n is a vector with C elements. Each element shows how many smaples
% in the training set trset belongs to each class. For example n = [ 10 20
% 12] shows that classes 1, 2 and 3 have 10, 20 and 12 samples,
% respectively.
[N, p] = size(trset);
nintopnn = n;
offset = 0;
ise  = 0;  % inittial value of the objective function
C = length(n);

for i = 1:C
  for j = 1:n(i)
    xintopnn = trset(offset+j, :); % the sample going into the pnn
    % now form the training set, which is the given (input) trset without
    % the very smaple that is used as the input.
    for k = 1:(offset+j-1)
      trsetintopnn(k, :) = trset(k, :);
    end
    for k = (offset+j+1):N
      trsetintopnn(k-1, :) = trset(k, :);
    end
    % the samples of class i are decreased by 1 as one of them is used as
    % the input; so ...
    nintopnn(i) = n(i) - 1;
    % now call the pnn to see the respective output when the j-th
    % sample of the i-th class is presented to the network.
    G = pnn(xintopnn, sig, trsetintopnn, nintopnn);
    % update the objective function
    for i1 = 1:C
      q(i1) = G(i1)/sum(G);
    end
    for i1 = 1:C
      if i1==i
        %cccccccccccccccccccccccccccccccccccccccccccccccccccccccccccccccccccccccccc
        ise = ise + (1-q(i1))^2;
        %ise = ise + abs(1-q(i1));
      else
        ise = ise + q(i1)^2;
        %ise = ise + abs(q(i1));
        %cccccccccccccccccccccccccccccccccccccccccccccccccccccccccccccccccccccccccc
      end
    end
  end
  offset = offset+n(i);
```

```
   nintopnn = n;
end

%=====================

function anew = findsteplength(sig, aold, deriv, trset, n)

anew = aold;
while anew >= 0.0001
   % if the step length is less than 0.0001, we stop
   sigtemp1 = sig - anew*deriv;
   %if objf(sigtemp1.^2, trset, n) < objf(sig.^2, trset, n)
   if objf(sigtemp1, trset, n) < objf(sig, trset, n)
      sigtemp2 = sig - 1.5*anew*deriv;
      %if objf(sigtemp2.^2, trset, n) < objf(sigtemp1.^2, trset, n)
      if objf(sigtemp2, trset, n) < objf(sigtemp1, trset, n)
         anew = 1.5*anew;
         return
      else
         return
      end
   else
      sigtemp2 = sig - 0.5*anew*deriv;
      %if objf(sigtemp2.^2, trset, n) < objf(sig.^2, trset, n)
      if objf(sigtemp2, trset, n) < objf(sig, trset, n)
         anew = 0.5*anew;
         return
      else
         anew = 0.25*anew;
         continue
      end
   end
end
```

## B.17 Script BIRDLIGHTFEAT

```
% Script BIRDLIGHTFEAT
% Input: None.
% Output: The features obtained using physical properties of bird and
% lightning classes.
% This m-file contains the visually extracted features from the classes of
% bird and lightning.

clear all, clc

% Duration of the transients in the class of bird
bdu = [6000-1500, 6000-1500, 4000-1500, 6000-3800, 6000-1500, 6000-1500, 6000-1300, 5500-1500, ...
      6000-1500, 4000-1500, 4000-1500, 4000-1500, 4000-1500, 4000-1500, 6000-1500, 6000-1500, ...
      5000-1500, 5000-1500, 6000-2000, 6000-1500, 6000-1500, 6000-1500, 5000-1500, 4000-1500] /
5760;

% Initial voltage drop in the class of bird
bvd = [1800-1730, 1800-1720, 1800-1620, 1800-1770, 1800-1730, 1800-1680, 1800-1680, 1800-1600,
1800-1600, 1800-1900, ...
      1800-1810, 1800-1810, 1800-1500, 1800-1810, 1800-1630, 1800-1750, 1800-1760, 1800-1840, 1820-
1800, ...
      1800-1720, 1800-1780, 1800-1680, 1800-1560, 1800-1810];

% Duration of the transients in the class of ligthning
ldu = [2500-1500, 2800-600, 4000-1200, 6000-1500, 6000-1500, 4000-1500, 4000-1500, 4000-1500, 4000-
1500, ...
      2500-1500, 4000-1500, 4000-1500] / 5760;

% Initial voltage drop in the class of lightning
lvd = [2000-700, 1950-2000, 1900-1750, 1800-100, 1950-1530, 1900-1250, 1830-1500, 1850-800, 1930-
1900, ...
      1830-1610, 1800-1810, 1800-1880];

save phyfeatures bdu bvd ldu lvd

figure (1),
plot( bdu, bvd, '+', 'linewidth', 2), hold, plot( ldu, lvd, 'ro', 'linewidth', 2),
xlabel('Duration of transient [sec]'), ylabel('Initial voltage drop [V]')
legend('Bird', 'Lightning')

% combine features with vfdt and wavelet
load wave_features
load rvfdtmv

figure (2),
plot3(bdu, wave_bird, bvd, '*', ldu, wave_light, lvd, 'o'), grid on,
xlabel('Mean'), ylabel('Duration'), zlabel('Voltage drop')
legend('Bird', 'Lightning')
```

## B.18 Function RDATA2VFDT

```
% Function RDATA2VFDT
% Input: The signal to be submitted for VFDT calculation.
% Output: The VFDT.

function sig_vfdt = rdata2vfdt(fname, a, b, kmax)
% This function reads the data file containing the recorded
% transient (given in fname) and calculates its VFDT from
% sample number a to sample number b. The sampling time is
% 1/5760 sec.
% kmax is the number of points used for the linear approximation on the
% log-log plot (is an integer and is larger than 1).

signal = load(fname);
signal = signal(a:b, :);

sig_vfdt = rvfdt(signal, kmax);

% This function should be applied on all the recorded data and the results
% should be stored for later use.
```

## B.19 Function VFDT_MVAR

```
% Script VFDT_MVAR
% Input: The VFDT of recorded signals.
% Output: The VFDT-based features.
% This script loads the .mat file rvfdt_data.
% The .mat file contains six matrices:
% vfdt_bird [24*30], vfdt_light [12*30], vfdt_storm [12*30], vfdt_tran
% [10*30], vfdt_swit [4*30], vfdt_nflt [2*30]
%
% This script also calculates the mean and variance (and more) of each row and stores
% the results in respective matrices.
%
% Output: the mat-file rvfdtmv

clear all, clc, close all

load rvfdt_data

for i = 1:24,
   mean_vfdt_bird(i) = mean(vfdt_bird(i, :));    % mean of the VFDT for class bird
   var_vfdt_bird(i) = mean(vfdt_bird(i, :).^2);  % E{x^2} for class bird
end

for i = 1:12,
   mean_vfdt_light(i) = mean(vfdt_light(i, :));    % mean of the VFDT for class lightning
   var_vfdt_light(i) = mean(vfdt_light(i, :).^2);  % E{x^2} for class light
end

for i = 1:12,
   mean_vfdt_storm(i) = mean(vfdt_storm(i, :));    % mean of the VFDT for class storm
   var_vfdt_storm(i) = mean(vfdt_storm(i, :).^2);  % E{x^2} for class storm
end

for i = 1:10,
   mean_vfdt_tran(i) = mean(vfdt_tran(i, :));    % mean of the VFDT for class transient
   var_vfdt_tran(i) = mean(vfdt_tran(i, :).^2);  % E{x^2} for class tran
end

for i = 1:4,
   mean_vfdt_swit(i) = mean(vfdt_swit(i, :));    % mean of the VFDT for class switching
   var_vfdt_swit(i) = mean(vfdt_swit(i, :).^2);  % E{x^2} for class switching
end

for i = 1:2,
   mean_vfdt_nflt(i) = mean(vfdt_nflt(i, :));    % mean of the VFDT for class no fault
   var_vfdt_nflt(i) = mean(vfdt_nflt(i, :).^2);  % E{x^2} for class no fault
end

for i = 1:24
   var_vfdt_bird(i) = var_vfdt_bird(i) - mean_vfdt_bird(i)^2;  % E{x^2}-(E{x})^2 = var(x) for class bird
end

for i = 1:12
   var_vfdt_light(i) = var_vfdt_light(i) - mean_vfdt_light(i)^2;  % E{x^2}-(E{x})^2 = var(x) for class light
```

```
end

for i = 1:12
   var_vfdt_storm(i) = var_vfdt_storm(i) - mean_vfdt_storm(i)^2;  % E{x^2}-(E{x})^2 = var(x) for class
storm
end

for i = 1:10
   var_vfdt_tran(i) = var_vfdt_tran(i) - mean_vfdt_tran(i)^2;  % E{x^2}-(E{x})^2 = var(x) for class tran
end

for i = 1:4
   var_vfdt_swit(i) = var_vfdt_swit(i) - mean_vfdt_swit(i)^2;  % E{x^2}-(E{x})^2 = var(x) for class swit
end

for i = 1:2
   var_vfdt_nflt(i) = var_vfdt_nflt(i) - mean_vfdt_nflt(i)^2;  % E{x^2}-(E{x})^2 = var(x) for class no fault
end

for i = 1:24
   min_vfdt_bird(i) = min(vfdt_bird(i, :));
   max_vfdt_bird(i) = max(vfdt_bird(i, :));
end

for i = 1:12
   min_vfdt_light(i) = min(vfdt_light(i, :));
   max_vfdt_light(i) = max(vfdt_light(i, :));
end

for i = 1:12
   min_vfdt_storm(i) = min(vfdt_storm(i, :));
   max_vfdt_storm(i) = max(vfdt_storm(i, :));
end

for i = 1:10
   min_vfdt_tran(i) = min(vfdt_tran(i, :));
   max_vfdt_tran(i) = max(vfdt_tran(i, :));
end

for i = 1:4
   min_vfdt_swit(i) = min(vfdt_swit(i, :));
   max_vfdt_swit(i) = max(vfdt_swit(i, :));
end

for i = 1:2
   min_vfdt_nflt(i) = min(vfdt_nflt(i, :));
   max_vfdt_nflt(i) = max(vfdt_nflt(i, :));
end

figure(1)
plot(mean_vfdt_bird, var_vfdt_bird, 'o', mean_vfdt_light, var_vfdt_light, '*', mean_vfdt_storm,
var_vfdt_storm, '+', ...
   mean_vfdt_tran, var_vfdt_tran, '^', mean_vfdt_swit, var_vfdt_swit, 'd', mean_vfdt_nflt, var_vfdt_nflt, 's')

legend('Bird', 'Lightning', 'Strom', 'Transient', 'Switching', 'No Fault')
xlabel('Mean'), ylabel('Variance')
```

```
figure(2)
plot(mean_vfdt_bird, min_vfdt_bird, 'o', mean_vfdt_light, min_vfdt_light, '*', mean_vfdt_storm,
min_vfdt_storm, '+', ...
   mean_vfdt_tran, min_vfdt_tran, '^', mean_vfdt_swit, min_vfdt_swit, 'd', mean_vfdt_nflt, min_vfdt_nflt,
's')

legend('Bird', 'Lightning', 'Strom', 'Transient', 'Switching', 'No fault')
xlabel('Mean'), ylabel('Min')

figure(3)
plot(mean_vfdt_bird, max_vfdt_bird, 'o', mean_vfdt_light, max_vfdt_light, '*', mean_vfdt_storm,
max_vfdt_storm, '+', ...
   mean_vfdt_tran, max_vfdt_tran, '^', mean_vfdt_swit, max_vfdt_swit, 'd', mean_vfdt_nflt, max_vfdt_nflt,
's')

legend('Bird', 'Lightning', 'Strom', 'Transient', 'Switching', 'No Fault')
xlabel('Mean'), ylabel('Max')

figure(4)
plot(min_vfdt_bird, max_vfdt_bird, 'o', min_vfdt_light, max_vfdt_light, '*', min_vfdt_storm,
max_vfdt_storm, '+', ...
   min_vfdt_tran, max_vfdt_tran, '^', min_vfdt_swit, max_vfdt_swit, 'd', min_vfdt_nflt, max_vfdt_nflt, 's')

legend('Bird', 'Lightning', 'Strom', 'Transient', 'Switching', 'No Fault')
xlabel('Min'), ylabel('Max')

save rvfdtmv mean_vfdt_bird var_vfdt_bird mean_vfdt_light var_vfdt_light mean_vfdt_storm
var_vfdt_storm mean_vfdt_tran var_vfdt_tran ...
mean_vfdt_swit var_vfdt_swit min_vfdt_bird max_vfdt_bird min_vfdt_light max_vfdt_light
min_vfdt_storm max_vfdt_storm min_vfdt_tran max_vfdt_tran ...
min_vfdt_swit max_vfdt_swit mean_vfdt_nflt var_vfdt_nflt min_vfdt_nflt max_vfdt_nflt

clear all
```

## B.20 Function RDATA2WAVE

```
% Function RDATA2WAVE
% Input: The recorded signals.
% output: The wavelet-based features.
function sig_wave = rdata2wave(fname, a, b)
% This script reads the transient data into MATLAB and submits them for
% wavelet analysis.
%
% The wavelet analysis is carried out to yield the first detail
% coefficients of the signal. They are then squared and averaged and used as
% features. So each waveform is distilled into only one feature.

signal = load(fname); % load the data file

signal = signal(a:b, 3);

[C , L] = wavedec(signal, 3 , 'db4');
cD1 = detcoef(C , L , 1);
%cD2 = detcoef(C , L , 2);
%rmsD1 = sqrt(2*mean(cD1.^2)/(b-a));
%rmsD2 = sqrt(2*mean(cD2.^2)/(b-a));
f1 = mean(cD1);
f2 = var(cD1);
%meanD2 = mean(cD2.^2);

sig_wave = [f1 f2];
%plot(cD1);

clear signal C L cD1

% All real data files need to be analyzed using this function. Once this is
% done, the features should be save in the data file WAVE_FEATURES.MAT
```

## B.21 Script WAVEVFDTCOMBNN

```
% Function WAVEVFDTCOMNN
% Input: The pointer to a sample input.
% Output: The corresponding class of the input, using the k-NN method.

function sampclass = wavevfdtcombnn(row_num)
% This function does the following tasks:
% 1) combines the features from the vfdt with the features form the wavelet
% analysis;
% 2) for a sample in the training set (specified by rom_num), it discards
% the sample from the training set and uses it as a test sample.
% 3) The class of the test sample is returned in the sampclass
% The row_num has to be lass than 49

%load wave_features
load wave_features2
load rvfdtmv
load phyfeatures

training = [
   bvd' bdu' mean_vfdt_bird' wave_bird
   lvd' ldu' mean_vfdt_light' wave_light];

% Format of the data:
% Rows 1 to 24 --> Bird
% Rows 25 to 36 --> Lightning

% Original numbers
birdc = 24;
lightc = 12;

% Update numbers
if (1 <= row_num & row_num <= birdc)
   birdc = birdc-1;
elseif (25 <= row_num & row_num <=birdc+lightc)
   lightc = lightc-1;
end

new_training = [ training(1:row_num-1, :); training(row_num+1:length(training), :)];

nn3 = findclose(new_training, training(row_num, :));

birdind = find( nn3 <= birdc);

if (length(birdind) >= 3)
   sampclass = 'Bird';
else
   sampclass = 'Lightning';
end

%sampclass

function nn = findclose( Tmat, Samp)
D = 0;
```

```
[N,fnum] = size(Tmat);

% Firstly normalize the training set and the input smaple
for i=1:fnum
   mm = mean(Tmat(:,i));
   Tmat(:, i) = Tmat(:, i) / mm;
   Samp(i) = Samp(i) / mm;
end

for i = 1:length(Tmat)
   D(i) = 0;
   for j = 1:fnum
     % if fnum == 4
       %  G = 1000;
       % else
       %  G = 1;
       %end
      D(i) = D(i)+(Samp(j)-Tmat(i,j))^2;
   end
   D(i) = sqrt(D(i));
end
n1 = find( D == min(D));
% D(n1) = Inf;
% n2 = find( D == min(D));
% D(n2) = Inf;
% n3 = find( D == min(D));
% D(n3) = Inf;
% n4 = find( D == min(D));
% D(n4) = Inf;
% n5 = find( D == min(D));
% nn = [n1 n2 n3 n4 n5];
% nn = nn(1:5);
```